University of Kentucky
UKnowledge

University of Kentucky Doctoral Dissertations | Graduate School

2007

MICROELECTRODE ARRAY RECORDINGS OF L-GLUTAMATE DYNAMICS IN THE BRAINS OF FREELY MOVING RATS

Erin Cathleen Rutherford
University of Kentucky, eruth2@gmail.com

Right click to open a feedback form in a new tab to let us know how this document benefits you.

Recommended Citation

Rutherford, Erin Cathleen, "MICROELECTRODE ARRAY RECORDINGS OF L-GLUTAMATE DYNAMICS IN THE BRAINS OF FREELY MOVING RATS" (2007). *University of Kentucky Doctoral Dissertations*. 523.
https://uknowledge.uky.edu/gradschool_diss/523

This Dissertation is brought to you for free and open access by the Graduate School at UKnowledge. It has been accepted for inclusion in University of Kentucky Doctoral Dissertations by an authorized administrator of UKnowledge. For more information, please contact UKnowledge@lsv.uky.edu.

ABSTRACT OF DISSERTATION

Erin Cathleen Rutherford

The Graduate School

University of Kentucky

2007

MICROELECTRODE ARRAY RECORDINGS OF L-GLUTAMATE DYNAMICS IN THE BRAINS OF FREELY MOVING RATS

ABSTRACT OF DISSERTATION

A dissertation submitted in partial fulfillment of the
requirements for the degree of Doctor of Philosophy in the
College of Medicine
at the University of Kentucky

By
Erin Cathleen Rutherford

Lexington, Kentucky

Director: Dr. Greg Gerhardt, Professor of Anatomy and Neurobiology

Lexington, Kentucky

2007

Copyright © Erin Cathleen Rutherford 2007

ABSTRACT OF DISSERTATION

MICROELECTRODE ARRAY RECORDINGS OF L-GLUTAMATE DYNAMICS IN THE BRAINS OF FREELY MOVING RATS

L-glutamate (Glu) is the predominant excitatory neurotransmitter in the mammalian central nervous system (CNS) and is associated with a wide variety of functions including motor behavior and sensory perception. While microdialysis methods have been used to record tonic levels of Glu, little is known about the more rapid changes in Glu signals that may occur in awake animals. We have previously reported acute recording methods using an enzyme-based microelectrode array (MEA) with fast temporal resolution (800 msec), that is minimally invasive and is capable of detecting low levels of Glu (< 0.2 μM) in anesthetized animals with little interference from other analytes. We have made a series of modifications to the MEA design to allow for reliable measures in the brain of awake behaving rats. In these studies, we characterized the effects of chronic implantation of the MEA into the striatum and prefrontal cortex (PFC) of Fischer 344 and Long Evans rats. We measured resting levels of Glu and local application of Glu for 7 days without a significant loss of sensitivity and determined that Glu measures due to exogenous Glu varied between rat strain and brain region. In addition, we determined the viability of the recordings in the brains of awake animals. We performed studies of tail-pinch induced stress which caused an increase in Glu in the striatum and PFC of Long Evans and Fischer 344 rats. Histological data show that chronic implantation of our MEAs caused minimal injury to the CNS. Taken together, our

data support that chronic recordings of tonic and phasic Glu can be carried out in awake rats reliably for 7 days *in vivo* allowing for longer term studies of Glu regulation in behaving rats.

Keywords: L-Glutamate; Prefrontal Cortex; Striatum; Unanesthetized; Freely Behaving

Erin Cathleen Rutherford

03/06/07

MICROELECTRODE ARRAY RECORDINGS OF L-GLUTAMATE DYNAMICS IN THE BRAINS OF FREELY MOVING RATS

By

Erin Cathleen Rutherford

Greg A. Gerhardt
Director of Dissertation

Jennifer Brueckner
Director of Graduate Studies

03/06/07

RULES FOR THE USE OF DISSERTATIONS

Unpublished dissertations submitted for the Doctor's degree and deposited in the University of Kentucky Library are as a rule open for inspection, but are to be used only with due regard to the rights of the authors. Bibliographical references may be noted, but quotations or summaries of parts may be published only with the permission of the author, and with the usual scholarly acknowledgments.

Extensive copying or publication of the dissertation in whole or in part also requires the consent of the Dean of the Graduate School of the University of Kentucky.

A library that borrows this dissertation for use by its patrons is expected to secure the signature of each user.

Name	Date

DISSERTATION

Erin Cathleen Rutherford

The Graduate School

University of Kentucky

2007

MICROELECTRODE ARRAY RECORDINGS OF L-GLUTAMATE DYNAMICS IN THE BRAINS OF FREELY MOVING RATS

DISSERTATION

A dissertation submitted in partial fulfillment of the
requirements for the degree of Doctor of Philosophy
in the College of Medicine
at the University of Kentucky

By
Erin Cathleen Rutherford

Lexington, Kentucky

Director: Dr. Greg A. Gerhardt, Professor of Anatomy and Neurobiology

Lexington, Kentucky

2007

Copyright © Erin Cathleen Rutherford

Dedicated to my fiancé Kevin Hascup and my parents Gary Rutherford and Mike and Susan Leonard

ACKNOWLEDGEMENTS

The pursuit of this degree has led me down a long path and would not have been possible without the insight and direction of many people. I would like to begin by expressing my gratitude for my mentor, Dr. Greg Gerhardt, who has been instrumental in my personal and professional development. It has been a privilege to receive my graduate training in a laboratory that encourages independence and strives to continually remain on the cutting edge of research. I would also like to thank my graduate committee, comprised of Drs. Don Gash, Paul Glaser and Nada Porter, for their fostering of my ideas and intellectual contribution to the work contained in this dissertation, as well as Dr. Rodney Guttmann for graciously agreeing to serve in the role of outside examiner on this committee. Francois Pomerleau, Peter Huettl and Dr. Jason Burmeister have also played a pivotal role in my professional development that is much appreciated.

On a more personal note, I would like to thank those friends and family members whose support has allowed me to reach this point. First and foremost, my parents Gary Rutherford and Mike and Susan Leonard deserve special thanks for their support and guidance over the last 28 years, as well as for the emphasis they placed on dedication, achieving a quality education and following my dreams. Special thanks to my fiancé, Kevin Hascup, for his encouragement and his ability to keep me focused and make me laugh. I would also like to thank my entire family, brothers Gary and Robert, sisters Katie and Meghan, grandparents Lowell and Delores Rutherford and Russell and Dorothy Carpenter for their love and support. I would like to conclude by acknowledging the friends that have gone through the ups and downs with me, encouraged me, helped me find my way, and made this experience so much more enjoyable. Robin Lindsay, Dr. Jeorge Quintero, Dr. B. Keith Day, Dr. B. Matt Joyce, Dr. Justin Nickell, Garretson Epperly, Josh Fuqua, Katie Werner, Michelle Stephens, Pooja Talauliker, Theresa Currier Thomas, Jason Hinzman, Meagan Littrell, Stuart and

SaraBeth Blankenship, Sarah Bandomer, Megan Feichtner, Katy Raeman, Stewart Surgener and all my fellow IBS–ers…thanks for the memories.

TABLE OF CONTENTS

ACKNOWLEDGEMENTS iii
LIST OF TABLES vii
LIST OF FIGURES viii
Chapter One: Introduction 1
Techniques for Studying L-Glutamate: Microelectrode Arrays vs. Microdialysis 1
L-Glutamate in the Mammalian Central Nervous System 2
L-Glutamate Synthesis, Receptors, and Transporters 3
The Role of Anesthesia on the Glutamatergic System in the Central Nervous System 5
L-Glutamate in the Awake Animal Model 6
Thesis Outline 7
Chapter Two: Materials and Methods 16
Microelectrode Array Design and Fabrication 16
Microelectrode Preparation 17
Exclusion Layer 17
Enzyme-Based Microelectrode Design 17
Reference Electrodes 19
Printed Circuit Board Modification 19
Chronic Connector and MEA Attachment 20
Microelectrode Array /Cannula Assembly 21
Electrode Calibration 21
Animal Preparation for Awake Freely Behaving Amperometric Recordings 24
Electrode implantation 24
Awake Freely Behaving Recordings 25
Recording Apparatus 25
Recording protocol 26
Histopathology 27
Drugs and Reagents 28
Electrode Preparation and Calibration 28
Intracranial Ejection 28
Anesthetics and Special Use Drugs and Chemicals 29
Data Analysis 29
Chapter Three: Resting L-Glutamate Measures in Awake Male Fischer 344 and Long Evans Rats 36
Introduction 36
Methods 37
Results 37
Discussion 39
Chapter Four: Do Measures of Exogenous Glutamate Change Over Time, Between Brain Regions, and Between Rat Strains in Awake Rats? 54
Introduction 54
Methods 55
Results 55

Discussion 57
Chapter Five: The Extent of Damage on Surrounding Tissue due to Chronic Implantation of the Microelectrode Array 68
Introduction 68
Methods 69
Results 70
Discussion 71
Chapter Six: Does Tail-Pinch Stress Affect L-Glutamate Levels in the Striatum and Prefrontal Cortex of Male Fischer 344 and Long Evans Rats? 79
Introduction 79
Methods 80
Results 81
Discussion 82
Chapter Seven: Preliminary Studies and Future Directions 94
References 110
VITA 121

LIST OF TABLES

Table 1.1: Distribution of the Rat Brain Excitatory Amino Acid Transporters 11
Table 1.2: Ionotropic Glutamate Receptors 12
Table 1.3: Metabotropic Glutamate Receptors 13
Table 3.1: Resting L-Glutamate Levels in Awake Rats as Measured with Microdialysis or Enzyme-Based Amperometry 43
Table 3.2: Effects of Application of Urethane, TTX, CPG or LY379268 on Resting L-Glutamate Levels 44

LIST OF FIGURES

Figure 1.1: Neuronal Glutamate Metabolism Schematic 14
Figure 1.2: Glutamatergic Synapse Schematic 15
Figure 2.1: Freely Moving Microelectrode Design 30
Figure 2.2: L-Glutamate Self-Referencing Microelectrode Array Calibration 31
Figure 2.3: Slope Values for *In Vitro* Calibrations 32
Figure 2.4: Limit of Detection Values for *In Vitro* Calibrations 33
Figure 2.5: Microelectrode Implantation Surgery 34
Figure 2.6: Schematic Diagram of the *In Vivo* Freely Moving Recording System 35
Figure 3.1: Determination of Resting L-Glutamate Levels 45
Figure 3.2: Resting L-Glutamate Levels in the Striatum and Prefrontal Cortex of Fischer 344 and Long Evans Rats 46
Figure 3.3: Resting L-Glutamate Levels in the Prefrontal Cortex of Awake Long Evans Rats 47
Figure 3.4: Effects of Urethane on Resting L-Glutamate Levels in the Prefrontal Cortex of Long Evans Rats 48
Figure 3.5: Resting L-Glutamate Levels as Measured by Enzyme-Based Microelectrode Arrays in Fischer 344 Rats 49
Figure 3.6: Effects of Tetrodotoxin on Resting L-Glutamate Levels in the Prefrontal Cortex of Long Evans Rats 50
Figure 3.7: Effects of (S)-4-Carboxyphenylglycine on L-Glutamate in the Prefrontal Cortex of Long Evans Rats 51
Figure 3.8: Typical Changes in L-Glutamate with Local Application of a mGluR Agonist and Antagonist in the Prefrontal Cortex of Long Evans Rats 52
Figure 3.9: Effects of mGluR Agonist and Antagonist on L-Glutamate Levels in the Prefrontal Cortex of Long Evans Rats 53
Figure 4.1: Representative Tracing of Local Application of 5 mM L-Glutamate (1 µL) in the Striatum of a Long Evans Rat 60
Figure 4.2 Local Application of L-Glutamate at +0.7 V and +0.2 V vs. Ag/AgCl Reference Electrode 61
Figure 4.3: Local Application of 5 mM L-glutamate (1 µL) Days 3, 5, and 7 Post-Implantation in the Right Prefrontal Cortex of Long Evans Rats 62
Figure 4.4: Local Application of 5 mM L-glutamate (1 µL) Day 3 Post-Implantation in the Striatum and PFC of Fischer 344 and Long Evans Rats 63
Figure 4.5: t_{80} on Days 3, 5, and 7 Post-Implantation in the Prefrontal Cortex of Fischer 344 Rats 64
Figure 4.6: t_{80} on Days 3, 5, and 7 Post-Implantation in the Prefrontal Cortex of Long Evans Rats 65
Figure 4.7: t_{80} in the Striatum of Long Evans and Fischer 344 Rats 66
Figure 4.8: t_{80} in the Striatum of Awake and Anesthetized Fischer 344 Rats 67
Figure 5.1: Cresyl Violet Staining of Microelectrode Arrays Chronically Implanted in the Right Prefrontal Cortex of a Long Evans Rat 73

Figure 5.2: GFAP Staining of the Right Prefrontal Cortex of Long Evans Rats with Chronic Microelectrode Array Implantations 74
Figure 5.3: GFAP Staining of Right Prefrontal Cortex of a Long Evans Rat after an 8 Week Implant 75
Figure 5.4: Image of GFAP and Iba1 Staining in the Prefrontal Cortex of Long Evans Rats after 3 Day, 1 Week, 4 Week, and 24 Week Implantations 76
Figure 5.5: Iba1 staining of the Right Prefrontal Cortex of Long Evans Rats with Chronic Microelectrode Array Implantations 77
Figure 5.6 :Iba1 Staining of the Right Prefrontal Cortex of a Long Evans Rat after an 8 Week Implant 78
Figure 6.1: Representative Tracing of a Five Minute Tail-Pinch Response in the Striatum of a Long Evans Rat 85
Figure 6.2: Representative Tracing of a Five Minute Tail-Pinch Response in the Prefrontal Cortex of Long Evans Rats 86
Figure 6.3: Representative Tracing of a Five Minute Tail-Pinch Response in the Striatum of Fischer 344 Rats 87
Figure 6.4: Representative Tracing of a Five Minute Tail-Pinch Response in the Prefrontal Cortex of Fischer 344 Rats 88
Figure 6.5: Duration of Response to a Five Minute Tail-Pinch in the Striatum and Prefrontal Cortex of Fischer 344 and Long Evans Rats 89
Figure 6.6: Maximum Amplitude during Tail-Pinch Response in the Striatum and Prefrontal Cortex of Fischer 344 and Long Evans Rats 90
Figure 6.7: Area Under the Curve for Tail-Pinch Response in the Striatum and Prefrontal Cortex of Fischer 344 and Long Evans Rats 91
Figure 6.8: Number of Peaks during Tail-Pinch Response in the Striatum and Prefrontal Cortex of Fischer 344 and Long Evans Rats 92
Figure 6.9: Total Peak Area for Tail-Pinch Response in the Striatum and Prefrontal Cortex of Fischer 344 and Long Evans Rats 93
Figure 7.1: Tail-Pinch Response in the Fischer 344 Rat Striatum 99
Figure 7.2: Fischer 344 Tail-Pinch Striatal Spike Response 100
Figure 7.3: Fischer 344 Tail-Pinch Striatal Plateau Response 101
Figure 7.4: Local Application of Dopamine (200 µM, 1 µL) in the Striatum of a Long Evans Rat 102
Figure 7.5: Dopamine Tail-Pinch Response in the Striatum of a Long Evans Rat 103
Figure 7.6: Achetylcholine Tail-Pinch Response in the Prefrontal Cortex of a Long Evans Rat 104
Figure 7.7: Glutamatergic Response to Fox Urine Exposure in the Striatum of a Fischer 344 Rat 105
Figure 7.8: Glutamatergic Response to a NMDA Receptor Antagonist (MK-801) in the Somatosensory Cortex of a Long Evans Rat 106
Figure 7.9: Glutamatergic Response to Contralateral Vibrissae Stimulation in the Somatosensory Cortex of a Long Evans Rat 107
Figure 7.10: Continuous Second-By-Second Recording of L-Glutamate over Light and Dark Cycles 108

Figure 7.11: T1 MRI of an Implanted MEA in the Prefrontal Cortex of a Long Evans Rat 109

Chapter One: Introduction

Techniques for Studying L-Glutamate: Microelectrode Arrays vs. Microdialysis

Historically, Glu neurotransmission has been studied in brain tissue using microdialysis and electrophysiological methods such as patch-clamp recordings (Bagley and Moghaddam, 1997; Fitzpatrick *et al*., 2001; Kennedy *et al*., 2002; Shou *et al*., 2004; Tucci *et al*., 1997). Currently, the most common technique employed to study Glu levels in the intact mammalian brain is *in vivo* microdialysis. Many microdialysis studies of Glu levels have been performed in anesthetized and awake animal models (Bagley and Moghaddam, 1997; Kennedy *et al*., 2002; Shou *et al*., 2004; Tucci *et al*., 1997). Microdialysis allows for the simultaneous measurements of multiple analytes at low detection levels. However, the fast dynamics of Glu regulation may be muted when using microdialysis due to the limits in temporal resolution of this method. Progress on increasing the temporal resolution by coupling microdialysis with capillary electrophoresis (Tucci *et al*. 1997; Kennedy *et al*., 2002) has decreased sampling rates to every 12-18 seconds which is still far above the subsecond rates required. In addition, several microdialysis studies have reported that the Glu overflow measured with this technique is not tetrodotoxin (TTX) -dependent, supporting the idea that the Glu signals measured using microdialysis are not neuronally derived (Timmermann and Westerink, 1997; Baker *et al*., 2002; Melendez *et al*., 2005). Furthermore, it has been shown that there is extensive damage to the brain tissue up to 1.4 mm away from the microdialysis probe implant site (Clapp-Lilly *et al*., 1999; Borland *et al*., 2005) which may affect neurotransmitter signaling, release, and uptake. Despite the incorporation of capillary electrophoresis, it is doubtful that microdialysis can achieve the temporal resolution required to see the subsecond dynamics of Glu, mainly due to the physical limitations associated with the diffusional process required to cross the dialysis membrane. Since neurochemical levels and behaviors are capable of changing rapidly (sub-second), it is important to develop a technique that has an adequate temporal resolution.

Our laboratory has recently developed an enzyme-based microelectrode array (MEA) that is capable of selectively detecting low levels (0.2 μM) of Glu with sub-second (500 - 800 msec) time resolution that is virtually free from CNS interferents, such as 3,4-dihydroxy-phenylacetic acid (DOPAC) and ascorbate (Burmeister *et al*., 2000, 2003). The present studies address the adaptation and validation of MEA recordings in the awake, freely moving rat, as well as address clinically relevant issues, such as measures of Glu resting levels, the effects of chronic implantation of the MEAs on surrounding brain tissue, Glu clearance, variance in phasic and tonic Glu between brain regions, and the effects of stress on Glu levels. First, we adapted our methodology for chronic recordings of tonic (resting) levels and phasic (rapid) changes of Glu in awake rats. Second, we investigated the reproducibility of such methods for chronic measures in the rat PFC and striatum over several days. Third, studies with pharmacological agents were carried out to better understand the specificity of these measures for Glu and the *in vivo* source(s) of these signals. Fourth, extracellular levels of Glu were investigated during a behavior related situation (stress induced by a tail-pinch) in the brain of awake rats. Finally, we carried out histopathological studies to determine the damage produced by the MEA's to surrounding brain tissue.

L-Glutamate in the Mammalian Central Nervous System

There are four main classification criteria for a neurotransmitter: 1) presynaptic localization, 2) release by a physiological stimuli, 3) identical action with naturally occurring transmitter, and 4) mechanism for rapid termination of transmitter action. In the mid – 1980s, Glu met these criteria and was accepted as a candidate for a neurotransmitter (Krnjevic, 1986; Watkins, 1986). Today we know that Glu is the predominant excitatory neurotransmitter in the mammalian CNS. Glu has been shown to link many structures within the brain, including the cerebral cortex, hippocampus, basolateral amygdala, substantia nigra, nucleus accumbens, striatum, superior colliculus, caudate nucleus, red nucleus, and the pons. Studies that examine the exact localization of Glu have been hard to accomplish successfully, mainly due to the abundance of Glu in the CNS and its

metabolic functions and the role of Glu as a precursor for γ-aminobutyric acid (GABA), the major inhibitory neurotransmitter in the brain. Glu has been shown to play a role in development, plasticity, learning and memory, cognition, sensory systems, and motor systems through its interactions in the CNS. In addition, Glu has also been associated with many brain disorders, including schizophrenia, addiction, stroke, traumatic brain injury, Huntington's Disease, amyotophic lateral sclerosis, Parkinson's Disease and epilepsy.

For the scope of these studies, the brain areas of interest were the striatum and the PFC. In the rodent, the medial PFC (infralimbic and prelimbic areas) is suggested to be the brain area responsible for executing function, including working memory (Aultman and Moghaddam, 2001; Delatour and Gisquet-Verrier, 1996; Floresco *et al*., 1996; Granon and Poucet, 1995; Kesner *et al*., 1996; and Seamans *et al*., 1995) and other cognitive functions. All PFC efferents and the majority of the afferents to the PFC, such as projections from the thalamus, hippocampus, and amygdala, are glutamatergic. Glu is also abundant in the striatum, which is important to these studies because the PFC and striatum send and receive input from each other and are interconnected via the limbic system and motor controls, which are implicated in various behavioral functions including the stress response.

L-Glutamate Synthesis, Receptors, and Transporters

Glu in the brain is derived almost entirely through local synthesis. This may occur through multiple pathways. In the brain, Glu is formed primarily through the Krebs cycle, by the transamination of α-ketoglutarate by Glu dehydrogenase, and also from glutamine derived from glial cells that can be converted in the nerve terminal to Glu via glutaminase. A brief overview of the pathways mentioned here can be seen in Figure 1.1. Glu in the nerve terminal is then transferred, via a highly specific Cl^- -dependent vesicular Glu transporter (vGluT), and stored in synaptic vesicles until it is released into the synaptic cleft. In glutamatergic neurons, Glu is released through a calcium-dependent

exocytotic process where the synaptic vesicle fuses with the presynaptic neuronal cell membrane when the nerve terminal is depolarized.

Once Glu is released into the synaptic cleft, the signal is terminated mainly by uptake into glial cells through high affinity sodium-dependent plasma membrane Glu transporters; the Glu aspartate transporter (GLAST-1) and Glu transporter-1 (GLT-1) (Danbolt, 2001; Fillenz, 1995). Glu is then converted to glutamine and can be transported back to the presynaptic glutamatergic nerve terminal, where it can again be converted into Glu and stored in synaptic vesicles and used for release. Glu near the synaptic cleft may also be terminated through uptake on the postsynaptic nerve terminal by a sodium-dependent plasma membrane excitatory amino acid carrier (EAAC). Additionally, in the human brain, there are two more transporters, EAAT4 (cerebellum) and EAAT 5 (retina). As the primary area of interest for this document lies in the striatum and PFC of rats, EAAT4 and EAAT 5 will not be discussed. A review of the primary location of Glu transporters in the rat brain can be found in Table 1.1.

There are two types of Glu receptors, ionotropic (iGluR) and metabotropic (mGluR). The iGluRs consist of α-amino-3-hydroxy-5-methyl-4-isoxazole propionate (AMPA), kainate, and N-methyl-D-aspartate (NMDA) receptors, named after select agonists. The AMPA receptor is involved in the fast neurotransmission of excitation and utilizes sodium and Glu as endogenous agonists. The NMDA receptor is involved in slow, prolonged neuronal depolarization. This receptor is unique in that it requires two ligands, Glu and glycine, for receptor activation. Additionally, the NMDA receptor is both ligand-gated, using sodium, calcium, and Glu as endogenous agonists, and voltage-gated due to the magnesium channel block. A brief review of iGluRs can be found in Table 1.2.

mGluRs are divided into three groups (I, II, and III). mGluRs contain seven transmembrane spanning domains with their ligand-binding sites located on the extracellular N-terminus and are coupled to G-proteins. mGluRs require subsequent second messenger signaling to elicit a response and are therefore generally slower acting than iGluRs. The mGluR Group I (mGluR 1 and 5) are

linked to phospholipase C (PLC) and are generally excitatory. While mGluR Group II (mGluR 2 and 3) and III (mGluR 4, 6, 7, and 8) act by inhibiting adenyl cyclase, and therefore cAMP formation, making mGluR Group II and III generally inhibitory. mGluRs are thought to modulate brain excitability through their presynaptic, postsynaptic, and glial activity (Table 1.3). As is evident from this brief discussion, the glutamatergic synapse is highly involved with its iGluRs, mGluRs, and transporters. As such, Figure 1.2 outlines a typical glutamatergic synapse.

The Role of Anesthesia on the Glutamatergic System in the Central Nervous System

The effects of anesthesia on the glutamatergic system in the CNS have only recently begun to be studied. Various anesthetics may have widely differing effects on the glutamatergic system, based on their target of action. One anesthetic of interest, isoflurane, a halogenated ether commonly used in the operating room, was first used clinically in 1981 affects Glu neurotransmission. Liachenko *et al.* (1999) reported inhibition by isoflurane on both the release and re-uptake of Glu with an EC_{50} in the clinical dose range. Additionally, patch-clamp recordings have shown a decrease in glutamatergic neuronal excitability with isoflurane. However, these affects have been shown to return to normal within 30 minutes after the cessation of administration, making it a good candidate for use with humans as well as for recovery surgery with rodents.

Another anesthetic commonly used when studying rodents is urethane due to its ability to produce a high plane of anesthesia for approximately eight hours without the need for re-administration. While urethane is thought to have minimal effects on the dopaminergic system (Sabeti *et al*., 2003), little is known about its effects on the glutamatergic system. Bindman *et al.* (1988) reported that there was no difference observed between *in vitro* brain slices and urethane-anesthetized rats in resting membrane potential, action potential amplitude or membrane capacitance. However, a diminished neuronal activity associated with urethane was observed in several studies (Albrecht and Davidowa, 1989; Dyer

and Rigdon, 1987; Girman *et al*., 1999). Resting Glu levels in the anesthetized rat striatum were reported to be approximately 1.3 – 2.7 μM (Cellar, *et al.,* 2005), whereas, in an awake rat model resting Glu levels in the striatum were reported to be 0.20-0.82 μM (Di Cara *et al.,* 2001; Segovia *et al.,* 2001). Additionally, microdialysis measures of resting Glu in the frontal cortex of the awake rat ranged between ~2 μM and ~9 μM (Baotell *et al.*, 1995; Rocha *et al*., 1996). These discrepancies observed in resting Glu levels using microdialysis may be explained by differences in the sampling time employed, or the origin of the Glu pool being sampled, the brain region, as well as the effects of anesthesia. It is entirely possible that there may be differences observed in tonic (resting levels) and phasic Glu levels in the brain as a result of the use or type of anesthetic.

L-Glutamate in the Awake Animal Model

Several methods have been employed to measure Glu in the awake rat model, including microdialysis. However, none have the combined advantages of sub-second recording times, low levels of detection for Glu, and minimally invasiveness. Recordings of Glu in freely moving animals have several distinct advantages. First, this approach allows for monitoring Glu neurotransmission without the effects of anesthesia. Anesthetics are known to alter resting levels and phasic Glu release dynamics (Liachenko *et al*., 1998, 1999). Second, our microelectrodes can reliably record Glu for at least one week in the brain of the freely moving rat. This means that subsequent measures can be made over multiple days rather than only one day as in anesthetized amperometric recordings as well as anesthetized and awake microdialysis studies. Third, freely moving animal recordings can be coupled to behavioral studies to investigate changes in Glu that are due to behavior. This allows us to directly couple a behavioral event with a physiological response.

Of particular interest to us is the involvement of stress in neurological disorders, such as addiction, schizophrenia, and Parkinson's disease. Stress can play a major role in the development, progression and exacerbation of symptoms associated with these disorders (Carlsson and Carlsson, 1990; Grace,

1991; Greenamyre, 1993; Del Arco *et al*., 1998, 1999). It has been suggested that Glu neurotransmission activation in the PFC is a common mechanism that may allow stress to influence both normal and abnormal processes that maintain cognition and affect (Moghaddam, 2002). Glutamatergic neurotransmission in the PFC modulates or mediates many aspects of the stress response, such as activation of the hypothalamic-pituitary-adrenal (HPA) axis and monoamine neurotransmission. Previous studies (Bagley and Moghaddam, 1997; Bland *et al*. 1999; Jedema and Moghaddam, 1994; Takahata and Moghaddam, 1998) have reported on stress response and Glu involvement in unanaesthetized animals, however, these studies did not have the temporal and spatial resolution that is possible with our ceramic MEAs and therefore, may not have detected the fast dynamics of Glu as a neurotransmitter. In many psychiatric disorders, such as addiction, depression, and schizophrenia, stress appears to be a major influence in the course and outcome of the disease. A better understanding in these areas may lead to more effective treatments.

Thesis Outline

As is evident from this discussion of the possible effects of anesthesia on the glutamatergic system and the techniques available for studying Glu in the awake animal, there is a great need to examine the glutamatergic system in a model that is free from anesthetics and has the capabilities to record low levels of Glu with high temporal resolution over long durations. The work presented herein serves not only to develop and characterize a new technique designed to record Glu in the freely moving animal, but also to serve as a means to expand on the current knowledge of resting levels and behavior-evoked Glu in the awake rat. In Chapter Three, we investigated resting Glu levels in the striatum and PFC of two rat strains, the Fischer 344 rat commonly used in age-related studies, and the Long Evans rat commonly used in behavioral based studies. We accomplished this by using an enzyme-based ceramic microelectrode array configured to selectively measure Glu utilizing a self-referencing technique. We determined resting Glu levels on days 3, 5, and 7 post-implantation prior to

stimulation. We also examined potential mechanisms of action for regulating resting levels of Glu as well as the effect of urethane anesthetic on resting Glu levels. Our results show that tonic Glu levels were significantly higher in the PFC of Long Evans rats compared to the PFC of Fischer 344 rats and the striatum of Long Evans rats and urethane significantly decreased tonic Glu levels (58%) in the PFC of Long Evans rats. In addition, we showed that independent local application of TTX and $mGluR_{2/3}$ agonist (LY379268) decreased resting Glu levels while the $mGluR_{2/3}$ antagonist (LY341495) increased those levels. Taken together, these results show that the pool of Glu being sampled was partially neuronally derived and was regulated presynaptically through mGluRs. In addition, data showed that tonic Glu levels were significantly different between rat strains as well as brain regions and resting Glu levels decreased with urethane administration.

Chapter Four further examines the glutamatergic system in the awake rat through local application of exogenous Glu and the differences observed in relation to time, brain region, and rat strain. We showed that Glu measures from locally applied Glu were not significantly different throughout the first seven days post-implantation in a given brain region. Additionally, exogenous Glu measures in the PFC of Long Evans and Fischer 344 rats were significantly increased compared to the striatum in the respective rat strain. Also, exogenous Glu measures in the PFC were significantly increased in Long Evans rats compared to Fischer 344 rats. However, no difference was observed in the striatum between the two rat strains. These observations show that there were differences in the clearance of Glu between brain regions and rat strains. These differences in clearance may be due to potential differences in brain tissue morphology, either the density of tissue or the type of cells present, or differences in the number, location, or efficiency of the Glu transporters. We also examined changes in clearance in the PFC of Fischer 344 rats and observed a trend in increased clearance time associated with longer implant durations. These results also show that our enzyme-based ceramic MEA can reliably

measure Glu when chronically implanted in the brain for at least one week post-implantation.

In Chapter Five we examined the extent of damage, measured by astrocyte density and activated microglia, caused by chronic implantation of our ceramic MEAs in the PFC of Long Evans rats. GFAP staining showed that there were no significant changes in astrocytes in rats with chronic MEA implantations for up to eight weeks. However, at 16 and 24 weeks post-implantation there was a significant increase in GFAP density. There was also a significant increase in mean density ionized calcium binding adaptor molecule 1 (Iba1) at the 1 week time point. However, the Iba1 levels return to control levels by 24. In all implantation durations examined, astrocytic changes indicating damage were contained to within 50-100 μm from the implantation site. These results show that chronic implantation of our ceramic MEAs caused minimal damage to surrounding tissue and the electrode was well tolerated by the host for an extended length of time. Furthermore, the results support that as we improve upon the technology and methodology of our enzyme-based coating, we will be able to extend the duration that we accurately and reliably measure Glu in the CNS.

In Chapter Six we applied our newly developed technology in freely moving rats to a behavioral paradigm in an effort to enhance the current understanding of the affects of stress on Glu levels in the striatum and PFC of Fischer 344 and Long Evans rats. Our results show that while there was no significant difference in the maximum Glu amplitude elicited between brain regions or rat strain, the duration of the Glu response observed in the striatum and PFC of Fischer 344 was significantly increased compared to that seen in the striatum and PFC of the Long Evans rats. An analysis of the Glu response vs. time showed no significant difference in the tail-pinch response area under the curve. However, there was a trend with the PFC showing elevated levels as compared to the striatum in both rat strains. These results suggest that there may be multiple short-lived Glu peaks above the general rise and fall of the tail-pinch response, not just a single maximum amplitude peak. The number of

peaks during the tail-pinch response showed an increased trend in the PFC of both rat strains compared to the striatum. This supports the need for a technique with high temporal resolution that is capable of distinguishing fast fluctuations in Glu coupled with advanced analytical techniques that can accurately depict changes of fast neurotransmitters, such as Glu.

Copyright © Erin Cathleen Rutherford 2007

Table 1.1: Distribution of the Rat Brain Excitatory Amino Acid Transporters

Transporter Subtype	Primary Localization
GLAST-1	Astrocytes
GLT-1	Astrocytes
EAAC	Postsynaptic neurons
EAAT4	Cerebellar Purkinje neurons (human)
EAAT5	Retina (human)

Table 1.2: Ionotropic Glutamate Receptors

	Ionotropic Receptors		
	NMDA	**AMPA**	**Kainate**
Select Agonist	NMDA	AMPA	Kainate
Functional Characteristics	Activation of NA^+, K^+, and Ca^{2+} channels	Activation of NA^+, K^+, and Ca^{2+} channels	Activation of NA^+, K^+, and Ca^{2+} channels
Other Agonists	Ibotenate, quinolinate	Quisqualic acid	Domoate,
Competitive Antagonists	2-AP5	CNQX, DNQX	CNQX, DNQX
Allosteric Modulators	Glycine, D-serine	Benzothiazide A (Con A)	concanacalin
Antagonists on allosteric binding sites	5,7-diCl-Kyn		
Channel Blockers	PCP, MK-801	Jorospider toxin (JST)	

2-AP5, 2-amino-5-phosphonopentanoic acid; CNQX, 6-cyano-7-nitroquinoxaline-2,3-dione; DNQX, 6,7-dinitroquinoxaline-2,3-dione; 5,7-diCl-Kyn, 5,7-dichlorokynurenic; PCP, phencyclidine; MK-801, dizocilpine.

Table 1.3: Metabotropic Glutamate Receptors

	Receptor	Coupling	Localizations and Functions	Agonists	Antagonist
Group I	mGluR1	Gq; increase PLC	primarily postsynaptic in neurons; activation enhances postsynaptic glutamatergic excitability	3,5-DHPG quisqualate	CPCCOEt (noncompetitive)
	mGluR5	Gq; increase PLC	Primarily postsynaptic in neurons and glia		MPEP (noncompetitive)
Group II	mGluR2	Gi, Go; decrease AC	Pre- and postsynaptic in neurons; high expression levels in rat forebrain	DCG-IV 2R,4R-APDC LY354740 LY379268	EGLU LY341495 LY307452
	mGluR3	Gi, Go; decrease AC	Primarily postsynaptic in neurons and glia		
Group III	mGluR4	Gi, Go; decrease AC	Pre- and postsynaptic in neurons; high expression levels in rat cerebellum	L-AP4 L-SOP PPG 3,4-DCPG is a selective mGluR8 agonist	CPPG MAP4
	mGluR6	Gi, Go; decrease AC	Localized to retinal tissue; low expression in brain tissue		
	mGluR7	Gi, Go; decrease AC	Pre- and postsynaptic in neurons; targeted presynaptically to active zone of glutamate release		
	mGluR8	Gi, Go; decrease AC	Pre- and postsynaptic in neurons; negative modulation of glutamate		

3,5-DHPG, 3,5-dihydroxyphenylglycine; CPCCOEt, 7-hydroxyiminocyclopropane[b]chromen-1a-carboxylic acid ethyl ester; MPEP, 2-methyl-6-(phenylethynyl)-pyridine; DCG-IV, (2S, 2'R,3'R)-2-(2',3'-dicarboxycyclopropyl)glycine; 2R,4R-APDC, 2R,4R-4-aminopyrrolidine-2,4-dicarboxylic acid; EGLU, (S)-α-ethylglutamic acid; L-AP4, 1,2-amino-4-phosphonobutyrate; L-SOP, S-serine-O-phosphate; PPG, (RS)-4-phosphonophenyl glycine; CPPG, (2S,2'R,3'R)-2-(2',3'-dicarboxycylcopropyl)glycine; MAP4, (S)-α-methyl-2-amino-4-phosphonobutanoic acid.

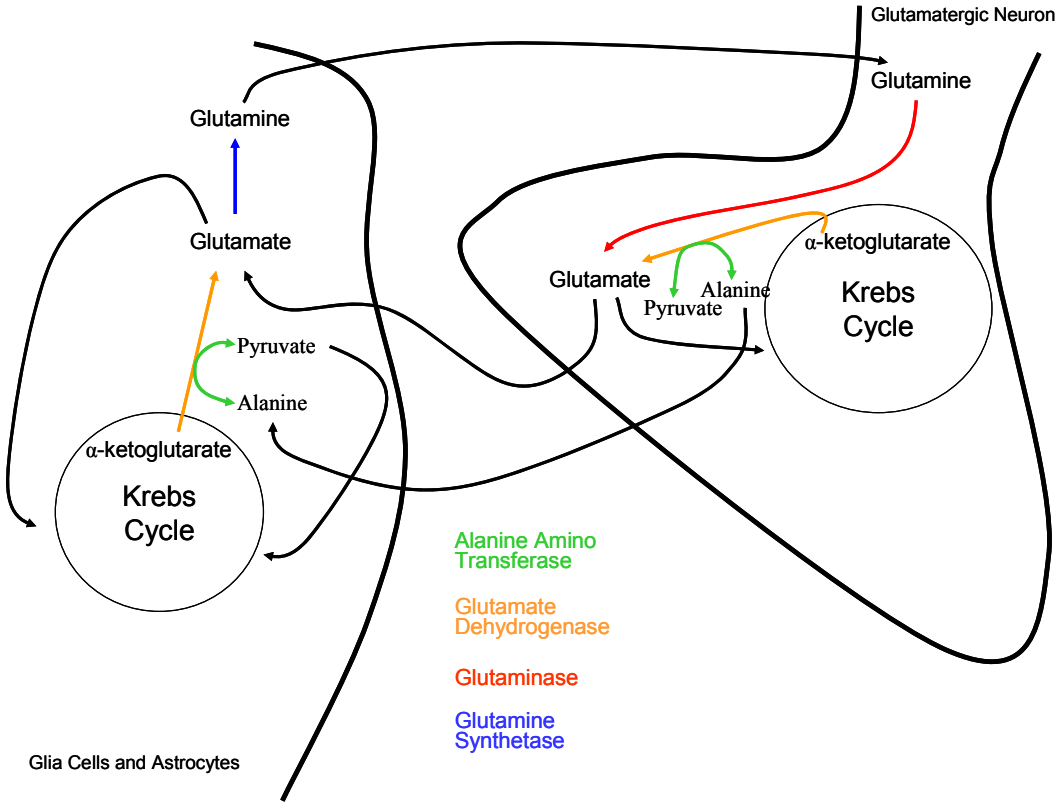

Figure 1.1: Neuronal Glutamate Metabolism Schematic
Schematic showing basic Glu metabolism and release at a glutamatergic synapse. Glutamatergic neurons release Glu derived from glutamine and the Krebs Cycle into the synaptic cleft. Glu is taken up into glial cells where it is converted to glutamine. Glutamine can then be transported to the glutamatergic neuron where it can be deamidated back into Glu and packaged into synaptic vesicles for release. In glia, Glu from the Krebs Cycle can also be converted into glutamine and transported to glutamatergic neurons where it can be converted back into Glu for release. Adapted from Waagepetersen *et al*., 2000.

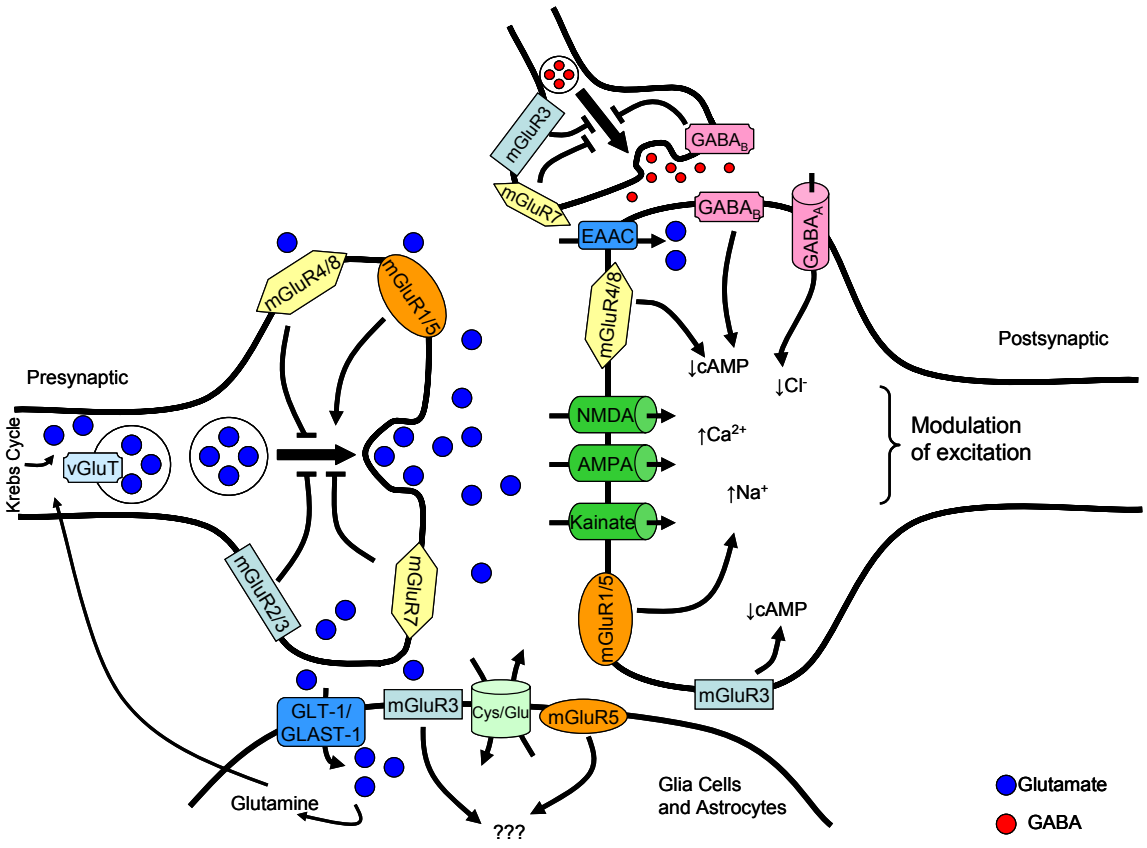

Figure 1.2: Glutamatergic Synapse Schematic
Schematic representation of a typical glutamatergic synapse. Glu from the Krebs Cycle is loaded into synaptic vesicles by vGluTs. The synaptic vesicles fuse with the neuronal membrane releasing Glu into the synaptic cleft. Glu can be transported into postsynaptic neurons via EAAC and into glia via GLT-1 and GLAST-1. Glu in the synaptic cleft can induce downstream signaling via post-synaptic neurons through mGluRs (groups I, II, and III) as well as through iGluRs (NMDA, AMPA, and kainate). Glu can excite or inhibit presynaptic neurons through mGluR groups I, II, and III. mGluR group I and II as well as the cystine-Glu exchanger are located on glia. GABAergic neurons, which can be influenced by mGluR group II and III, can also act on postsynaptic neurons through $GABA_A$ and $GABA_B$ receptors. Adapted from Schoepp, 2001.

Chapter Two: Materials and Methods

Microelectrode Array Design and Fabrication

Our multisite microelectrodes were constructed in conjunction with Thin Films Technology, Inc. (Buellton, California). In these studies, MEAs were produced with the desired recording site array layout (S2 microelectrode arrays consisting of four (two side-by-side pairs) Pt recording sites, each 15 x 333 μm). Microelectrode photographic masks were designed on a computer aided design program where arrays of 4 recording sites were arranged on templates. A 2.5 x 2.5 cm x 125 μm thick ceramic wafer (alumina, Al_2O_3, Coors Ceramic, Coors Superstrate 996) served as a substrate for the MEAs. Ceramic was used for its ability to reduce cross-talk from adjacent connecting lines. Ceramic also allowed for stereotaxic placement into tissues without flexing or breaking due to ceramic's strong and rigid nature.

The ceramic wafer was cleaned and a photoresist was spun onto the wafer. Light passing through the photomask exposed the photoresist, transferring the microelectrode images onto the wafer. Spaces for the recording sites, connecting lines and bonding pads were not exposed to light. Unexposed photoresist was removed from the wafer using solvents. Titanium (500 Å thick) was sputtered onto the ceramic wafer that was covered with developed photoresist. The titanium acted as an adhesion layer that helped the Pt adhere to the ceramic substrate. The active recording metal layer, Pt, was sputtered onto the substrate (~1.5 μm thick) on top of the titanium adhesion layer. Next, the developed photoresist and unwanted metals were removed with solvents resulting in the ceramic wafer covered only with the Pt recording sites and connecting lines. Finally, a protective polyimide layer (2-4 μm thick) was applied using a second photomask step, leaving the 4 active Pt recording sites uncoated. The individual microelectrodes tips were cut out using a diamond saw, which produced highly polished edges for reduced tissue damage during implantation. The ceramic wafer with Pt recording sites was attached to a small printed circuit

board (PCB) that allowed for easy handling and modification for use in the freely moving rat.

Microelectrode Preparation

Exclusion Layer

Microelectrodes were coated with an exclusion layer to block undesirable electrochemically active compounds that exist in high concentrations in the brain. The Pt recording sites were dip coated with the exclusion layer, Nafion® (an anionic Teflon® derivative with negatively charged sulfonic acid groups), which acted to repel anions, such as ascorbate and DOPAC (Burmeister and Gerhardt, 2001). This was accomplished by first aliquoting Nafion® into a 300 µl centrifuge tube. The microelectrode tip was then lowered approximately half-way into the aliquot of Nafion® and rotated in a circle three times and the tip was pulled straight out of the Nafion® solution. Microelectrodes were then placed in an oven at 165-175°C for five minutes to allow the Nafion® layer to cure on the tip. Microelectrodes were allowed to cool to room temperature for approximately 30 minutes prior to enzyme coating.

Enzyme-Based Microelectrode Design

Enzymes provided a means to convert a molecule, such as Glu, that is not inherently electrochemically active and therefore not measurable by a 16 bit Fast Analytical Sensing Technology (FAST-16) recording system (Quanteon, LLC, Nicholasville, KY), into a reporter molecule, such as peroxide (H_2O_2), that is oxidizable at the Pt recording sites of the microelectrodes. The current measured from the oxidation of peroxide generated during the enzymatic breakdown was directly proportional to the analyte (Glu) concentration. Microelectrode recording sites 1 and 2 (the lower pair) were coated with a 1% Glu oxidase (GluOx) coating solution. In order to induce cross-linking of GluOx and increase the adhesion of GluOx to the Pt recording sites, glutaraldehyde (0.125%) and BSA (1%) were added to the GluOx solution. To prepare the GluOx solutions, first, all proteins were brought to room temperature and 0.10 g

of bovine serum albumin (BSA) was dissolved by manual agitation in a 1.5 mL microcentrifuge tube containing 985 µl ddH_2O. Once dissolved, glutaraldehyde solution (5 µl) was added to the BSA mixture and manually mixed by inversion five times. The solution was set aside for five minutes. The BSA served as a matrix to protect the oxidase enzyme activity during immobilization. Next, the BSA/glutaraldehyde mixture (9 µl) was added to a 300 µl microcentrifuge tube and 1 µl of the Glu stock solution (1 UI/µl) was added and mixed by pipette agitation.

All enzymes were applied to the Pt recording sites by hand. Solutions were drawn up into a 10 µl Gastight® Hamilton microsyringe and dispensed to form a single small droplet of solution at the tip of the microsyringe. The droplet was briefly applied to the Pt recording sites under a dissecting microscope. Two additional coats of enzyme were applied in the same way with one minute dry times between each coat. The GluOx layer was required by our approach to measure Glu, as it caused the enzymatic break-down of Glu to α-ketoglutarate and H_2O_2. When a potential of +0.7 V vs. a Ag/AgCl reference electrode was applied to the MEA, the reporter molecule, H_2O_2, was oxidized and donated two electrons and the resulting current was then amplified and recorded by the FAST-16 recording system.

The advantage of using multisite microelectrodes was that a pair of recording sites were coated with the enzyme mixture and the adjacent sites were coated with the inactive protein matrix (BSA and glutaraldehyde) in the same manner as applying the enzyme mixture. Our laboratory refers to this technique as “self-referencing”. Microelectrode recording sites 3 and 4 (self-referencing or sentinel sites) were coated similar to sites 1 and 2, with the exception that the coating solution did not contain GluOx (Figure 2.1). This means that sites 3 and 4 recorded everything not repelled by Nafion® (any possible interferents, etc.) except Glu. When the current from sites 3 and 4 were subtracted from the current on sites 1 and 2, the resulting signal was due solely to Glu (Burmeister and Gerhardt, 2001 & Burmeister *et al.,* 2003). The combination of the exclusion

layer and the self-referencing technique resulted in a microelectrode with minimal background noise and an increased selectivity for the analyte of interest, Glu.

Once the enzyme and/or inactive protein matrix was applied, microelectrodes were stored at room temperature. Enzyme-coated microelectrodes cured at room temperature for 48-72 hours prior to calibration and experimentation. Complete curing increased enzyme layer adhesion to the microelectrode surface. This provided increased sensitivity to Glu as well as increased the shelf-life of the microelectrodes. If the enzyme/protein layers were not allowed to fully dry, they might have dissolved when put into solution or the brain and the maximum number of possible chronic Glu recording days may have been diminished.

Reference Electrodes

Ag/AgCl reference electrodes were prepared by first stripping the Teflon® coated silver wire (0.08 in bare, 0.110 in coated; A-M Systems, Inc., Carlsborg, WA) ¼ inch on each end. One of the stripped ends was soldered to a gold-plated socket (Ginder Scientific, Ottawa, ON) for connection to the FAST-16 headstage for freely moving recordings and the other end was coated with AgCl by placing the tip of the stripped sliver wire (cathode) into a 1 M HCl plating bath saturated with NaCl containing a Pt wire (anode) and applying 9 V DC current using a power supply to the cathode vs. the anode. The applied potential attracted Cl^- on the wire to form AgCl thus making the Ag/AgCl reference. The plating potential was applied for approximately 10-15 minutes.

Printed Circuit Board Modification

The pedestal was the portion of the system that was chronically implanted on the rat's head and contained the microelectrode. The pedestal connected to the miniaturized rat hat, which contained the miniature 4-channel pre-amplifier that was connected to a low torque commutator. The PCB was altered during MEA production to change the electrode PCB from the design used in slice and anesthetized animal recordings to a smaller design required for use in freely

moving animals. The resulting shorter paddle was termed “stub” (Figure 2.1). The stub MEA was designed to allow for future advances to the MEAs with up to 16 individual recording sites. The number of recording sites can be changed simply by using the same stub PCB and substituting a ceramic tip with a different configuration. The ceramic-based Glu MEAs were prepared for freely moving recordings first by cleaning the MEA. This was done by dipping the bottom portion of the ceramic electrode tip in filtered, stirred isopropyl alcohol for five minutes. This was followed by a five minute wash with stirred ddH_2O to aid in removing any residues from the recording sites. The Pt recording surfaces were carefully wiped twice with Kimwipes® to further remove any residual particles that may be on the recording sites and would have hindered the adhesion of the enzyme matrix. MEAs were dried for fifteen minutes at 105-115°C to ensure there was no residual water on the sites. Next, the MEAs were coated with Nafion®, cured at 170 ºC for five minutes followed by applying the coating solutions (either containing or not containing GluOx) as described previously.

Chronic Connector and MEA Attachment

In order to attach the chronic connector to the modified MEA for freely moving recordings, connecting wires were prepared by first stripping both ends of 30 AWG varnished copper wire (Radioshack). One end of the copper connecting wire was soldered to a gold-plated socket (Ginder Scientific, Ottawa, ON). The other end of the wire was soldered to the PCB for each of the four corresponding recording sites, using eutectic solder, a low heat soldering iron (200° C) and heat sinks to prevent heat transfer damage to the enzyme matrix on the Pt recording sites (Figure 2.1). The PCB portion of the microelectrode was coated with water proof five-minute epoxy to secure the assembly and protect the interface from moisture. The epoxy was allowed to dry for approximately one hour. The gold-plated socket ends of the reference and microelectrode wires were inserted into a 9 pin miniature connector (Ginder Scientific, Ottawa, ON) so that the sockets were completely encompassed by the connector. The varnished copper wires were tucked around the miniature connector and the MEA tip was carefully

positioned parallel to the miniature connector. Correct positioning of the MEA tip was essential for accurate stereotaxic placement in the brain. Water proof five-minute epoxy was used to secure the paddle and wires to the miniature connector, making sure that the exposed part of the sockets on the end of the connector closest to the microelectrode tip and wires were covered with epoxy to ensure that moisture did not penetrate the pedestal. The completed assembly was allowed to air dry for at least 1 hour.

Microelectrode Array /Cannula Assembly

In order to locally apply small quantities of Glu and other pharmacological agents near the MEA tip, a 26-gauge stainless steel guide cannula with inserted dummy cannula (Plastics One, Roanoke, VA) was attached to the PCB so the tip of the dummy cannula, protruding 1 mm past the guide cannula, was aimed between the four recording sites at a distance of approximately 100 μm away from MEA tip. This was accomplished by attaching modeling clay to the PCB and using the modeling clay to hold the guide cannula steady while it was positioned between the recording sites. Once the guide cannula was properly positioned, it was held more firmly in place by applying melted Sticky Wax (Kerr Corp., Orange, CA) onto the PCB and encasing the modeling clay. Since the MEAs were coated with Nafion® and once they have been soaked the tips had to remain wet to prevent cracking in the exclusion layer, the guide cannula were attached pre-calibration. Local applications of Glu or drug solutions for local pharmacological studies of the CNS were performed through a 33-gauge internal cannula, which protruded 1 mm past the guide cannula. A stainless steel dummy cannula remained in the guide whenever the animal was not in the recording chamber (Figure 2.1).

Electrode Calibration

Pt recording sites on the microelectrodes may respond differently to peroxide and Glu, and therefore must be calibrated *in vitro* prior to chronic implantation to determine standard curves. These calibrations were used to

equate a change in current from the oxidation of peroxide to a proportional change in Glu (analyte) concentration. Calibration also allowed us to determine the individual Pt recording sites sensitivity and selectivity against ascorbic acid, a major interferent in the brain. Constant potential amperometry was performed using a FAST-16 system designed for recording simultaneously from the four-channel microelectrodes with a primary gain of 0.2 nA/V and secondary gain of 10 X generating a final gain of 2 nA/V for all calibrations.

Nafion® coated microelectrode tips were soaked in a solution of 0.05 M phosphate buffered saline (PBS) for at least one hour prior to calibration. The soaking time allowed for better diffusion of analytes through the Nafion® layer as well as activation of the enzyme layer. However, once the Nafion® coated MEA has been wet, it must remain in solution at all times. If the soaked Nafion® coated MEA was allowed to dry, the Nafion® layer would crack, allowing interferents to pass through the exclusion layer, therefore, decreasing the selectivity of the Pt recording sites for Glu.

After soaking the MEA tip for at least one hour, the tip of the modified MEA was placed in a continuously stirred solution of 0.05 M PBS (40 mL; pH 7.4) using a battery operated, portable magnetic stir plate (Barnant Co.). A recirculating water bath (Gaymar Co.) was used to maintain a constant buffer temperature of 37ºC to allow the enzyme layer to function properly and to mimic physiological conditions. The calibrations were operated at a constant applied potential of +0.7 V vs. a Ag/AgCl reference electrode, allowing approximately 15 minutes prior to the addition of calibration solutions for the current to reach a stable baseline. Calibrations were performed by achieving final buffer concentrations of 250 μM ascorbic acid and 20, 40, and 60 μM Glu through additions of aliquots of 20 mM ascorbic acid and 20 mM Glu stock solutions (prepared in ddH_2O) and allowing for stable baseline conditions between each addition. Also, after the final addition of Glu was added, two test substances, 2 mM DA (2 μM, final beaker concentration) and 8.8 mM H_2O_2 (8.8 μM, final beaker concentration) (40 μL additions; made in ddH_2O), were added. The test substances were used to determine the relative response and sensitivity of the

individual Pt recordings sites on each MEA and if needed, could be used as a means to normalize the experimental data. The test substances did not affect the calibration slope, or any calculations derived from the slope (Figure 2.2). Another test substance addition was performed when a new substance was to be used for local or systemic application experiments to ensure that the compound was not electrochemically active on the Pt recording surfaces at +0.7 V. The FAST-16 system software recorded the current for each addition of analyte (Glu), created a calibration curve for each Pt recording site, and stored the slope of this calibration. Selectivity ratios for Glu over ascorbic acid were calculated in addition to the slope (sensitivity), limit of detection (LOD), and linearity (R^2) for MEA Pt recording sites coated with GluOx. Due to the highly reproducible fabrication process of the MEA, Glu responses were extremely linear and were only used if linear regression curves fit with $R^2 \geq 0.99$.

Sensitivity of the MEA corresponded to how well the change in Glu was measured. The slope from the *in vitro* calibration was used to equate a change in current to a change in Glu concentration and can be applied to determine the Glu concentration *in vivo*. The slope was also used to calculate LODs, which were the main criteria used to select microelectrodes. LOD is the limit of detection for the MEA and was defined as the analyte concentration that resulted in an electrode response that was equivalent to 3 times the background noise of the FAST-16 recording system. This was a conservative determination of the lowest detectable change in analyte concentration that cannot be attributed to noise. The LODs for our microelectrodes range from approximately 0.2 to 1.0 μM, depending on the stability of the sites. Our laboratory normally recommends using MEAs with LODs ≤ 1 μM, depending on the expected Glu response, with 0.2 μM being optimal.

Selectivity refers to the ratio of the microelectrodes sensitivity for Glu over interferents, such as AA. Selectivity was determined by dividing the Glu slope by the AA slope. A MEA with a selectivity of 100:1 refers to a 100 μM concentration increase of AA results in an apparent 1 μM concentration increase in Glu, or that the MEA is 99% effective at blocking AA. Selectivity ratios of 100:1 or greater

are ideal, however, selectivity ratios as low as 20:1 were still used and extremely effective since this ratio is not a linear correlation. *In vitro* calibrations showed that slope and LOD values were not significantly different over 7 days (Figures 2.3 and 2.4).

Animal Preparation for Awake Freely Behaving Amperometric Recordings

Male Long Evans or Fischer 344 (Harlan) rats 3-6 months of age at the time of surgery were used for all experiments. Fischer 344 rats weighed 375-450 g, while Long Evans rats weighed 400-600 g at the time of surgery. The animals were group housed in a 12 hour light/dark cycle with free access to food and water in the AAALACI-approved animal resource center at the University of Kentucky. Animals were allowed at least 7 days to acclimate to the environment prior to any experiments. All appropriate animal care (food, water, bedding, cage cleaning, etc.) was performed by the Animal Resource Center staff. There were no procedures involving undue discomfort to the animals. Following surgery, rats were individually housed under the same conditions. Animal care was approved by the University of Kentucky Institutional Animal Care and Use Committee and was in accordance with the *Guide for the Care and Use of Laboratory Animals*.

Electrode implantation

Following a successful calibration of the microelectrode, rats were anesthetized with 2% isoflurane, and placed in a stereotaxic apparatus (Kopf Instruments, Tujunga, CA). Animal body temperature was maintained at 37°C with an isothermal heating pad (Braintree Scientific, Braintree, MA). The animals' eyes were coated with artificial tears (The Buttler Company, Columbus, OH) to help maintain moisture and prevent infection. All surgeries were performed in a Vertical Laminar Flow Workstation (Microzone Corp., Ottawa, ON), which filtered lab air through a HEPA filter. Prior to incision, the skin directly on top of the animals head (between the ears and from just behind the eyes to the neck) was wiped with Betadine solution to keep the incision area clean and to prevent infection. The skin on top of the rat's head was reflected,

making as small an incision as possible. Three small holes were drilled in the skull in the opposite quadrants of where the MEA was implanted for placement of stainless steel skull screws. A fourth hole was drilled contralateral from the recording site for insertion of the Ag/AgCl reference electrode (see above). The animals underwent a 2 mm x 2 mm craniotomy and were implanted with a Glu selective MEA pedestal assembly into the right striatum (AP: +1.0 mm; ML: -2.5 mm; DV: -4.3 mm vs. bregma) or the right prefrontal cortex (AP: +3.2 mm; ML: -0.8 mm, DV: -4.5 mm vs. bregma), based on the coordinates from Paxinos and Watson (2005) with the incisor bar set so that the skull was level (-2.3 mm). Three small stainless steel screws (Small Parts, Inc) were threaded into the skull to serve as anchors and care was taken so that the tip of the screw did not touch the brain (Figure 2.5). The assembly was secured with approximately four layers of dental acrylic (Lang Dental MFG, Wheeling, IL), taking care to cover as much of the MEA assembly as possible. The dental acrylic had a smooth texture and care was taken to remove excess dental acrylic from the fur surface so as not to promote the rat to scratch its head.

Following surgery, rats were placed in their cage and monitored until the rat recovered from anesthesia (rats were usually fully awake within 5-10 minutes after removing from isoflurane). One subcutaneous injection of Rimadyl® (carprofen) sterile injectable solution (10 mg/kg) (Pfizer, New York) was administered immediately following surgery for post-surgery inflammation and pain. Rats were allowed to recover for a minimum of two days prior to initial recordings.

Awake Freely Behaving Recordings

Recording Apparatus

The recording apparatus consisted of a large wooden box with a Plexiglas® insert. The recording headstage consisted of a round miniature connector with 5 connector pins (one connecting each of the four Pt recording sites and one connecting the Ag/AgCl reference electrode). The connector pins lead to the 4 channel low noise potentiostat (Rat Hat 4, Quanteon, LLC,

Nicholasville, KY), which once connected sat as close as possible to the animal in order to minimize noise artifacts. The potentiostat created a potential difference between the microelectrode array and a reference electrode to carryout electrochemical recordings. Connecting wires, encompassed by an insulator, lead to the low torque commutator at the top of the box. The recording assembly hung from the top center of the box from a 12 lead commutator (Airflyte, Bayonne, NJ). This allowed the animal to freely move to all areas of the box. The outputs of the commutator were connected to the FAST-16 system where the electrochemical analog signals generated by oxidation reactions were amplified and then digitized in the FAST-16 microcomputer using a fast A/D-D/A board (National Instruments) (Figure 2.6). In addition, control voltages for amperometric measurements were controlled by the data acquisition board. The digitized second-by-second (1 Hz) representation of the data was then visualized and recorded using the FAST-16 software (Quanteon, LLC, Nicholasville, KY). Recorded files were exported to other Windows™ based applications, such as Excel™, for easier data processing.

Recording protocol

Typical recording sessions involved allowing the rat to freely roam around the recording chamber for ten minutes to acclimate to the surroundings before connecting the pedestal to the potentiostat. Data acquisition was started and the rat underwent a minimum thirty minute acclimation period, or until baseline was stabilized, before an ejection cannula was inserted or animal manipulations/behavior studies were initiated. At this point, resting, or basal, Glu measures were taken. The ejection cannulae were only inserted on days when chemicals needed to be ejected. After the ejection cannula was inserted (connected to a 10 µL Hamilton syringe), another acclimation period of ~ 30 minutes was allowed so that baseline was again established. Following this period, the effects of locally applied Glu, urethane injections (i.p.), or other compounds, or a 5 minute tail-pinch were studied for up to three additional hours. The volumes of locally applied Glu were kept constant at 1 µL.

Following completion of the experiments (after multiple days of recordings), rats were anesthetized with isoflurane and transcardially perfused with 0.9% saline followed by 4% paraformaldehyde. The brain was removed and stored in 4% paraformaldehyde for three days followed by storage in 0.1 M phosphate buffer (10% sucrose) for sectioning and staining to confirm MEA placement and examining possible tissue damage.

Histopathology

Male Long Evans rats between the age of 3 and 6 months at the time of surgery were chronically implanted with pedestal microelectrodes as previously described. Animals were then anesthetized with isoflurane and transcardially perfused after 1, or 3 days, 1, 2, 4, 8, 16, or 24 weeks. The brains were stored as previously described. After rinsing in sucrose, cryostat sections (14 µm) were collected from the area of implantation. The sections were postfixed in acetone for 3 minutes prior to being processed for indirect immunohistochemistry. Antibodies used were raised against glial fibrillary acidic protein (GFAP anti-mouse, diluted 1:400; Chemicon) as a marker for astrocytes and Iba1 (anti-rabbit, diluted 1:1000; Wako Chemicals, Germany), a pan-microglia marker (Imai *et al*., 1996; Ito *et al*., 1998). Incubations were performed for 48 hours at 4°C. After washing, the sections were incubated in Alexa 488 and Alexa 594 secondary antibodies (diluted 1:500, Molecular Probes) for 1 hour at room temperature. Antibodies were diluted in PBS containing 0.3% Triton-X. After additional rinsing the sections were mounted in 90% glycerin in PBS. Double labeling of GFAP and Iba1 were performed in sequence such that each type of antibody was applied one at a time. Sections were evaluated using image analysis and Improvision software. The densities of GFAP and Iba1 immunoreactivities were calculated using NIH image software on binary images and expressed as mean grey density. Mean values from four sections from each brain were analyzed using a one-way ANOVA followed by Tukey's post hoc analyses. All measurements were performed on blind-coded slices.

Drugs and Reagents

All chemicals were used as received unless otherwise stated.

Electrode Preparation and Calibration

Nafion® (5% in a mixture of aliphatic alcohols and water), BSA, glutaraldehyde, ascorbate, Glu monosodium salt, and 3-hydroxytrypamine HCl (dopamine, DA) were obtained from Sigma-Aldrich Corp. (St. Louis, MO). GluOx was purchased from Seikagaku America, Inc. (East Falmouth, MA). The 3% H_2O_2 solution was purchased from a local retailer. 0.05 M PBS was created using sodium chloride, sodium phosphate monobasic, and sodium phosphate dibasic obtained from Fisher Scientific. The DA stock solution was prepared in 1% perchloric acid for prolonged stability. Glutaraldehyde was stored at -20 ºC. Special care was taken to ensure that the stock Nafion®, BSA, and glutaraldehyde solutions were only used for 1-2 months. All solutions were prepared using distilled water, which was de-ionized using a Millipore® water treatment system.

Intracranial Ejection

All solutions administered intracranially were prepared in 0.9% saline solution, adjusted to pH 7.4, and filtered prior to use through a sterile syringe filter (0.22 μm pore size, Costar, Corning, NY). All components of the 5 mM Glu, 0.9% saline solution, 4% paraformaldehyde, 0.1 M PB with 10% sucrose, were purchased from Fisher Scientific. Tetrodotoxin (TTX) was obtained from Sigma-Aldrich Corp. (St. Louis, MO, USA). (S)-4-carboxyphenylglycine (CPG) was obtained from Tocris Cookson Inc. (Ellisville, MO). mGluR agonist (LY379268) and mGluR antagonist (LY341495) were obtained from Eli Lilly & Co. (Indianapolis, Indiana).

Anesthetics and Special Use Drugs and Chemicals

Isoflurane, used as anesthetic for recovery surgery and perfusions, was obtained from Baxter Pharmaceutical. Rimadyl®, used for post-operative pain and inflammation, was obtained from Pfizer.

Data Analysis

The FAST-16 recording system saved amperometric data, time, and ejection data marks for all four recording channels. Unless otherwise noted, calibration data, in conjunction with a modified spreadsheet program, was used to determine parameters for the signal differences recorded between data marks. Measures derived from the data file included maximum amplitude, measured from baseline to the peak concentration of the signal, the time in seconds, or duration, of the signal, and t_{80}, or the time it takes for 80% of the signal to decay. Unless otherwise noted, ejection (local application) volumes remained constant at 1 µL. Additionally, for stress-evoked Glu measures, area under the curve was calculated from the beginning of the tail pinch until the Glu levels returned to baseline measures. An analysis of variance (ANOVA) with a Tukey's post hoc test was used to analyze the significance of all data. Significance was defined as $p < 0.05$.

Copyright © Erin Cathleen Rutherford 2007

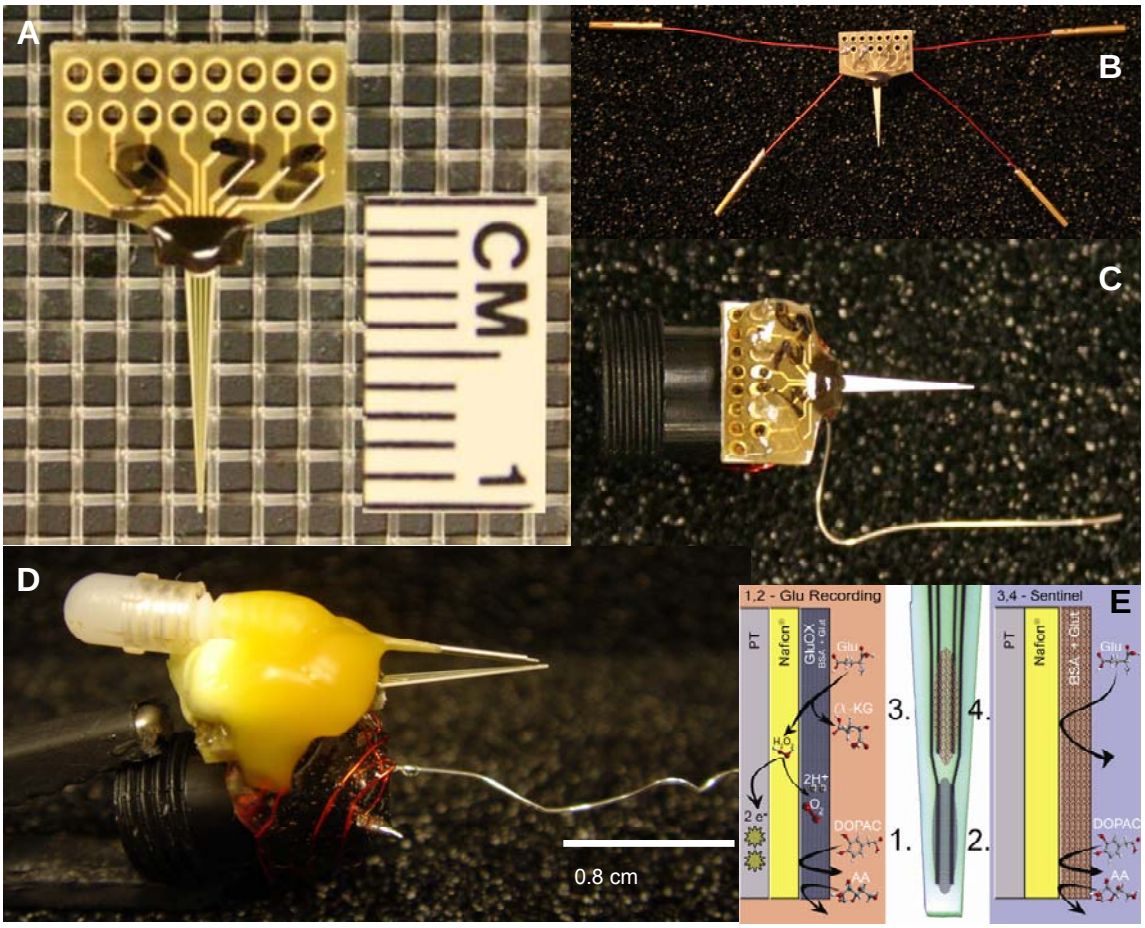

Figure 2.1: Freely Moving Microelectrode Design
A) Stub PCB with attached ceramic tip, or the stub MEA. B) Stub MEA with connecting copper soldered to stub at the positions for channels 1, 2, 3, and 4. Gold-plated sockets are attached to the ends of the copper wire. Only the varnished section of the copper wire is showing. C) Photograph of the pedestal MEA consisting of the stub MEA, Ag/AgCl reference electrode, and miniature connector. Epoxy was used to mount the stub MEA on the miniature connector. D) Pedestal MEA with attached guide cannula. Dummy cannula is inserted in the guide cannula and protrudes past the guide cannula. The guide cannula is held in place with sticky wax. E) Illustration showing a Nafion® coated self-referencing MEA. Pt recording sites are 333 x 15 µm with 20 µm/100 µm spacing. E1,2) Glu recording sites. E3,4) Self-referencing sites. Adapted from Rutherford *et al.*, 2007.

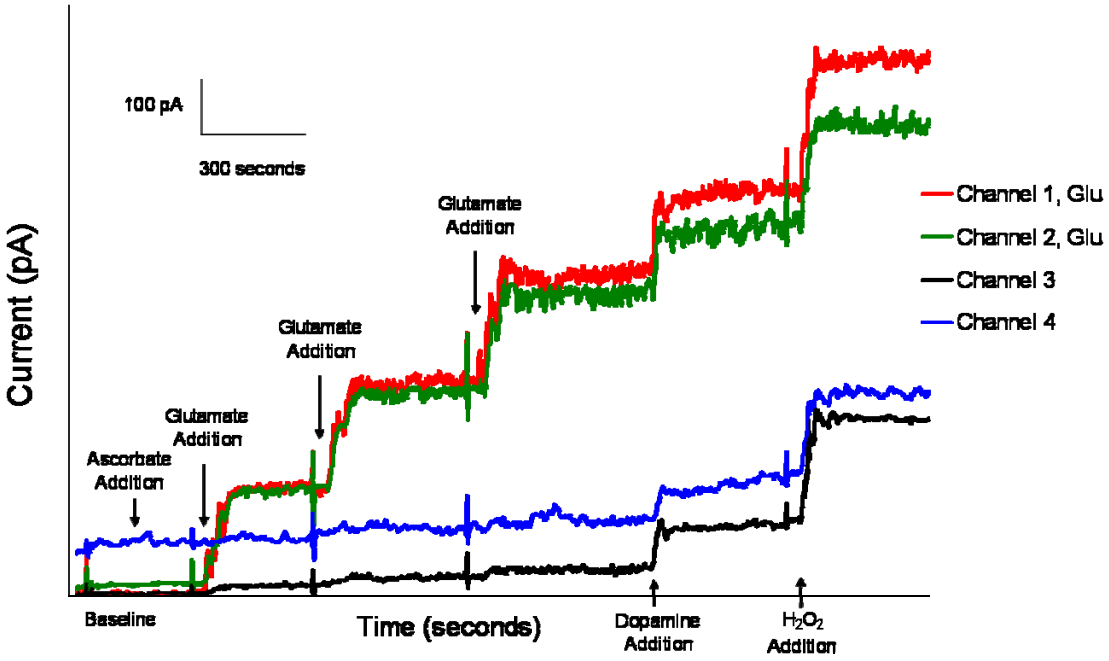

Figure 2.2: L-Glutamate Self-Referencing Microelectrode Array Calibration
Representative tracing of a typical calibration of a self-referencing Glu selective pedestal MEA. A single 500 µL addition of 20 mM ascorbate shows little to no change in current. This was followed by three 40 µL additions of 20 mM Glu yielding a linear increase in Glu response on the GluOx coated sites (channels 1 and 2) but not the self-referencing sites (channels 3 and 4). DA (2 mM) and H_2O_2 (8.8 mM) were added (40 µL) as test substances and changes in current were measured on all four recording sites.

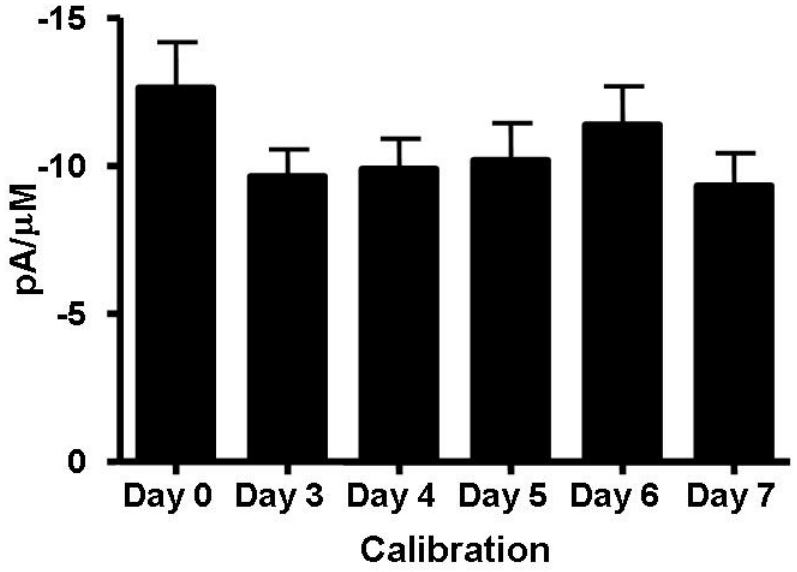

Figure 2.3: Slope Values for *In Vitro* Calibrations
In vitro calibrations were performed on MEAs to determine their slope values over days. MEAs were Nafion® coated and continuously soaked in 0.05 M PBS. Slope values were not significantly different over 7 days of calibration.

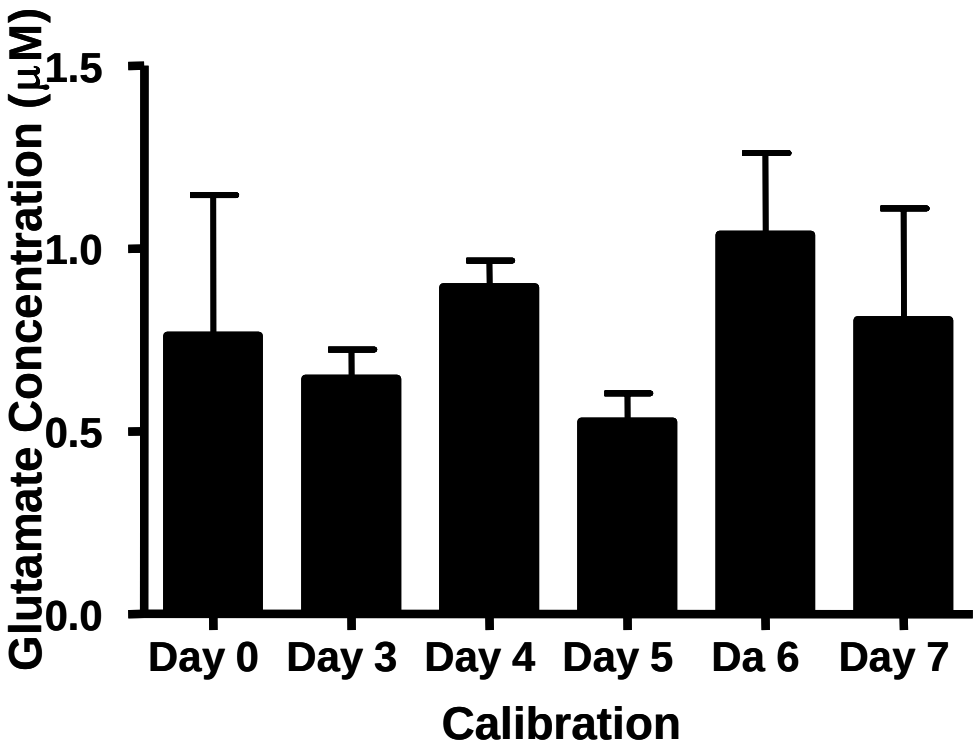

Figure 2.4: Limit of Detection Values for *In Vitro* Calibrations
In vitro calibrations were performed on MEAs to determine their LOD values over days. MEAs were Nafion® coated and continuously soaked in 0.05 M PBS. LOD values were not significantly different over 7 day calibrations.

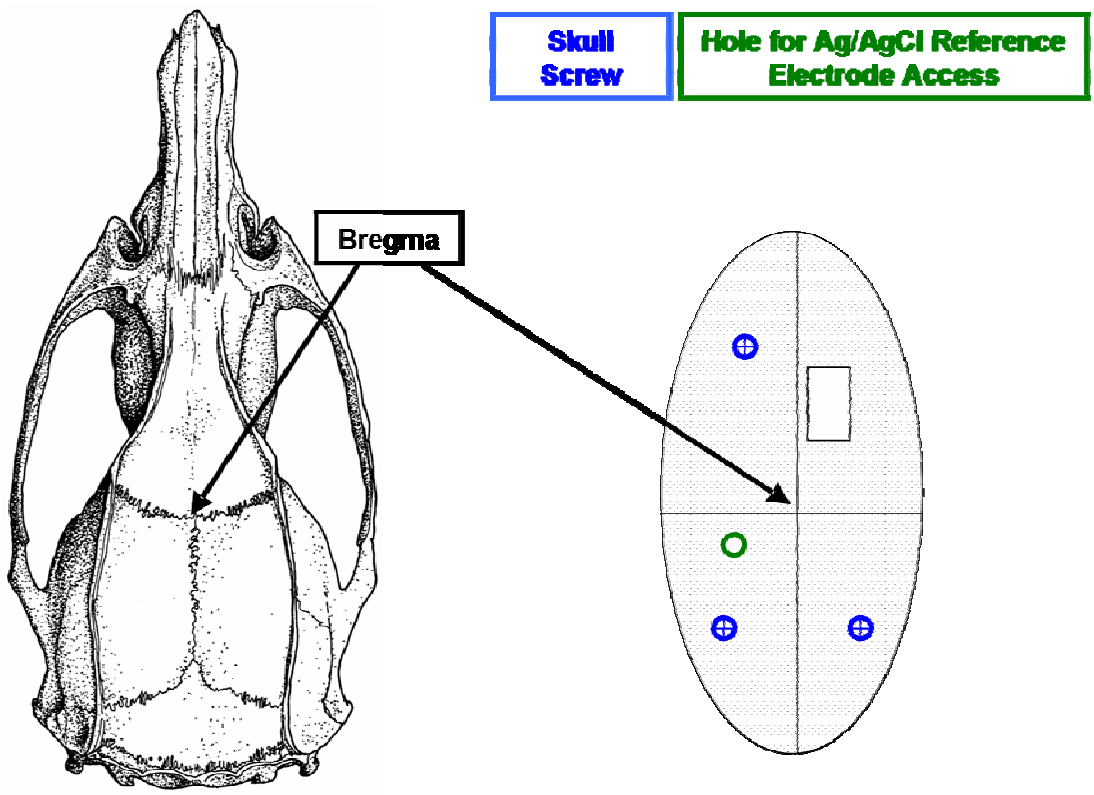

*Adapted from Paxinos and Watson, 2005

Figure 2.5: Microelectrode Implantation Surgery
Drawing of rat skull (left) and schematic of pedestal MEA implantation surgery in the right PFC of a Long Evans rat (right). Three skull screws were threaded into the skull (blue), a hole was drilled for placement of the reference electrode (green), a separate larger hole in the shape of a rectangle was drilled for MEA placement and the skull section was removed. Adapted from Paxinos and Watson, 2005.

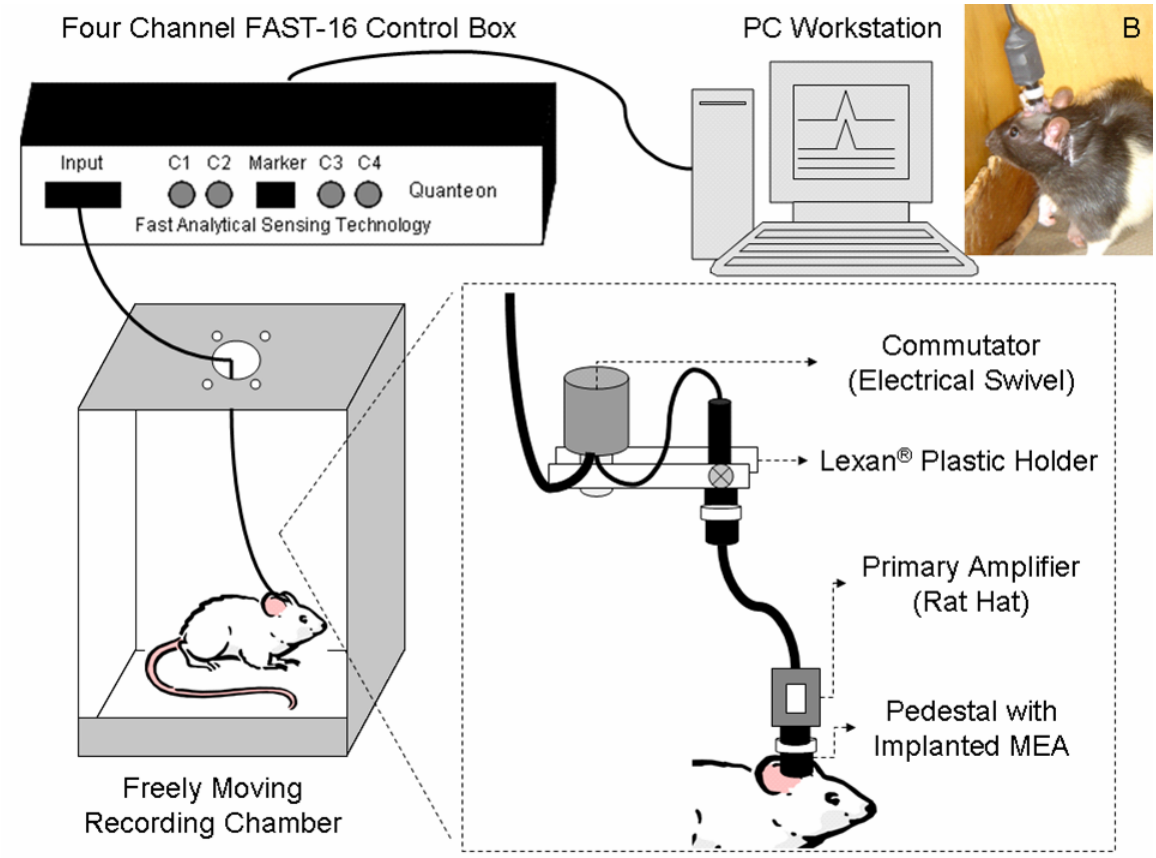

Figure 2.6: Schematic Diagram of the *In Vivo* Freely Moving Recording System
The pedestal MEA is implanted in to the rat brain. When the MEA is connected to the FAST-16 recording system, the signal travels from the implanted MEA to the pre-amplifier rat hat. The signal then travels through the commutator, which is located at the top of the recording chamber, and finally in to the FAST-16 control box and PC workstation. The commutator allows for the connecting wires to freely rotate as the rat moves throughout the recording chamber without hindrance. Gold sockets from the miniamplifier/rat hat connect to the gold sockets embedded in the miniature connector of the pedestal to allow for continuous recordings. Dental acrylic surrounds the implanted pedestal apparatus. The rat is able to move to all areas of the recording chamber, performing everyday activities while Glu is simultaneously recorded from the CNS of the rat. Rutherford *et al*., 2007.

Chapter Three: Resting L-Glutamate Measures in Awake Male Fischer 344 and Long Evans Rats

Introduction

Resting Glu measures in awake animals have been established using microdialysis; however, this method may not be capable of detecting subtle second-by-second changes in neuronal Glu and the origin of the glutamatergic pool being sampled is controversial. Additionally, resting levels may be altered through a variety of mechanisms, including the effects of anesthesia. Anesthetics, including urethane, have been shown to decrease neuronal activity (Albrecht and Davidowa, 1989; Dyer and Rigdon, 1987; Girman *et al*., 1999) while maintaining excitatory Glu-mediated synaptic signal transmission (Sceniak and MacIver, 2006). More specifically, previous studies have reported on reduced tonic Glu levels in anesthetized preparations (Liachenko *et al*., 1998, 1999). Urethane, the anesthetic currently used in our laboratory for acute recordings, was initially used because it was believed to have minimal affects on DA signaling, also of interest to our laboratory. However, little is known as to how urethane affects glutamatergic neurotransmission. There is precedence that anesthetics affect Glu neurotransmission *in vitro;* isoflurane was shown to decrease activation of both NMDA and non-NMDA glutamatergic receptors as well as reversibly reduce field potentials (Ranft *et al*., 2004).

Little is known about potential mechanisms involved in regulating resting Glu and Glu release, such as the role inhibitory autoreceptors play in Glu signaling. There is evidence that supports the involvement of Glu receptors, specifically mGluRs. Some mGluRs have been shown to act as inhibitory presynaptic autoreceptors (groups II and III) while others may be excitatory (group I) (Schoepp, 2001). Additional glutamatergic factors that may be involved in regulating resting extracellular Glu levels are iGluRs, Glu transporters, and the cystine-Glu exchanger, all of which are commonly present at glutamatergic synapses.

This study was aimed at determining resting Glu levels and the factors that influence these levels in the brain of awake behaving rats. In these studies,

we examined the differences in resting Glu in the striatum and PFC of two different rat strains, Fischer 344 and Long Evans rats. Additionally, we determined the effect of anesthesia on resting Glu levels and made direct comparisons between resting Glu in the striatum and PFC of the awake and anesthetized rats using an amperometric recording technique. We also examined the influences of TTX, a sodium channel blocker, mGluR group II agonist and antagonist, and a cystine-Glu exchanger blocker on resting Glu levels.

Methods

Animals were housed in the conditions described in Chapter Two. Male Fischer 344 and Long Evans rats were between three and six months of age at the time of implantation surgery. Surgical procedures, MEA implantation in the striatum and PFC, and recording procedures followed those outlined in Chapter Two. Briefly, male Fischer 344 and Long Evans rats were implanted either in the striatum or PFC under isoflurane anesthesia and allowed to recover for two days prior to recording sessions. On recording days, rats were allowed approximately ten minutes to acclimate to the recording chamber prior to establishing a connection between the implanted MEA and the FAST-16 recording system. Once a connection was established and recordings started, a sampling rate of 1 Hz was maintained throughout the recording session. After recording for approximately 30 minutes, or longer if needed, and baseline was established, a 15 second interval was used to determine resting Glu levels. Recordings continued for other experimental use, such as, local application of Glu. Data analysis involved an ANOVA with a Tukey's post hoc test. Significance was determined at $p<0.05$.

Results

Resting Glu levels in awake rats were measured in the striatum and PFC of Fischer 344 and Long Evans rats using the self-referencing technique described above. Briefly, the self-referencing site currents were subtracted from

the Glu recording site currents during unstimulated recordings (Figure 3.1). We observed a highly significant difference in resting levels of Glu in the PFC (37.4 ± 3.0 μM Glu; n=7) of Long Evans rats compared to resting measures in the striatum (5.8 ± 0.4 μM Glu; n=7) of Long Evans rats and measures in the striatum (10.4 ± 0.7 μM Glu; n=3) and PFC (9.8 ± 0.7 μM Glu; n=7) of Fischer 344 rats (Figure 3.2). No other significance difference was observed in resting Glu levels in the striatum and PFC in the Fischer 344 and Long Evans rats. A comparison with microdialysis in the awake rat on resting Glu levels in the striatum and PFC is shown in Table 3.1.

After verifying that our MEA recording system was able to reliably measure Glu in chronically implanted and behaving rats over multiple days (Figure 3.3), we wanted to determine the effects of anesthesia, specifically urethane, on resting Glu levels in the brain. After verifying that the MEA was functioning properly by locally applying Glu (see Chapter 4), the rats were administered urethane (1.25 mg/kg, i.p.) as per our usual protocols for anesthetizing rats in our laboratory for acute *in vivo* amperometry measures (Day *et al*., 2006; Nickell *et al*., 2005). In this study, the resting Glu levels significantly decreased by an average of 58% (resting measures of 35.3 ± 2.5 μM dropped to 14.9 ± 3.1 μM; n=4; $p<.001$) in the 2.5 hours following the initial urethane injection (Figure 3.4). Additionally, resting Glu levels in anesthetized Fischer 344 rat striatum (1.4 ± 0.2 μM) and frontal cortex (1.6 ± 0.3 μM) were significantly decreased compared to resting Glu levels in the awake Fischer 344 rat striatum and PFC (Figure 3.5) as measured by enzyme-based amperometry (anesthetized data taken from Day *et al*., 2006).

The effect of TTX was studied in the PFC of awake male Long Evans rats. TTX was determined to decrease resting Glu levels in the PFC of Long Evans rats on average approximately 25 % (Figure 3.6). However, TTX did not completely diminish the resting Glu levels, as was observed in recordings in the anesthetized rat (Day *et al*., 2006). These results showed that resting Glu levels in the PFC of awake Long Evans rats were at least partially neuronally derived. However, the resting Glu levels must also have other contributing components.

For this reason, we wanted to determine the effects of (S)-4-carboxyphenylglycine (CPG) on resting Glu levels. CPG has been reported to be a cystine-Glu exchanger blocker (Baker *et al*., 2002; Melendez *et al*., 2005) as well as a competitive group I mGluR antagonist/weak group II mGluR agonist (Tocris Bioscience, Ellisville, MO). This would suggest that when locally applying CPG, there should be an observed decrease in resting Glu levels. However, upon local application of CPG in the PFC of awake Long Evans rats, we observed a rapid, robust increase in Glu with the spike lasting approximately 2 minutes, followed by a prolonged slight decrease in Glu levels, lasting approximately 15 minutes (Figure 3.7). Additionally, group II mGluR agonist and antagonist were examined for their effect on resting Glu levels. The agonist (LY379268) decreased resting Glu levels 3.0 ± 0.4 μM below basal levels while the antagonist (LY341495) increased resting Glu levels 13.8 ± 4.7 μM above basal levels (Figures 3.8 and 3.9).

Discussion

The current self-referencing recording techniques with MEAs can be used to effectively and reliably measure resting (tonic) Glu levels. Our data show that there was a significant difference in resting Glu levels between the striatum and PFC in Long Evans rats as well as between the PFC of Ficher 344 and Long Evans rats. Direct comparisons to previous studies performed in our laboratory using the same method for detecting Glu have reported that the resting Glu levels in the frontal cortex of the anesthetized Fischer 344 rats were 1.6 ± 0.3 μM and in the striatum they were 1.4 ± 0.2 μM (Day, *et al*., 2006), or on average approximately 84% to 87% decreased compared to our freely moving Fischer 344 recordings. The differences observed in resting Glu between the anesthetized and awake rat were not surprising. Studies using microdialysis report resting Glu in the anesthetized rat striatum to be approximately 1.3 – 2.7 μM when sampling 20-24 seconds, which is comparable to our value of 1.4 μM (Cellar, *et al.,* 2005). However, in an awake rat model using microdialysis measures in the striatum, resting Glu levels were reported to be 0.202-0.82 μM

when sampling every 15-20 minutes (Di Cara *et al.,* 2001; Segovia *et al.,* 2001). Additionally, 10 to 20 minute microdialysis measures of resting Glu in the frontal cortex of the awake rat ranged between ~2 μM and ~9 μM (Baotell *et al.*, 1995; Rocha *et al*., 1996; Table 3.1). Resting Glu discrepancies using microdialysis may be explained by the sampling time and method, the extent of damage, and the origin of the Glu pool being sampled. In addition, our faster sampling rates coupled with decreased tissue damage may have contributed to the observed higher resting Glu levels in the awake rat. Westerink's group (Oldenziel *et al*., 2006a) has also reported an elevated resting Glu levels (18.2 ± 9.3 μM) in the striatum of anesthetized rats using an enzyme-based hydrogel-coated microsensor with an osmium-containing redox polymer. However, previous studies using redox hydrogel-coated enzyme-based Glu biosensors were limited by their response time of 8-10 seconds (Belay *et al*., 1998; Oldenziel *et al*., 2006a; Oldenziel *et al*., 2006b).

There was no significant difference observed in resting Glu levels between the striatum and PFC of Fischer 344 rats. This finding was similar to the lack of significant difference seen by Day *et al*. (2006) between the striatum and frontal cortex in anesthetized Fischer 344 rats. However, there remains an 84-87% increase observed in the current awake Fischer 344 striatum and PFC studies compared to those observed in the anesthetized Fisher 344 rats by Day *et al*. (2006). The biggest contributor to the increased resting Glu levels in the awake animal model is most likely due to the system being relieved from the suppressive effects caused by anesthesia.

We hypothesized that observed differences in resting levels of Glu between the awake and anesthetized animals using our enzyme-based MEAs were largely due to an effect of the anesthetic (urethane) on resting Glu levels. We tested the effects of urethane on resting Glu by administering urethane to freely behaving rats using the same protocols used in anesthetized studies. Our freely moving studies in the PFC showed a 58% decrease in resting Glu levels following urethane dosing. The point at which there is a 58% decrease in Glu levels was the time point at which surgery would begin for typical anesthetized

recordings. However, typical anesthetized recordings in our studies would occur following approximately 0.5-3 hours additional time allowing for a deeper plane of surgical anesthesia. These data show that anesthetics affected resting Glu levels in the rat brain and contributed to the previous poor estimates of resting Glu levels.

In anesthetized animals, TTX diminished resting Glu by approximately 100% (Day *et al*., 2006), whereas in the awake animals, TTX decreased resting Glu by approximately 25%. The current data supplemented with work in the anesthetized animal by Day *et al* (2006) suggests that, while both the anesthetized and awake animal models exhibit resting Glu levels that are at least in part sodium channel-dependent as shown by the TTX data, anesthesia may block or inhibit other pools of Glu that contribute to resting levels resulting in diminished resting Glu. Additionally, the awake rat may have the capability to better clear TTX from the extracellular space compared to the anesthetized rat.

Since, in the awake rat model, urethane anesthesia was observed to decrease resting Glu levels by 58% and TTX decreased resting levels 25% in the PFC, there must still be other contributors to resting Glu. One possible mechanism contributing to resting Glu levels could be group II mGluR, which act as inhibitory autoreceptors. This suggested that a mGluR group II agonist acting presynaptically would actually have an inhibitory effect on Glu release into the synaptic cleft. The mGluR group II agonist (LY379268) was shown to decrease resting Glu levels by approximately 8 % in the PFC of Long Evans rats, supporting the idea that there may still be other mechanisms affecting extracellular Glu levels.

Another mechanism proposed to regulate resting Glu levels was the cystine-Glu exchanger (Baker *et al*., 2002; Melendez *et al*., 2005). This exchanger is located on glial cells and acts via uptake of cystine into the glia cells coupled with the release of Glu into the extracellular space. CPG is thought to act by blocking the cystine-Glu exchanger. As such, a decrease in extracellular Glu would be expected when CPG was applied. Additionally, Tocris Bioscience reported CPG as a mGluR group I competitive antagonist and a weak mGluR

group II agonist, which when acting presynaptically on Glutamatergic neurons should induce a decrease in extracellular Glu. However, we observed an unexpected initial increase in Glu. The increase peaked within seconds at approximately 20 μM above resting Glu levels and the entire duration lasted approximately two minutes, and therefore, may not have been detected, or the response may have been muted, in previous microdialysis studies. One explanation for the increase in Glu may be because the group II mGluR also resides on GABAergic neurons, and act to inhibit GABA release. If this inhibitory action on GABA was increased via an mGluR group II agonist, it could lead to a decrease on the GABAergic inhibition on glutamatergic neurons. Following the initial increase in Glu there was a prolonged decrease that averaged approximately 4 μM below resting Glu levels and lasted approximately 15 minutes which was most likely the decrease observed in previous microdialysis studies. A summary of the approximate decreases observed in resting Glu levels due to urethane, TTX, CPG and LY379268 can be seen in Table 3.2.

Taken together, the data show that while resting Glu levels remained consistent over multiple days within a given brain region, there were differences between brain regions as well as rat strains. We also determined that the Glu pool sampled using our technique is at least partially neuronally derived and that there are many factors located throughout the synapse that may influence Glu levels, including mGluRs and the cystine-Glu exchanger. Furthermore, our results show that resting Glu levels were significantly decreased by the anesthetic urethane, promoting a need for studies in the awake, freely behaving animal model to have a more accurate knowledge about neurotransmitter function.

Copyright © Erin Cathleen Rutherford

Table 3.1: Resting L-Glutamate Levels in Awake Rats as Measured with Microdialysis or Enzyme-Based Amperometry

	Resting Glu Concentration	Technique	Rat Strain	Citation
Striatum	0.274 ± 0.072 μM	microdialysis	Wistar	Di Cara *et al.*, 2001 *J. Neurochem.*
	0.64 ± 0.18 μM	microdialysis	Wistar	Segovia *et al.*, 2001 *Neurochem. Res.*
	10.4 ± 0.7 μM	enzyme-based amperometry	Fischer 344	Rutherford *et al*. manuscript in preparation
	5.8 ± 0.4 μM	enzyme-based amperometry	Long Evans	Rutherford *et al*. manuscript in preparation
Frontal Cortex	~8 μM	microdialysis	Wistar	Rocha *et al*., 1996 *Epilepsy Res.*
	~2 μM	microdialysis	Sprague-Dawley	Boatell *et al., 1995 J. Neurochem.*
	9.8 ± 0.7 μM	enzyme-based amperometry	Fischer 344	Rutherford *et al*. manuscript in preparation
	37.4 ± 3.0 μM	enzyme-based amperometry	Long Evans	Rutherford *et al*. manuscript in preparation

Table 3.2: Effects of Application of Urethane, TTX, CPG or LY379268 on Resting L-Glutamate Levels

Substance Tested	Decrease from Resting Glu (%)
Urethane	~58
TTX	~25
CPG	~11
LY379268	~8

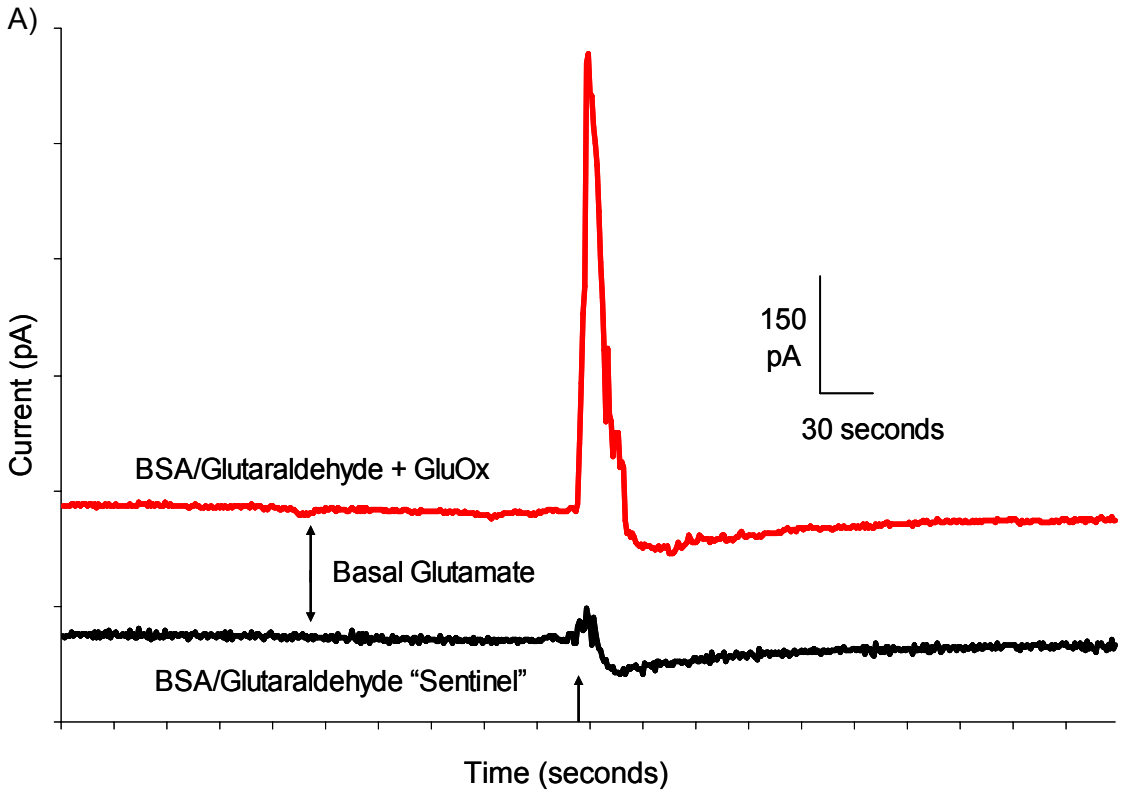

Figure 3.1: Determination of Resting L-Glutamate Levels
Representative tracing of GluOx coated recording site (red) and sentinel, or self-referencing site (black). The difference between the GluOx and sentinel baselines is an indication of resting (basal) Glu. Glu (5 mM, 1 µL) was locally applied (indicated by arrow) and detected using a self-referencing MEA. Taken from Rutherford *et al.*, 2007.

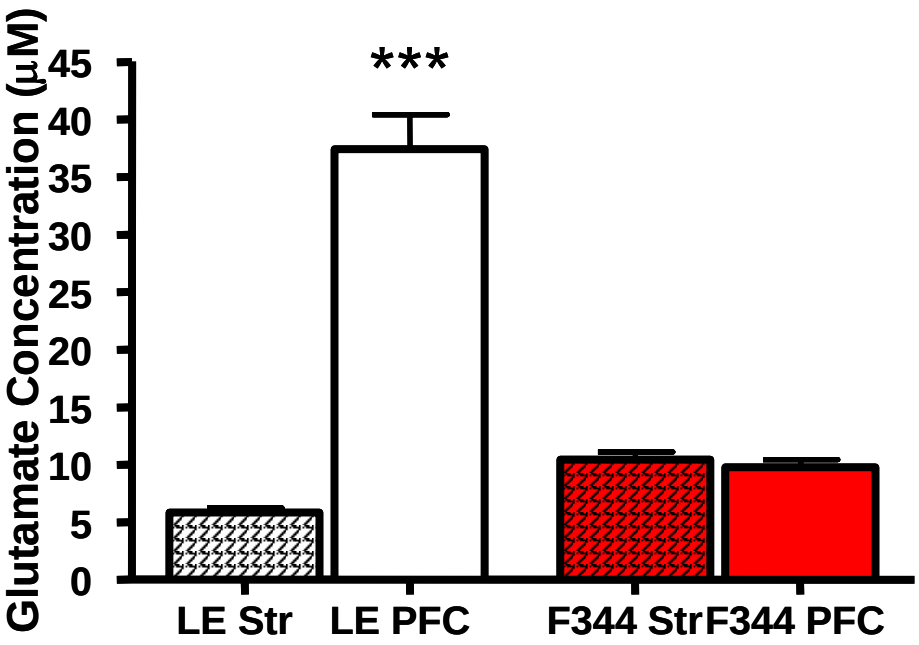

Figure 3.2: Resting L-Glutamate Levels in the Striatum and Prefrontal Cortex of Fischer 344 and Long Evans Rats

Resting Glu levels were measured in the striatum and PFC of Fischer 344 and Long Evans rats. The striatum of Long Evans rats and the striatum and PFC of Fischer 344 rats were significant compared to the PFC of Long Evans rats (***$p<0.001$).

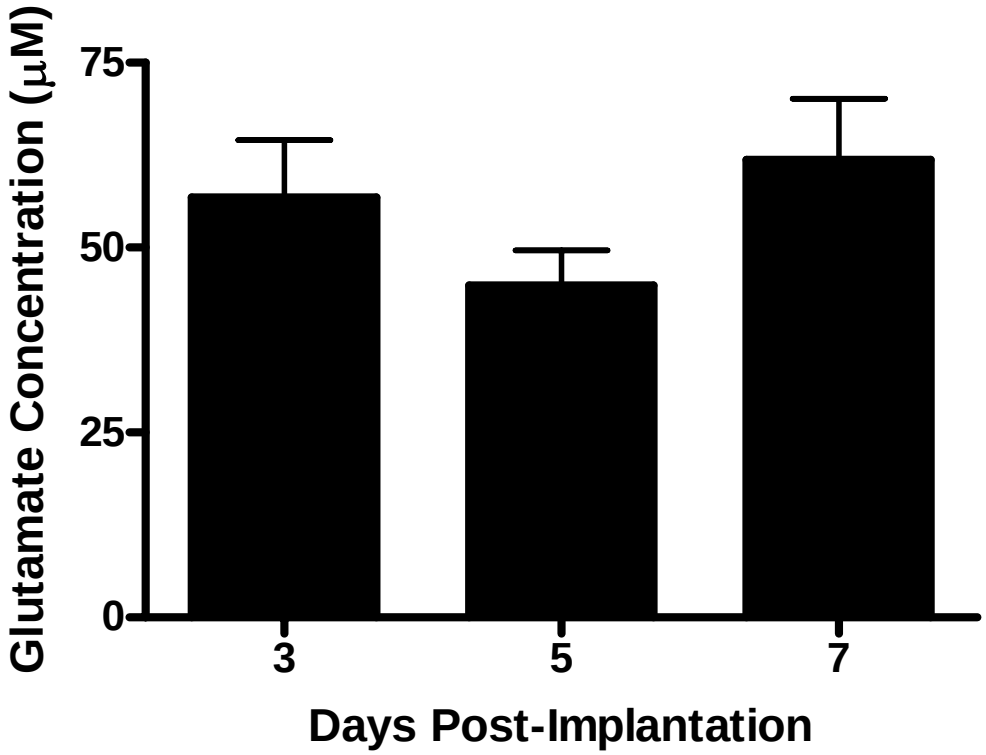

Figure 3.3: Resting L-Glutamate Levels in the Prefrontal Cortex of Awake Long Evans Rats
Resting Glu levels were recorded on days 3, 5, and 7 post-implantation in the PFC of freely behaving Long Evans rats using the self-referencing recording technique (n=7). Resting Glu levels were consistent up to one week post-implantation.

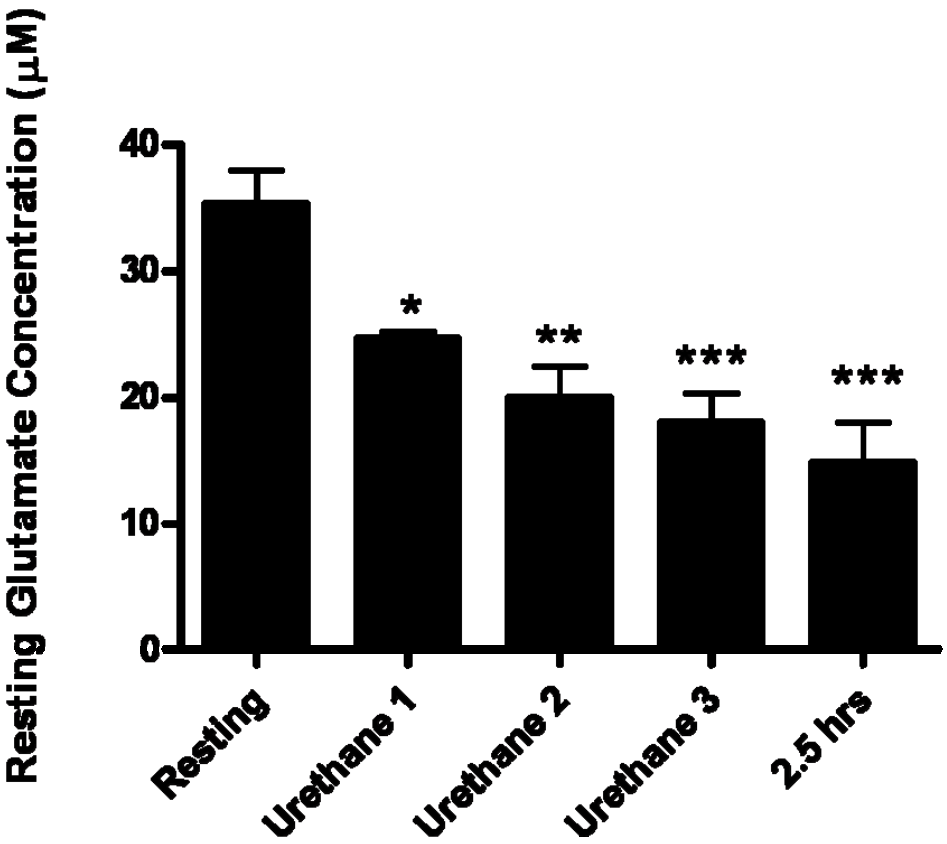

Figure 3.4: Effects of Urethane on Resting L-Glutamate Levels in the Prefrontal Cortex of Long Evans Rats

Resting Glu levels were continuously measured in the PFC of Long Evans rats. Rats were anesthetized during recordings with urethane (3 i.p. injections, 25 minutes apart, 1.25 g/kg total). Resting Glu levels decreased 58% over 2.5 hours (n=4; *p<0.05; **p<0.01; ***p<0.001). Taken from Rutherford *et al*. 2007.

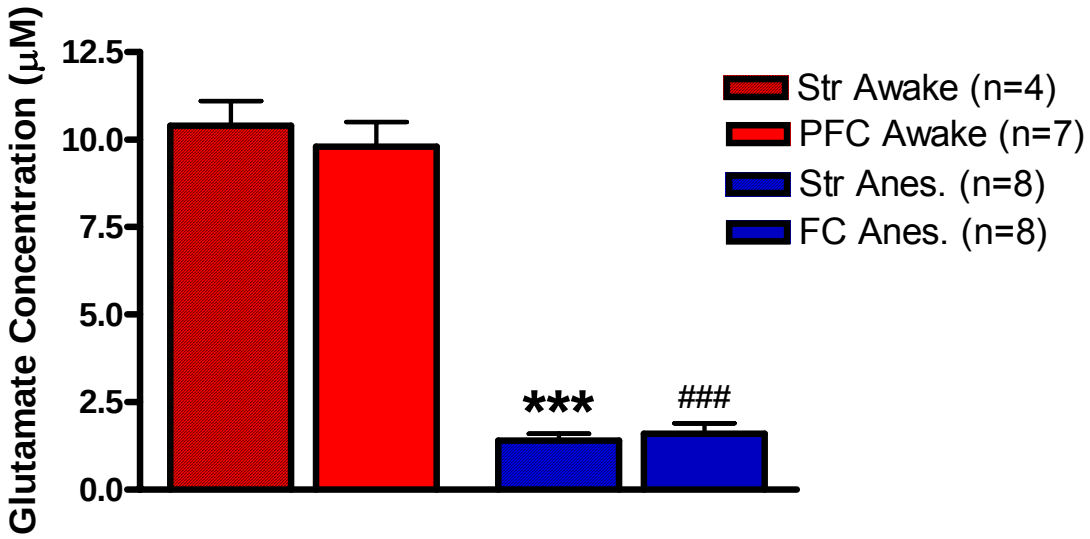

Figure 3.5: Resting L-Glutamate Levels as Measured by Enzyme-Based Microelectrode Arrays in Fischer 344 Rats

Resting Glu levels in the striatum and PFC of awake (red) and anesthetized (blue) Fischer 344 rats using the same enzyme-based self-referencing MEA recording technique (***$p<0.001$ vs. Str Awake; $^{###}p<0.001$ vs. PFC Awake). Anesthetized data was taken from Day *et al.*, 2006.

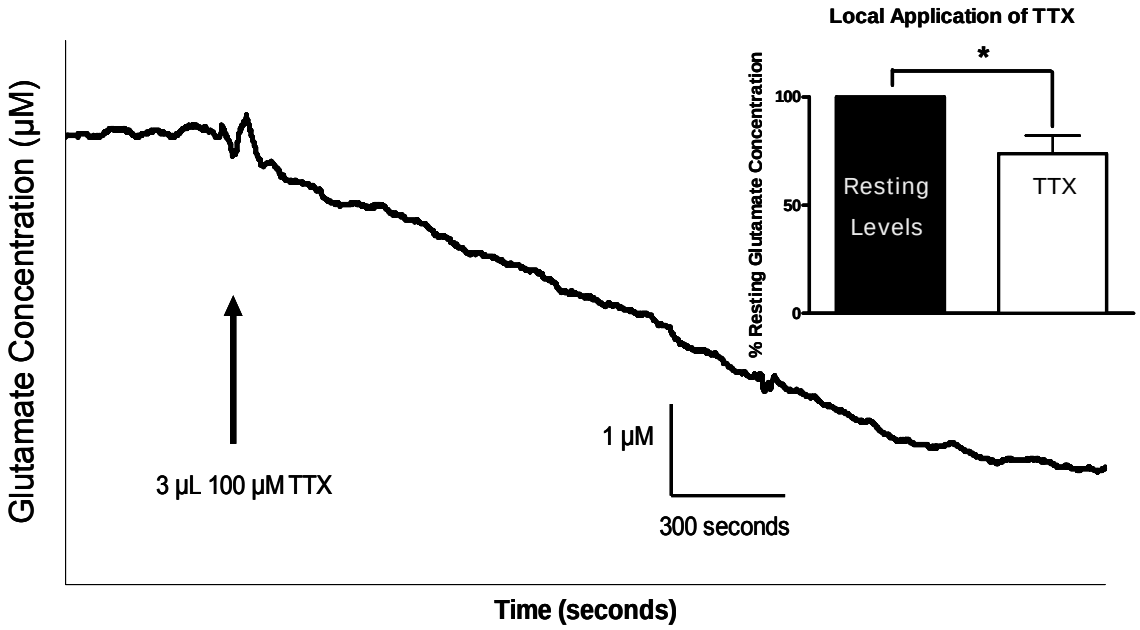

Figure 3.6: Effects of Tetrodotoxin on Resting L-Glutamate Levels in the Prefrontal Cortex of Long Evans Rats

Resting Glu levels were continuously measured in the PFC of Long Evans rats. TTX (100 µM, 3 µL) was locally applied (indicated by arrow). Resting Glu levels decreased ~ 25% as indicated by the inset (n=4; *p<0.05).

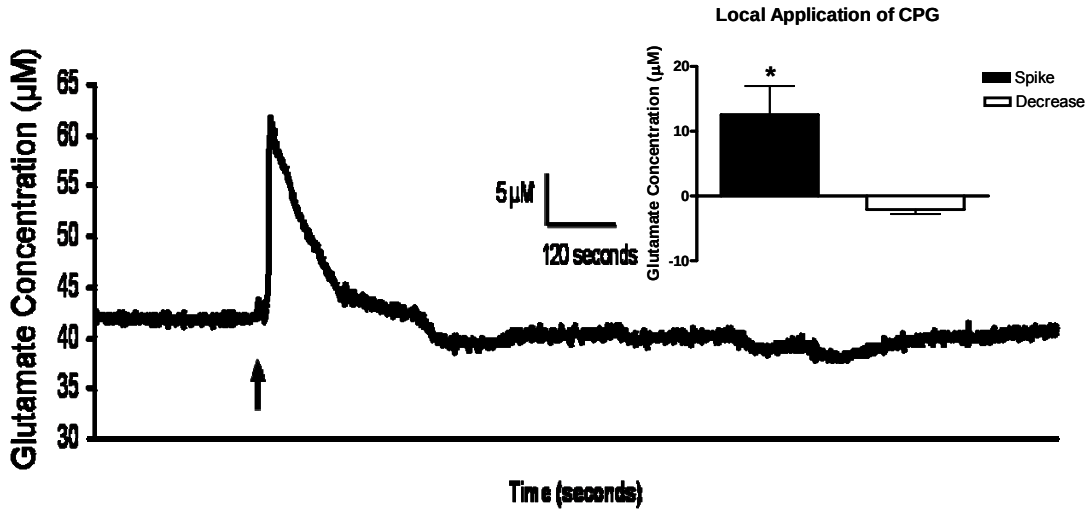

Figure 3.7: Effects of (S)-4-Carboxyphenylglycine on L-Glutamate in the Prefrontal Cortex of Long Evans Rats

Glu levels were altered due to local application of CPG (50 μM, 3 μL). There was an initial rapid increase in Glu followed by a prolonged decrease in Glu. The increase in Glu was significantly elevated over resting Glu levels (~12 μM; n=4; *$p<0.05$).

$mGluR_{2/3}$

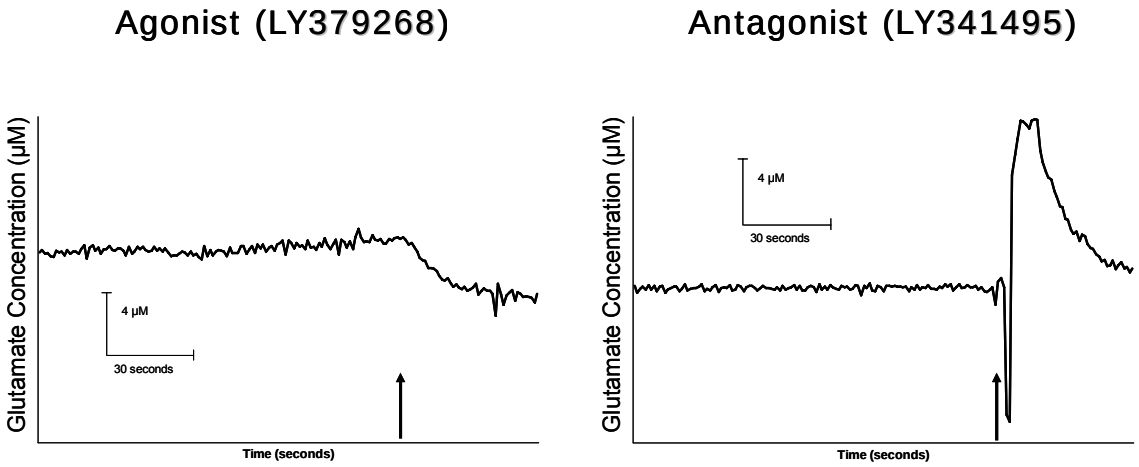

Figure 3.8: Typical Changes in L-Glutamate with Local Application of a mGluR Agonist and Antagonist in the Prefrontal Cortex of Long Evans Rats
Representative tracings of resting Glu levels continuously recorded in the PFC of Long Evans rats. mGluR agonist (LY379268) and antagonist (LY341495) were locally applied (100 μM, 3 μL, as indicated by arrows).

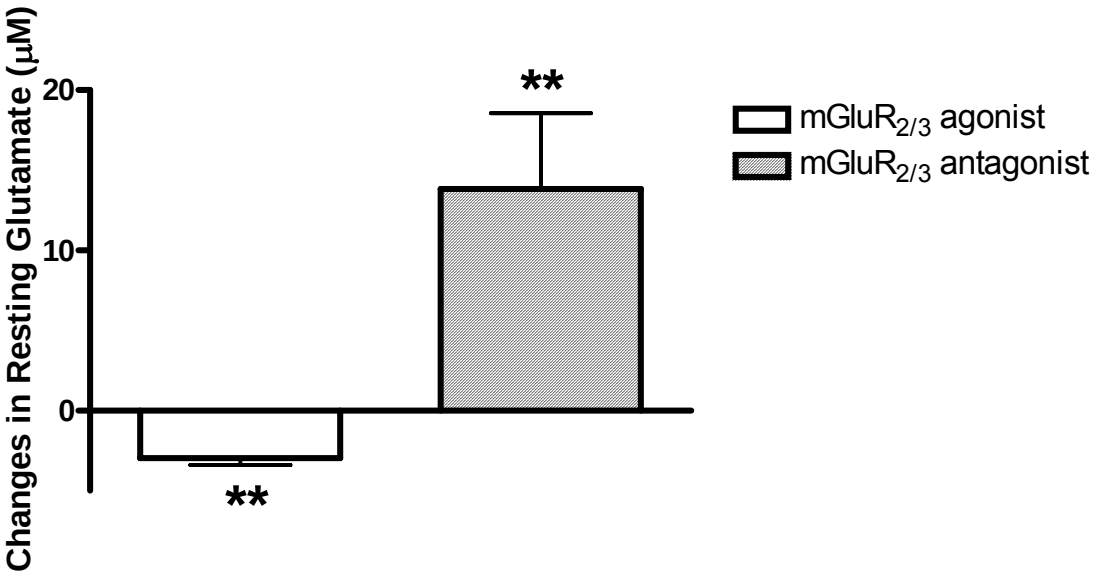

Figure 3.9: Effects of mGluR Agonist and Antagonist on L-Glutamate Levels in the Prefrontal Cortex of Long Evans Rats

$mGluR_{2/3}$ agonist (LY379268) and antagonist (LY341495) were locally applied (100 μM, 3 μL). Resting Glu levels were altered due to local applications of $mGluR_{2/3}$ agonist and antagonist. The agonist decreased resting Glu levels by ~2 μM, while the antagonist increased resting Glu levels ~12 μM (n=4; **p<0.01 vs. resting Glu levels).

Chapter Four: Do Measures of Exogenous Glutamate Change Over Time, Between Brain Regions, and Between Rat Strains in Awake Rats?

Introduction

Many similarities exist between rat strains as to their basic neuronal circuitry. The PFC is thought to be involved in executive functions, such as cognition, and the striatum is involved with motor function in both the Fischer 344 and the Long Evans rats. However, there are also many difference between rat strains. The Fischer 344 rat has been used primarily in age-related studies, while the Long Evans rat is used primarily in behavior-related studies. Another major difference between the strains is the Fischer 344 rat is inbred and albino, while the Long Evans rat is outbred and pigmented.

The neuronal circuitry and cell density is known to vary between brain regions, however, little work has been done to establish the effects of these differences on extracellular Glu clearance between brain regions and rat strains. Glu clearance can be affected by many things, including the density of Glu transporters present in a given brain area, the effectiveness of the transporters, and the regional cell density (Segovia *et al*., 2001b). Additionally, Glu uptake in the striatum has been shown to significantly decrease in aged rats compared to young adult rats (Nickell *et al*., 2006). One way to evaluate Glu clearance is through local applications of exogenous Glu. This allows for clearance to be studied independent of Glu release. While studying the effects of exogenous Glu alone can not give definitive answers as to the cause of differences in Glu clearance between brain regions, it can give some insight into the differences that may exist and the changes that may occur over time.

In the present study we examine the differences between extracellular Glu levels measured in the striatum and PFC of Fischer 344 and Long Evans rats due to the local application of 1 µL of 5 mM Glu. Differences in these levels may be an indication of differences in clearance. To examine this, t_{80} was determined for both brain regions in both rat strains. Although t_{80} cannot definitively

determine the cause of the potential differences observed, it can be used to determine differences in Glu clearance kinetics.

Methods

Animals were housed in the conditions described in Chapter Two. Male Fischer 344 and Long Evans rats were between three and six months at the time of implantation surgery. Surgical procedures, MEA implantation in the striatum and PFC, and recording procedures followed those outlined in Chapter Two. Briefly, male Fischer 344 and Long Evans rats were implanted either in the striatum or PFC under isoflurane anesthesia and allowed to recover for two days prior to recording sessions. On recording days, 3, 5, and 7 post-implantation, rats were allowed approximately ten minutes to acclimate to the recording chamber prior to establishing a connection between the implanted MEA and the FAST-16 recording system. Once a connection was established and recordings started, a sampling rate of 1 Hz was maintained throughout the recording session. After recording for approximately 30 minutes, or longer if needed, and baseline was established, a 33-guage internal cannula attached with connecting tubing to a 10 µL Hamilton syringe and filled with 5 mM Glu (isotonic; pH 7.2-7.4) was inserted into the guide cannula aimed among the four Pt recording sites on the implanted MEA. A series of four, 1 µL ejections of 5 mM Glu were performed, allowing time between each one for baseline to be re-established. Data analysis involved an ANOVA with a Tukey's post hoc test. Significance was determined at $p<0.05$.

Results

The FAST-16 recording system allowed for reliable second-by-second recordings of Glu in the striatum and PFC of awake, freely behaving rats. We were able to consistently implant the MEA assemblies and record Glu for as long as 3 weeks, reliable for 7 days, in the awake rats. Glu recordings were verified *in vivo* by locally applying a Glu solution (5 mM isotonic, pH 7.4, 1 µL) with the use of the cannula directed among the 4 recording sites approximately 100 µm from

the microelectrode surface. The Glu peaks produced by local application were robust and reproducible as can be seen in the representative tracing of the self-reference subtracted local applications of Glu in the striatum of a Long Evans rat (Figure 4.1). This measure was repeatable within animals, between animals, and over multiple days. This self-referencing subtracting technique (Burmeister and Gerhardt, 2001) was also used to measure resting Glu levels as discussed in Chapter Three.

Another method for verifying Glu signals *in vivo* was performed by locally applying Glu (1 µL) while recording at applied potentials of either +0.7 V or +0.2 V versus an Ag/AgCl reference electrode. A sharp, robust peak was observed with locally applied Glu recorded at +0.7 V vs. Ag/AgCl. However, when Glu was applied while the microelectrodes were polarized at +0.2 V vs. Ag/AgCl, little to no change in signal was observed (n=4) (Figure 4.2). Our prior studies have shown that H_2O_2 is oxidized primarily at +0.7 V vs. Ag/AgCl at the Pt recording sites (Pomerleau *et al*., 2004). Thus, this approach demonstrated that the *in vivo* signal derived from Glu is converted to H_2O_2 by the enzyme layer.

Based on the verification studies, we were assured that we were measuring Glu in the awake rat brain. The self-referencing technique was employed throughout these studies used both to verify that we were measuring Glu and to ensure that our maximum amplitudes reported were produced by Glu. Locally applied Glu measures were studied in the striatum and PFC of Fischer 344 and Long Evans rats. Measured responses in the PFC of Long Evans rats were not significantly different over days 3, 5, and 7 days post-implantation (Figure 4.3). However, responses observed in the PFC were significantly increased compared to the striatum within rat strains (Long Evans striatum: 17.3 ± 3.5 µM; Long Evans PFC: 53.0 ± 6.8 µM; Fischer 344 striatum: 8.7 ± 1.3 µM; Fischer 344 PFC: 26.9 ± 3.2 µM) (Figure 4.4). Additionally, the PFC in Long Evans rats was significantly increased compared to the PFC in Fischer 344 rats.

We were interested in Glu clearance in the brain and if it changed over time. When locally applying exogenous Glu on days 3, 5, and 7 post-implantation, we determined the time it took for 80% of the signal to decay, or t_{80}.

There was no significant difference in t_{80} over days; however, we did observe a trend in increased t_{80} as the duration of the implant increased in the PFC of Fischer 344 rats (Day 3: 33.4 ± 12.4 seconds; Day 5: 42.1 ± 16.4 seconds; Day 7: 72.7 ± 5.3 seconds) (Figure 4.5). Additionally, there was a decreasing trend observed in the PFC of Long Evans rats (Day 3: 8.5 ± 3.5 seconds; Day 5: 6.1 ± 0.8 seconds; Day 7: 5.5 ± 1.8 seconds) (Figure 4.6). Because the maximum amplitudes from local application of 5 mM Glu were not significantly different in the striatum of Fischer 344 and Long Evans rats, we were able to make a direct comparison of Glu clearance in these animals. The t_{80} in the striatum (6.8 ± 0.3 seconds) of Fischer 344 rats was significantly faster compared to the striatum (18.2 ± 3.0 seconds) of Long Evans rats (Figure 4.7). Additionally, a Glu clearance comparison was made between amplitude matched recordings from the striatum of anesthetized (5.9 ± 0.8 seconds) and awake Fischer 344 rats (anesthetized data is unpublished data from Dr. Justin Nickell). There was no significant difference in t_{80} in the striatum of anesthetized rats compared to awake rats (Figure 4.8).

Discussion

This study demonstrates that chronic enzyme-based MEA recordings in the awake freely moving rat offers a robust method for monitoring Glu *in vivo* with minimal tissue damage at the site of implant. Current microdialysis methods are limited in reliable temporal resolution (minutes) and are only capable of recording over a single day per animal in the anesthetized or unanesthetized rat models (Shou *et al*., 2004). In our studies, we extend this recording capacity to one week, routinely.

Locally applied Glu recordings in the striatum and PFC of Fischer 344 and Long Evans rats were reproducible in maximum amplitude from day 3 through day 7 post implant. Signals due to locally applied Glu were also measured in the striatum of unanesthetized Long Evans rats. In the striatum, Glu signals were reproducible through day 7, as in the PFC. However, the average maximum amplitudes of the Glu signals were smaller compared to the PFC, supporting

potential differential regulation of Glu in the rat PFC vs. rat striatum in the Long Evans rat.

When using *in vivo* amperometry, identifying the molecule of interest is frequently questioned. First the ability of the enzyme-based MEA to differentially record for a specific molecule, in this case Glu was due to the high selectivity of the enzyme (GluOx) for its substrate (Glu). Another way we addressed this issue was by varying the applied potential of the recordings. The reporter molecule, H_2O_2, resulting from the enzymatic breakdown of Glu by GluOx was oxidizable predominately at +0.7 V vs. a Ag/AgCl reference electrode. However, as we have shown, when one drops the applied potential to +0.2 V vs. a Ag/AgCl reference electrode, we lost the Glu signal because H_2O_2 was no longer oxidized at the surface of the MEA. To further support the ability of our enzyme-based MEA to detect Glu, we included an important and unique feature of our MEAs; the simultaneous self-referencing of the measured signal. By subtracting the signals obtained on the 2 adjacent sites (sentinel sites) that were not coated with GluOx from the signals obtained from the sites that measure Glu, we were able to ascertain that the resulting signal was derived from Glu. All possible interferents being detected by the Pt sites and/or noise were subtracted out of the signal. Thus self-referencing methods were employed throughout this study to ensure that resting levels and peak responses (maximum amplitude) were due primarily to changes in extracellular Glu levels.

Additionally, we determined the time it took for 80% of the signal to decrease in the PFC of Fischer 344 rats on days 3, 5, and 7 post-implantation. Signals were amplitude matched within brain regions and rat strains and t_{80}s were examined. There was no significant difference in t_{80} over days in the PFC of Fischer 344 or Long Evans rats. However, there was a trend observed in Fischer 344 rats with day 3 having the fastest t_{80} and day 7 having the slowest. These results show a trend in slower clearance over time which may suggest fewer glia surrounding the implantation site or an decrease in the number of transporters located on the glia. However, a decreasing trend was observed in the PFC of Long Evans rats with day 7 having the fastest t_{80}. These results show

a trend in faster clearance over time which may be due to an increase in glia surrounding the implantation site or an increase in the number of transporters located on the glia. Additionally, although a direct comparison cannot be made since the maximum amplitudes with volume matched local applications of Glu were significantly increased in the PFC of Long Evans rats compared to Fischer 344 rats, the t_{80} values for the PFC of Fischer 344 rats were approximately 4-13 fold increased compared to the Long Evans rats. This seems counterintuitive. One would expect slower t_{80}s to be associated with larger amplitudes. Additionally, amplitude matched samples were used to make a direct comparison in Glu clearance in the striatum of Long Evans and Fischer 344 rats. Glu clearance was significantly faster in the in the striatum of Fischer 344 rats compared to Long Evans rats. Taken together, these results suggest that there may be a difference in regulation of brain morphology and transporters between the two rat strains and that there may be further differentiation between the brain regions in the different rat strains. However, when comparing Glu clearance in the striatum of Fischer 344 rats between awake and anesthetized rats, there was no significant difference. These results suggest that while there are differences in Glu clearance that exist between rat strains and brain regions and the anesthetic urethane decreased resting Glu (Chapter Three), the urethane does not act on Glu levels through Glu clearance mechanisms.

Copyright © Erin Cathleen Rutherford

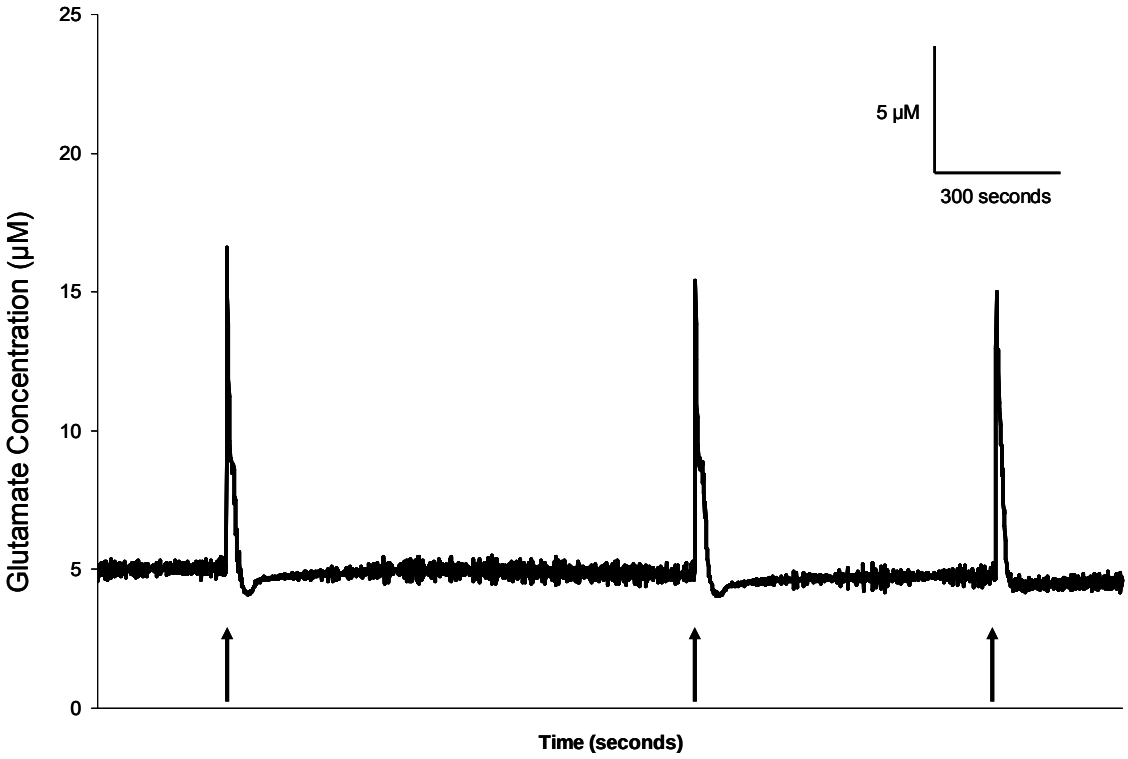

Figure 4.1: Representative Tracing of Local Application of 5 mM L-Glutamate (1 μL) in the Striatum of a Long Evans Rat

Representative tracing of locally applied Glu (5 mM, 1 μL) in the striatum of Long Evans rats. Glu was locally applied (indicated by arrows) and detected using a self-referencing MEA. Tracing shown is the result of subtracting the self-referencing site from the GluOx coated site. Glu peaks were rapid, robust, and reproducible.

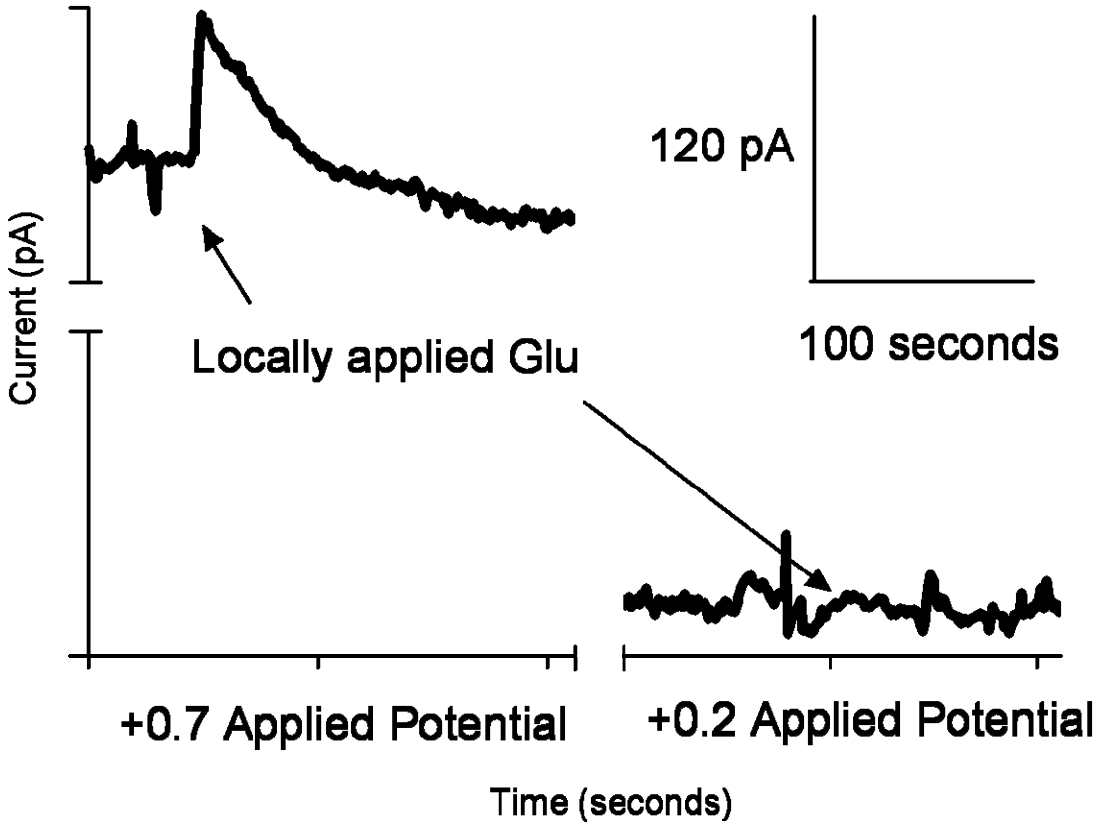

Figure 4.2 Local Application of L-Glutamate at +0.7 V and +0.2 V vs. Ag/AgCl Reference Electrode
Glu (5 mM, 1 µL) was locally applied (indicated by arrows) with either +0.7 V or +0.2 V vs. a Ag/AgCl reference electrode. At +0.7 V an increase in current (Glu) was observed. However, at +0.2 V no signal was observed, indicating that we are measuring Glu at +0.7 V vs. a Ag/AgCl reference electrode. Taken from Rutherford *et al.*, 2007.

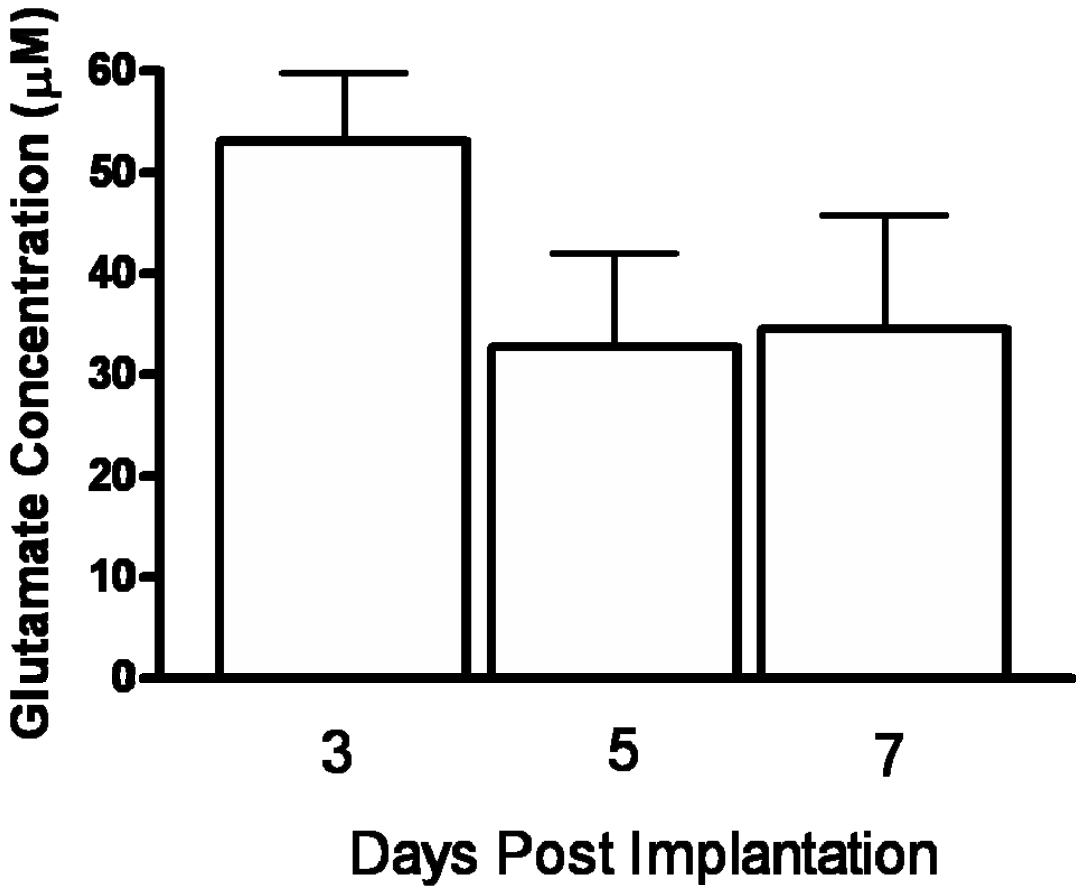

Figure 4.3: Local Application of 5 mM L-glutamate (1 μL) Days 3, 5, and 7 Post-Implantation in the Right Prefrontal Cortex of Long Evans Rats
Glu (5 mM, 1 μL) was locally applied over days in the PFC of Long Evans rats. There was no significant difference observed (n=7). Taken from Rutherford *et al.*, 2007.

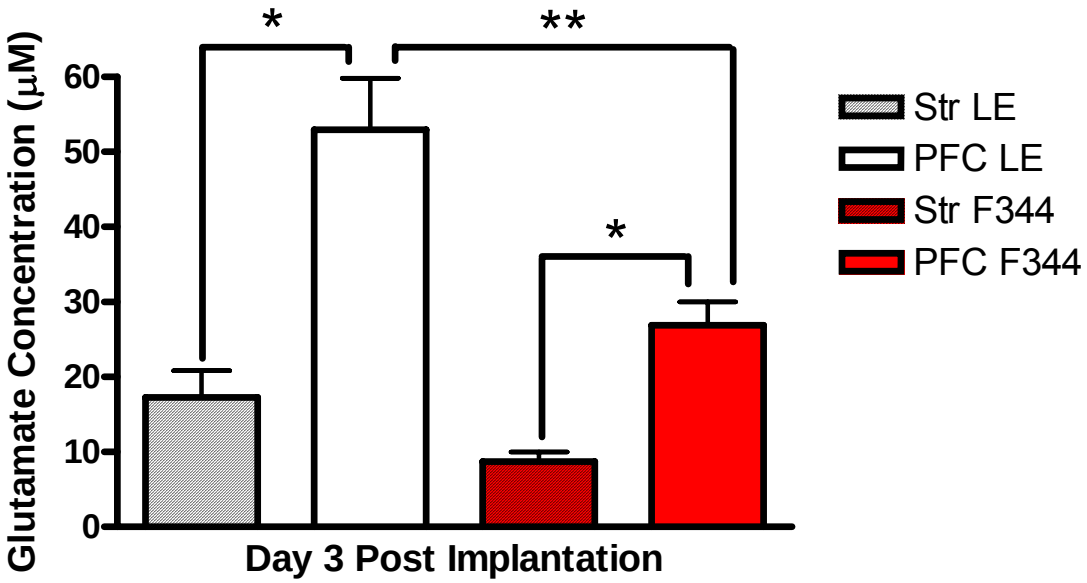

Figure 4.4: Local Application of 5 mM L-glutamate (1 µL) Day 3 Post-Implantation in the Striatum and PFC of Fischer 344 and Long Evans Rats

Glu (5 mM, 1 µL) was locally applied on day 3 post-implantation in the striatum (Str) and PFC of Fischer 344 (F344) and Long Evans (LE) rats. Levels in the PFC of Long Evans rats were significantly increased as compared to the striatum of Long Evans rats and the PFC of Fischer 344 rats. The PFC of Fischer 344 rats was also significantly increased compared to the striatum of Fischer 344 rats (n=7 except Str F344 n=4; *$p<0.05$; **$p<0.01$).

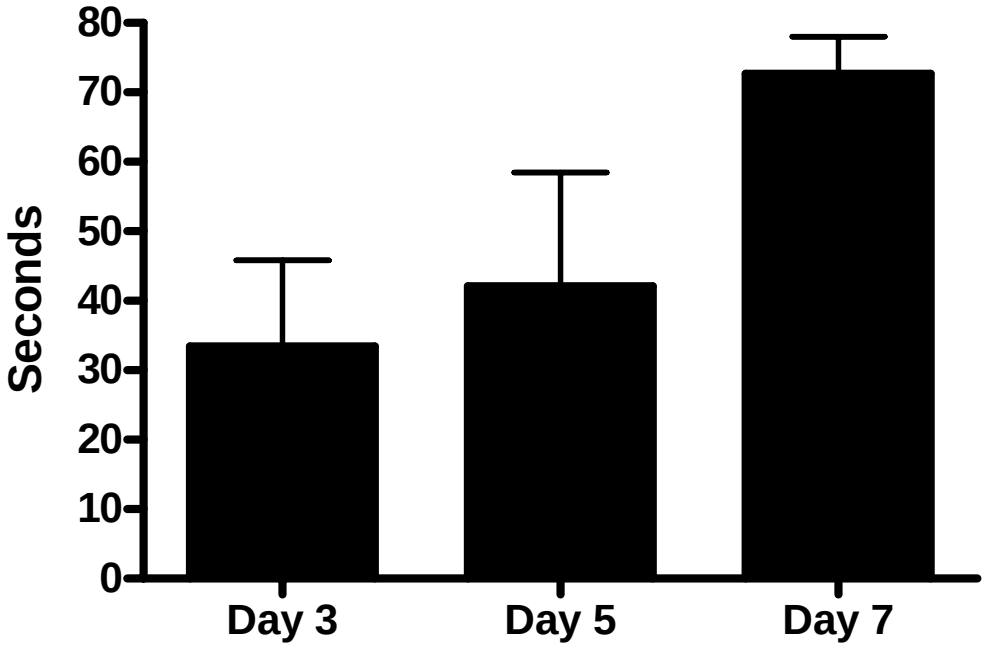

Figure 4.5: t_{80} on Days 3, 5, and 7 Post-Implantation in the Prefrontal Cortex of Fischer 344 Rats

t_{80}s over days following local application of Glu (5 mM, 1 µL) were calculated and analyzed in the PFC of Fischer 344 rats. No significance was observed between t_{80} over days 3, 5, and 7 post-implantation. However, a trend was observed in elongated t_{80} duration associated with longer implant durations (n=7).

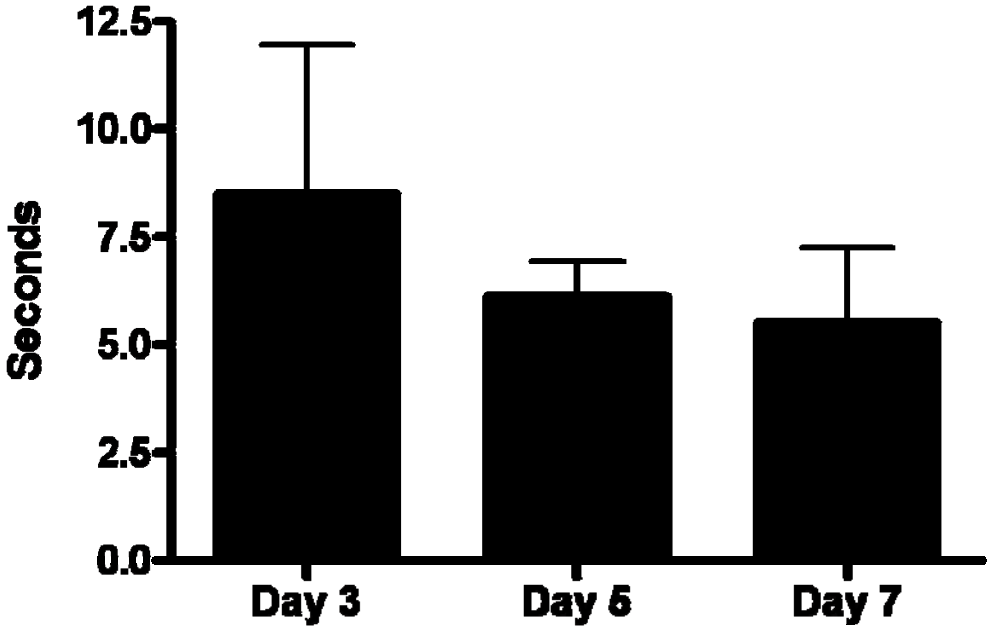

Figure 4.6: t_{80} on Days 3, 5, and 7 Post-Implantation in the Prefrontal Cortex of Long Evans Rats

t_{80}s over days following local application of Glu (5 mM, 1 µL) were calculated and analyzed in the PFC of Long Evans rats. No significance was observed between t_{80} over days 3, 5, and 7 post-implantation (n=7).

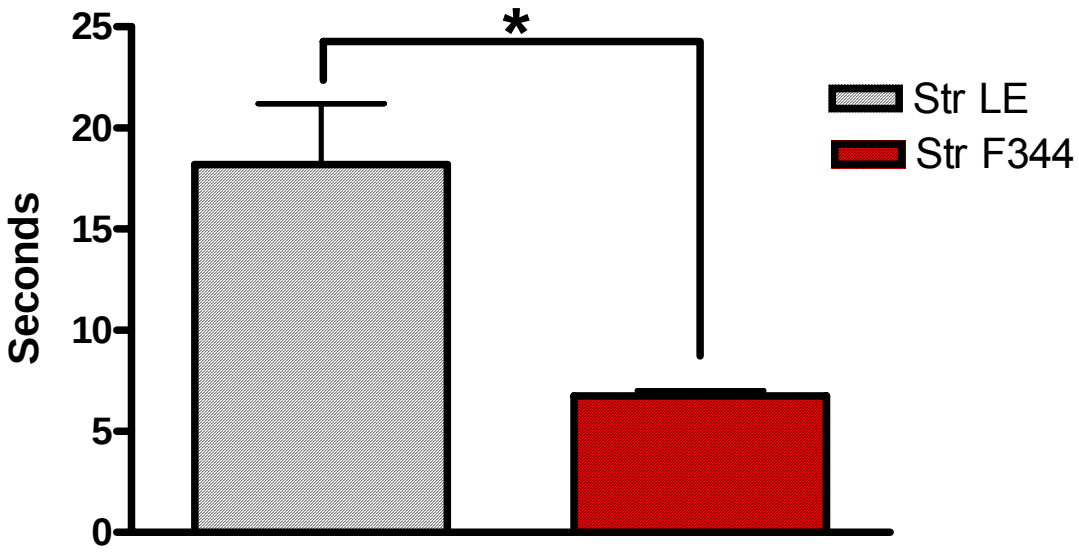

Figure 4.7: t_{80} in the Striatum of Long Evans and Fischer 344 Rats
t_{80}s in the striatum of Long Evans and Fischer 344 rats following local application of Glu (5 mM, 1 µL, amplitude matched) were calculated and analyzed. t_{80} in the striatum of Long Evans rats were significantly longer than those observed in the striatum of Fischer 344 rats (n=7 (LE); n=4 (F344); *p<0.05).

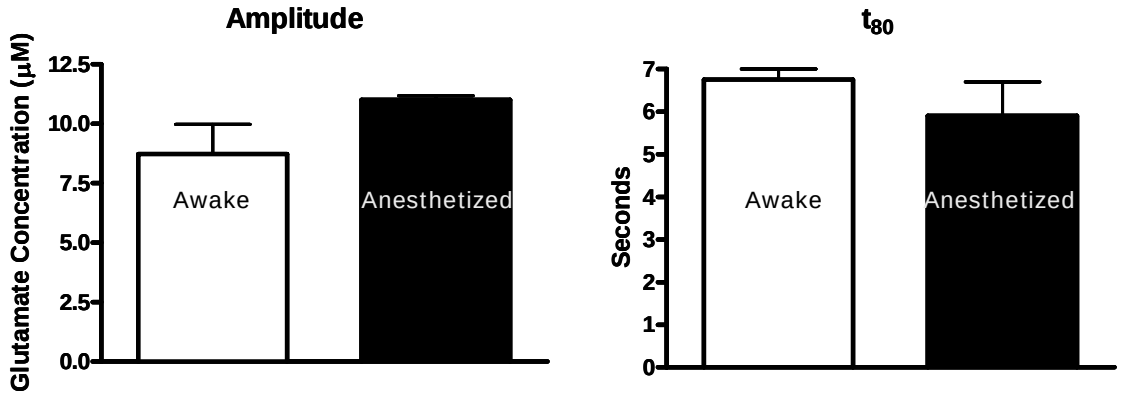

Figure 4.8: t_{80} in the Striatum of Awake and Anesthetized Fischer 344 Rats
t_{80}s in the striatum of awake and anesthetized Fischer 344 rats following local application of Glu (5 mM, amplitude matched) using the same enzyme-based self-referencing MEAs were calculated and analyzed. There was no difference in Glu clearance (t_{80}) in the striatum of awake and anesthetized Fischer 344 rat striatum (n=4 (awake); n=5 (anesthetized)). Anesthetized data is unpublished data from Dr. Justin Nickell.

Chapter Five: The Extent of Damage on Surrounding Tissue due to Chronic Implantation of the Microelectrode Array

Introduction

Many devices have been established to study Glu in the mammalian CNS including patch-clamp methods, carbon fiber microelectrodes, hydrogel-coated microsensors, and microdialysis probes. The ideal technique for measuring Glu *in vivo* is one that is minimally invasive, has the capability to chronically record Glu with low levels of detection and a high temporal resolution, and can record resting Glu levels. These methodologies can address several of these issues, however, none can address all by themselves. Patch-clamp methods allow membrane potentials associated with Glu to be measured in single cells, however, it is limited in its ability to be used in the whole animal over several days. Carbon fiber microelectrodes are minimally invasive and can be used in the awake animal, but it is hard to determine true resting Glu levels since there is only one recording channel and therefore no sentinel electrode. Microdialysis methods allow for low levels of detection, but produce damage up to 1.4 mm remote from the implant site and have slow response times (Tucci *et al*., 1997; Clapp-Lilly *et al*., 1999; Belay *et al*., 1998; Kennedy *et al*., 2002; Borland *et al*., 2005).

To address the need for a single technique with the capabilities to chronically record Glu in the CNS of awake animals with low limits of detection, high temporal resolution and the ability to record resting Glu levels, our laboratory has developed an enzyme-based multisite ceramic MEA that is light weight and has been used to routinely record in anesthetized animals (Nickell *et al*., 2005; Day *et al*., 2006). This technology has been successfully translated into chronic use in the freely moving animal (Pomerleau *et al*., 2003; Hascup *et al*., 2006; Rutherford *et al*., 2007) with Glu recordings possible through day 23 post-implantation and routinely through day 7 post-implantation without significant loss of sensitivity for Glu. Additionally, successful H_2O_2 test have been performed *in vivo* through day 90 post-implantation, suggesting that as we

improve upon our coating procedure we will be able to extend the duration that we are able to reliably record Glu.

As we extend the possible recording lifespan of our MEAs, it is important to establish the effects of chronic implantation on surrounding tissue. While the ceramic MEA tip is small and minimally invasive, the issue of tissue damage associated with chronic implantation of our ceramic MEAs has not been studied. These experiments were designed to address this issue. In this study, Long Evans rats were chronically implanted in the right PFC for either 1 or 3 days, 1, 2, 4, 8, 16, or 24 weeks. Following this time, animals were sacrificed and the brains were sectioned and stained for GFAP and Iba1 to determine changes in astrocytes and microglia levels surrounding the MEA implant site.

Methods

Animals were housed in the conditions described in Chapter Two. Long Evans rats were between three and six months at the time of implantation surgery. Surgical procedures, MEA implantation in the PFC, and histopathological studies followed those outlined in Chapter Two. Briefly, male Long Evans rats were implanted in the PFC under isoflurane anesthesia and allowed to recover. Following implantation surgery, rats were returned to the animal facilities and remained there for either 1 or 3 days, 1, 2, 4, 8, 16, or 24 weeks. At these time points, rats were briefly anesthetized with isoflurane and transcardially perfused with 4% paraformaldehyde. Brains were extracted and stored in 4% paraformaldehyde for three days. After three days, the storage solution was changed to 0.1 M phosphate buffer with 10% sucrose. Brains were then sliced and stained with a marker for astrocytes (GFAP) or a marker for microglia (Iba1) (courtesy of Dr. Ingrid Strömberg at Umeå University, Sweden). Pedestal MEAs did not have an attached guide cannula and were coated with Nafion® only, no GluOx. There were no recording sessions with these animals. Data analysis involved an ANOVA with a Tukey's post hoc test. Significance was determined at $p<0.05$.

Results

MEAs were chronically implanted in to the right PFC of Long Evans rats. Following 1 or 3 days, 1, 2, 4, 8, 16, or 24 weeks rats were sacrificed and their brains were extracted and sectioned. MEA placement in the PFC was verified with cresyl violet staining (Figure 5.1). Brain sections were analyzed to determine the extent of damage on tissue surrounding the MEA implantation site by staining with Iba1 (microglia) and GFAP (astrocytes). Mean densities for Iba1 and GFAP were reported. The shapes of the microglia were also examined to determine activation status.

GFAP staining was used to visualize astrocyte composition in the PFC of chronically implanted rats. GFAP mean density surrounding the implant site was elevated at 3 days, 1, 2, 4, and 8 weeks compared to 1 day implants (3.83 ± 1.64 mean density), however, a significant difference was only observed at 16 (39.47 ± 7.25 mean density) and 24 (33.60 ± 7.16 mean density) weeks post-implantation (Figure 5.2). Additionally, elevated GFAP staining was confined to within 50-100 μm surrounding the implantation site, regardless of the duration of the implant (Figure 5.3). However, glial scaring was observed at the implant site in the 6 month implants (Figure 5.4).

Iba1 staining was used to visualize microglia composition in the PFC of chronically implanted Long Evans rats (Figure 5.6, left). As seen with the GFAP staining, increased Iba1 staining was limited to within 50-100 μm of the implantation site. The levels observed did not reach an astrocyte density that would be associated with an injury. There was a dramatic increase in Iba1 staining observed in the contralateral hemisphere of an eight week implant where a skull screw came into contact with the brain (Figure 5.6, right). In rats implanted for 1 week (29.67 ± 5.50 mean density), there was a significant difference in Iba1 staining as compared to control hemispheres (10.30 ± 0.55 mean density) and 1 day implants (9.32 ± 2.38 mean density). However, the difference in Iba1 levels compared to control levels and 1 day implants returned to normal levels by 24 weeks (15.08 ± 3.86 mean density) with the implant (Figure 5.5). Additionally, when analyzing the individual microglia cell type, there

were very few rounded, or activated, cells, supporting that our ceramic MEAs are well tolerated by the rat brain (Figure 5.4) (Laurenzi *et al*., 2002).

Discussion

We investigated the histopathological effects from chronic MEA implantation. The implantation durations of 1 and 3 days yielded similar findings for GFAP (astrocytes) and Iba1 (microglia) staining. At close evaluation, both GFAP and Iba1 staining were seen to surround the MEA tracts, extending into tissue on average by 50 – 100 μm. No further increase in staining was seen in adjacent areas to the MEA tracts. There was a slight elevation observed in number of astrocytes immediately surrounding the site of implant that increased as the implant duration increased. However, this elevation was not significant until 16 weeks with the implantation and did not extend more than 50-100 μm into the surrounding tissue. These data correlate with Glu Clearance (t_{80}) data (Chapter Four) obtained from the PFC of Long Evans rats on days 3 and 7 post-implantation. As the relative staining for astrocytes (the majority of high affinity Glu transporters are located on astrocytes – See Chapter One) increases, Glu is cleared more rapidly. Furthermore the number of microglia was only significantly increased at 1 week (29.67 ± 5.50 mean density) post-implantation compared to control hemispheres (10.30 ± 0.55 mean density) and to 1 day (9.32 ± 2.38 mean density) implantations. However, Iba1 levels returned to normal by 24 week implantations. Figure 5.6 is an example of the microglia observed at the site of implantation and the degree of microglia activation that would be observed in an injury. This was produced by a skull screw that was placed too deep and came into contact with the tissue. Additionally, freely moving microdialysis studies yield a high degree of damage to the brain at the site of implant with extended damage observed up to 1.4 mm from the site of implantation within 30 hours (Clapp-Lilly *et al*., 1999; Borland *et al*., 2005). By contrast, our MEAs did not disrupt brain tissue more than 50-100 μm from the microelectrode tracts and cell morphology remained healthy with normal processes and cell shape up to 24 weeks post-implantation.

Additionally, pedestal MEA implants were cable of measuring H_2O_2 for up to 90 days in the awake, freely moving rat with no apparent adverse effects to the rat. This suggests that as we improve upon our enzyme-based technology, through cross-linking and coating procedures, we will be able to increase the number of consecutive days we can record Glu in the unanesthetized animal. Furthermore, our H_2O_2 data support that the loss of ability to record Glu is due to an enzyme coating related function, not due to loss of MEA function. The ability to record H_2O_2 longer than it is possible to detect Glu suggests that the enzyme layer may either be degrading or the enzyme may be dysfunctional (Valdes and Moussy, 2000) or detaching from the surface of the MEA. However, this must be further analyzed to determine the exact cause of the loss of enzyme function.

Current microdialysis studies report significant damage to brain tissue within 45 hours upto 1.4 mm of the area surrounding the probe implant site including altered mitochondria and endoplasmic reticulum. This supports an intracellular chemical disruption in the neuronal processes, in addition to an observed neuronal density loss up to 400 μm away from the microdialysis implant site (Clapp-Lilly *et al*., 1999). Additionally, Borland *et al*. (2005) observed disrupted dopamine release and uptake at least 220 μm remote from the microdialysis probe approximately 2 hours following probe placement. However, histological studies performed to examine the effects of chronic implantation of our MEA showed minimal damage (50-100 μm) on surrounding brain tissue up to 8 weeks post implant as measured by an astrocyte marker and one week as measured by a microglia marker with a return to control levels by 24-week post-implantation. The damage observed with chronic microdialysis implantations may account for the discrepancies between studies in terms of the source of the Glu measured.

Copyright © Erin Cathleen Rutherford

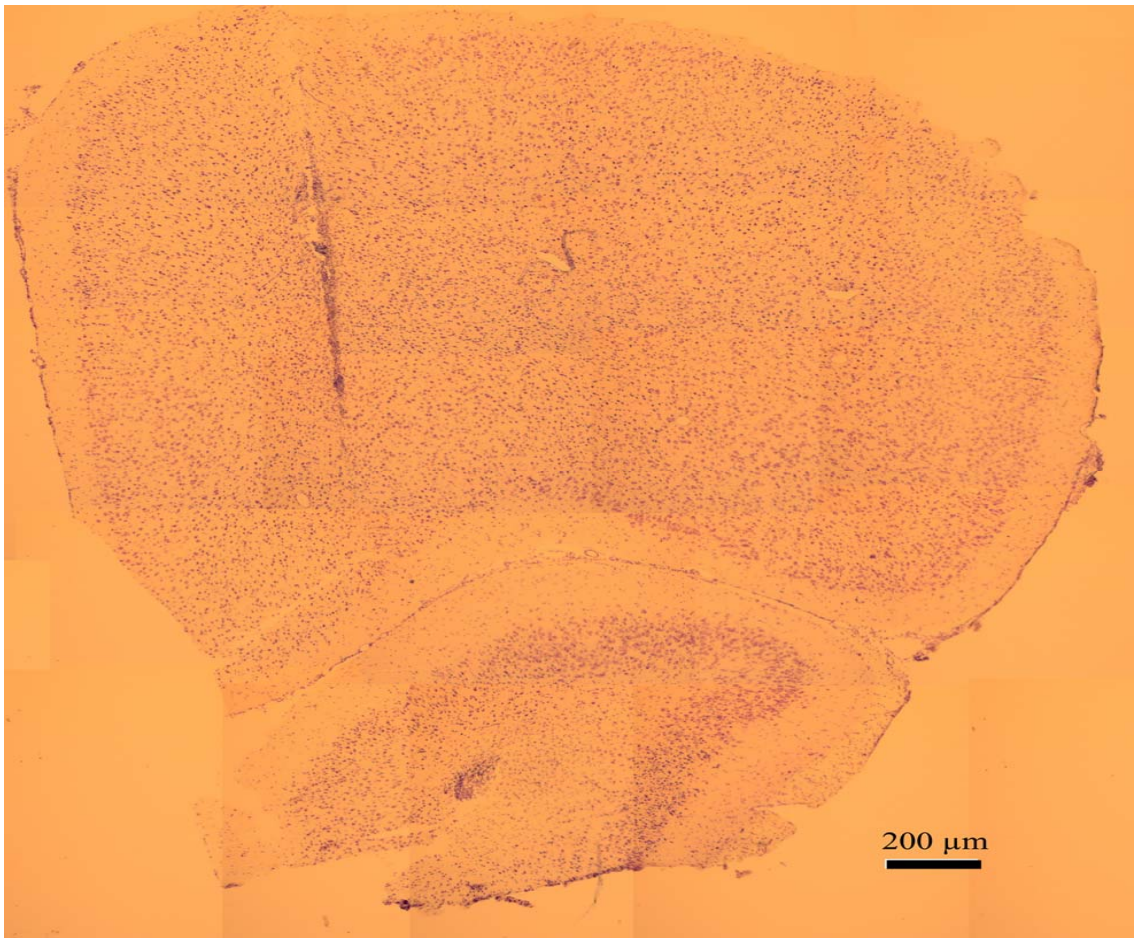

Figure 5.1: Cresyl Violet Staining of Microelectrode Arrays Chronically Implanted in the Right Prefrontal Cortex of a Long Evans Rat
Cresyl violet staining of neuropil. MEA tract is clearly visible in the right PFC.

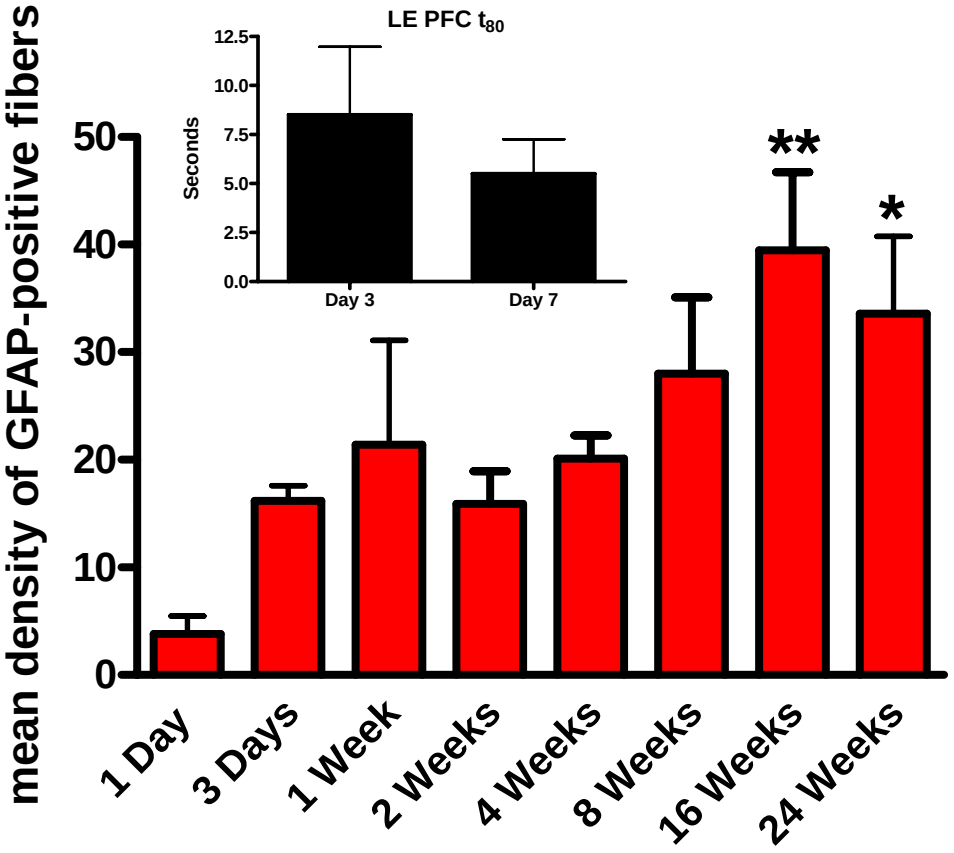

Figure 5.2: GFAP Staining of the Right Prefrontal Cortex of Long Evans Rats with Chronic Microelectrode Array Implantations
Rats were sacrificed after 1 or 3 days, 1, 2, 4, 8, 16, or 24 weeks with the implanted MEA. Significance was vs. 1 day implantations (n=4; *p<0.05; **p<0.01). Inset shows Glu clearance (t_{80}) on days 3 and 7 post-implantation in the PFC of Long Evans rats. Trend of faster Glu clearance correlates with trend of increased astrocyte density on days 3 and 7 post-implantation (n=7).

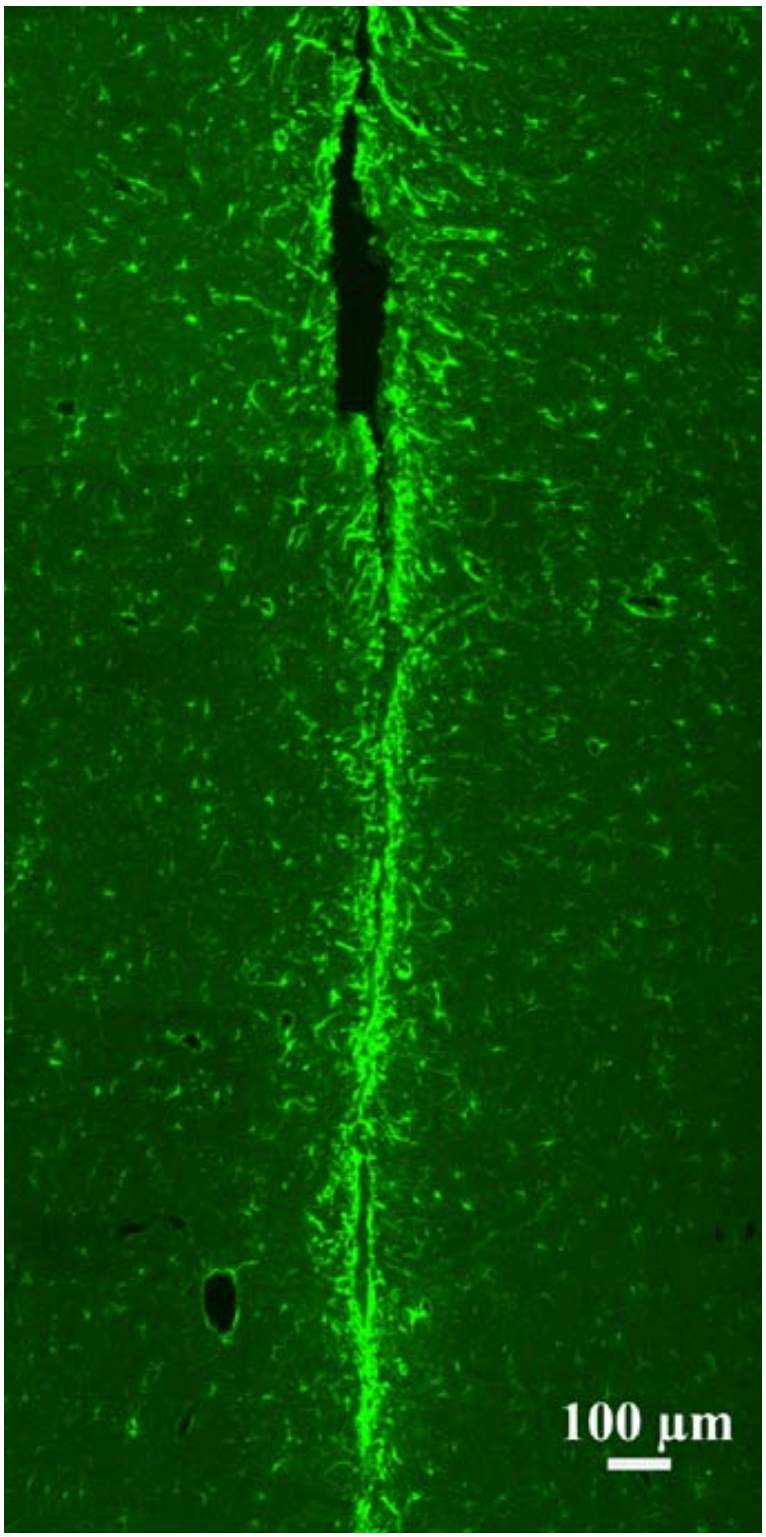

Figure 5.3: GFAP Staining of Right Prefrontal Cortex of a Long Evans Rat after an 8 Week Implant
Image of the right PFC of a Long Evans rat after an 8 week implantation stained with GFAP. MEA tract is clearly visible. Adapted from Rutherford *et al*., 2007.

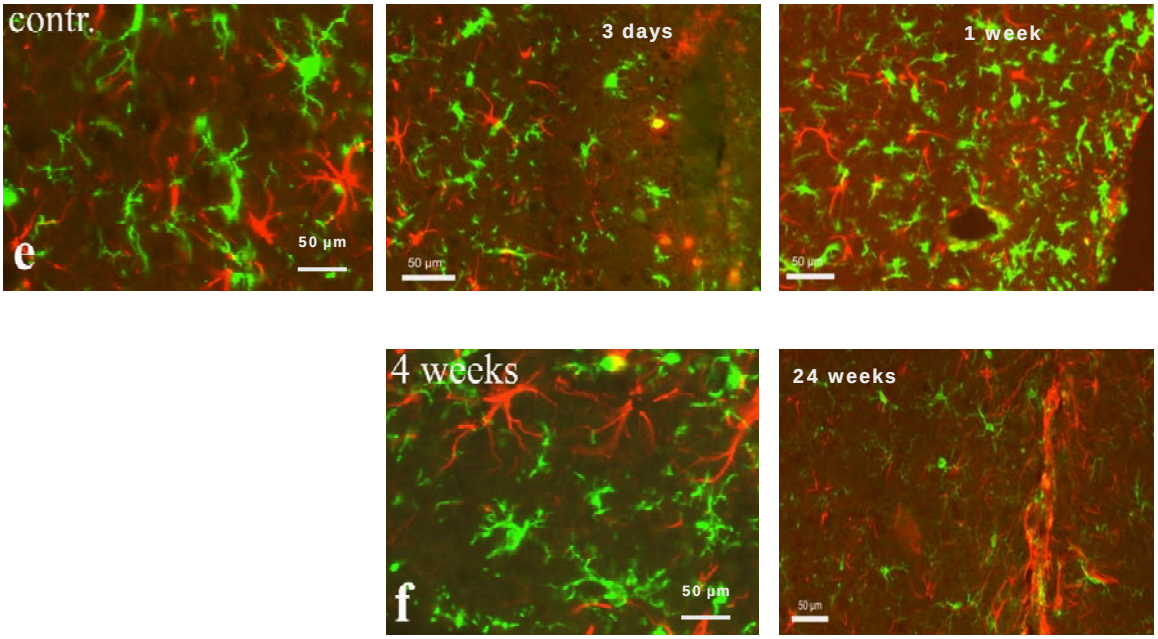

Figure 5.4: Image of GFAP and Iba1 Staining in the Prefrontal Cortex of Long Evans Rats after 3 Day, 1 Week, 4 Week, and 24 Week Implantations

Image of the control hemisphere (upper left) and implant site in the PFC of Long Evans rats after 3 days, 1 week, 4 weeks or 24 weeks implant stained with GFAP (red) and Iba1 (green). A glial scar can be seen along the MEA tract at 24 weeks.

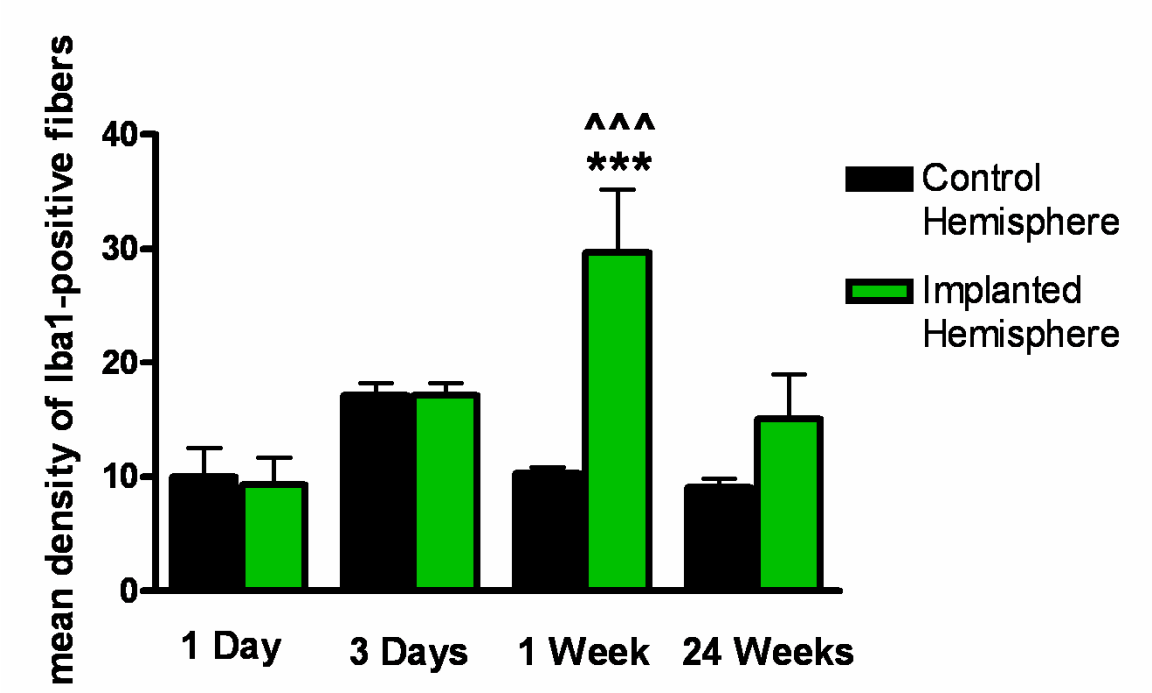

Figure 5.5: Iba1 staining of the Right Prefrontal Cortex of Long Evans Rats with Chronic Microelectrode Array Implantations
Rats implanted with pedestal MEAs were sacrificed after 1 or 3 days, 1, 2, 4, 8, 16, or 24 weeks. The contralateral hemisphere was used as controls (n=4; ***p<0.001 vs. 1 day; ^^^p<0.001 vs. 1 week control).

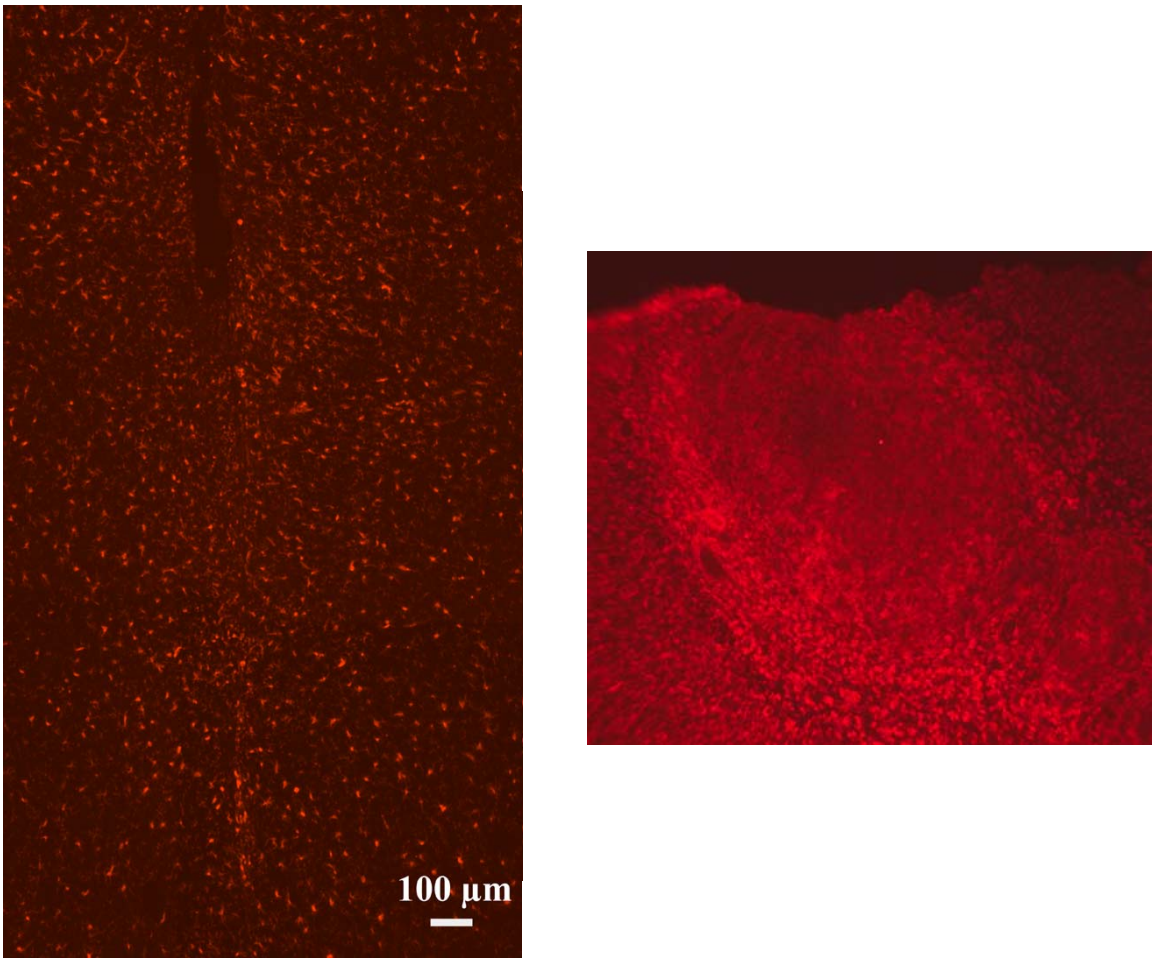

Figure 5.6 :Iba1 Staining of the Right Prefrontal Cortex of a Long Evans Rat after an 8 Week Implant

Image of the right PFC of a Long Evans rat after an 8 week implantation stained with Iba1 (left). MEA tract is clearly visible. Image of the contralateral hemisphere in a Long Evans rat after 8 week implantation stained with Iba1 (right). Increased GFAP staining is due to a stainless steel skull screw coming into contact with the brain and is indicative of an injury. Adapted from Rutherford *et al*., 2007.

Chapter Six: Does Tail-Pinch Stress Affect L-Glutamate Levels in the Striatum and Prefrontal Cortex of Male Fischer 344 and Long Evans Rats?

Introduction

Stress can play a major role in the development, progression and exacerbation of symptoms associated with many disorders, including addiction, schizophrenia, and Parkinson's disease. It has been suggested that Glu neurotransmission activation in the PFC is a common mechanism that may allow stress to influence both normal and abnormal processes that maintain cognition and affect (Moghaddam, 2002). The rodent medial PFC (infralimbic and prelimbic areas) is suggested to be the brain area responsible for executing function, such as working memory (Aultman and Moghaddam, 2001; Delatour and Gisquet-Verrier, 1996; Floresco *et al*., 1996; Granon and Poucet, 1995; Kesner *et al*., 1996; and Seamans *et al*., 1995) and other cognitive functions. All PFC efferents and the majority of the afferents to the PFC, such as projections from the thalamus, hippocampus, and amygdala, are glutamatergic. Glutamatergic neurotransmission in the PFC modulates or mediates many aspects of stress response, such as activation of the hypothalamic-pituitary-adrenal (HPA) axis and monoamine neurotransmission. Glu is also abundant in the striatum which is involved in the limbic system and motor functions and as such, is connected to the PFC through various pathways. Although the striatum is not commonly studied in conjunction with stress, the connection between the PFC and striatum present the striatum as another potential area to be influenced by stress.

Previous studies (Gilad *et al*., 1990; Moghaddam, 1993; Jedema and Moghaddam, 1994; Bagley and Moghaddam, 1997; Takahata and Moghaddam, 1998; Bland *et al*. 1999) have reported on stress response and Glu involvement in awake animals. Microdialysis studies evaluating handling and swimming stress showed elevated Glu stress response in the PFC compared to the striatum (Gilad *et al*., 1990; Moghaddam, 1998). Additionally, Glu response to stress was

shown to decrease with successive tail-pinch applications administered over a single day (Bagley and Moghaddam, 1997; Moghaddam, 2002). However, these studies did not have the temporal and spatial resolution that is possible with our chronic pedestal microelectrode implants.

In the present study we investigated the dynamics of Glu in response to tail-pinch stress in the PFC and striatum of Fischer 344 and Long Evans rats using our chronically implanted pedestal MEA. We examined the duration, maximum amplitude, and fast dynamics of the Glu signal change due to a physiological event (tail-pinch stressor). In addition, we were able to compare the changes in Glu response to stress in the striatum and PFC over multiple days.

Methods

Animals were housed in the conditions described in Chapter Two. Male Fischer 344 and Long Evans rats were between three and six months at the time of implantation surgery. Surgical procedures, MEA implantation in the striatum and PFC, and recording procedures followed those outlined in Chapter Two. Briefly, male Fischer 344 and Long Evans rats were implanted either in the striatum or PFC under isoflurane anesthesia and allowed to recover for two days prior to recording sessions. On recording days 4 and 6 post-implantation, rats were allowed approximately ten minutes to acclimate to the recording chamber prior to establishing a connection between the implanted MEA and the FAST-16 recording system. Once a connection was established and recordings started, a sampling rate of 1 Hz was maintained throughout the recording session. After recording for approximately 30 minutes, or longer if needed, and baseline was established, a five minute tail pinch stressor was performed by applying a clothespin approximately one inch from the base (where the tail meets the body) of the tail. Data analysis involved an ANOVA with a Tukey's post hoc test. Significance was determined at $p<0.05$.

Results

Five minute tail-pinch stressors were performed while recording Glu signals on a second-by-second basis in Fischer 344 and Long Evans rats chronically implanted either in the striatum or PFC (Figures 6.1, 6.2, 6.3, and 6.4). We were able to measure changes in Glu due to physiological stimuli in the awake behaving rat. Several parameters surrounding the tail-pinch were examined, including the duration of the tail-pinch response, the maximum amplitude of the tail-pinch, the area under the curve for the tail-pinch response, the number of peaks through out the tail-pinch response defined as a change of at least 15% over resting Glu levels, and the total peak area for the tail-pinch response.

The duration of the tail-pinch response was defined as the time from the beginning of the tail-pinch until the Glu levels returned to baseline. The duration of tail-pinch responses did not vary between brain regions within a single rat strain (either the Long Evans or Fischer 344 rats). However, both the striatum (26.5 ± 9.8 μM) and PFC (27.5 ± 6.2 μM) in the Fischer 344 rats were significantly elevated ($p < 0.05$) compared to their counterparts in the Long Evans rats (striatum: 11.5 ± 2.4 μM; PFC: 13.6 ± 2.9 μM) (Figure 6.5).

The maximum amplitude of the tail-pinch response was also examined. There were no significant differences observed between brain regions or rat strains. This could be due to the large variation observed with the PFC (8.9 ± 4.3 μM) and striatum (1.1 ± 0.4 μM) of the Long Evans rats and the striatum (7.9 ± 6.4 μM) and PFC (4.9 ± 2.0 μM) of the Fischer 344 rats (Figure 6.6). Similarly, when examining the area under the curve for the Glu tail-pinch response a large variance was observed in the PFC (8025 ± 4273 arbitrary units) and striatum (1061 ± 730.4 arbitrary units) of the Long Evans rats and the striatum (4648 ± 4021 arbitrary units) and PFC (6795 ± 5209 arbitrary units) of the Fischer 344 rats (Figure 6.7).

To get a better understanding of the shape of the tail-pinch response, the number of peaks was analyzed. There was no significance difference observed between rat strains or brain regions. However, there was a trend of elevated

number of peaks during the tail-pinch response observed in the PFC of the Long Evans (31.0 ± 9.4 peaks) and Fischer 344 (12.7 ± 5.5 peaks) rats compared to the striatum of their respective counterparts (Long Evans: 17.6 ± 2.8 peaks; Fischer 344: 9.5 ± 1.5 peaks) (Figure 6.8). Additionally, the total peak area for the tail-pinch response was analyzed. The striatum (725.5 ± 497.2 arbitrary units) and PFC (4581 ± 2322 arbitrary units) in the Long Evans rats and the striatum (4497 ± 4117 arbitrary units) and PFC (6690 ± 5148 arbitrary units) in the Fischer 344 rats had a large degree of variance (Figure 6.9).

Discussion

Our laboratory was interested in stress and how it affects Glu levels in the striatum and PFC of Fischer 344 and Long Evans rats. We wanted to determine if we could measure changes in extracellular Glu levels in a behaviorally relevant situation. To examine this, we performed a five minute tail-pinch stress on Fischer 344 and Long Evans rats with chronic MEA implants in the striatum or PFC. We observed large variations in tail-pinch response, even in an inbred rat strain (Fischer 344). We also observed fast, robust Glu responses that would not be able to be seen when using conventional microdialysis.

When analyzing the duration of the tail-pinch response, which we define as the beginning of the tail pinch and lasts until Glu levels return to resting levels, no significant difference was observed between the PFC and striatum within either the Long Evans or Fischer 344 rats. However, there was a significant difference observed between the Fischer 344 and Long Evans rats in the PFC (27.5 ± 6.2 minutes and 13.6 ± 2.9 minutes, respectively; $p<0.05$), and in the striatum of Fischer 344 and Long Evans rats (26.5 ± 9.8 minutes and 11.5 ± 2.4 minutes, respectively; $p<0.05$) with the response in the Fischer 344 rats lasting approximately two times those observed in the Long Evans rats. The tail-pinch response in the Long Evans rats lasted approximately 10-15 minutes, regardless of brain area, whereas the duration of the tail-pinch stress response in the Fischer 344 rats was approximately 20-30 minutes (Figure 6.5), suggesting that Fischer 344 rats remained stressed longer.

The maximum amplitude was also examined and was defined as the maximum peak height in Glu response during the duration of the tail-pinch response. There was no significant difference between the rat strains (Long Evans and Fischer 344) or between the brain regions (PFC and striatum) within the rat strains (Figure 6.6). In an effort to examine possible differences between rat strains and brain regions in response to tail-pinch stress more accurately, we analyzed the data using area under the curve. This method accounted for the duration of the Glu response to stress as well as the fluxuation of Glu response amplitudes throughout the duration of the Glu tail-pinch response. There was no significant difference in the area under the curve for tail-pinch stress between rat strains or brain regions. The averages for the area under the curve were decreased in the striatum of both rat strains compared to the PFC in the respective strains; however, the variance was too great to establish significance. The lack of significance suggests that there may be a regulatory mechanism in place in both the PFC and the striatum in the Fischer 344 and Long Evans rats that acts to limit the Glu response to stress such that over a period of time, there is a maximum total Glu concentration that can be achieved when the system is functioning properly.

However, when analyzing the PFC and striatum, there was significance observed in the duration of the Glu response to tail-pinch stress in Fischer 344 rats as compared to Long Evans rats, but no significance in either the maximum amplitude or the area under the curve. The current data suggest that the striatum and PFC in the Long Evans rats must either have an increased number of spikes in Glu concentration or an elevated Glu undertone in response to tail-pinch stress compared to the Long Evans rats. To examine this possibility, the number of peaks during the tail-pinch response was analyzed (Figure 6.8). There was no significance observed in the number of peaks between brain regions or rat strains. However, there was a trend with the number of peaks in the PFC of both rat strains having an increased average number of peaks as compared to the striatum in the respective rat strains (Figure 6.8). Additionally, there was no significant difference in the total peak area between the rat strains

or brain regions. Taken together, these data suggest that within a given rat strain and brain region there may be difference in the general rise and fall, or tone, of Glu.

The durations of the responses to tail-pinch were well within the sampling range that can be observed using microdialysis. Additionally, the maximum amplitudes observed using our recording technology would be detected using microdialysis. However, current microdialysis studies lack the response time necessary to see the fast changes in peak amplitudes that we were able to be distinguished using our second-by-second recording capabilities. Taken together, these studies support that the improved temporal resolution of enzyme-based MEAs can be used for reliable second-by-second measures of Glu in the CNS of freely moving rats and recordings in awake animals are necessary to accurately determine the fast dynamics of glutamatergic function.

Copyright © Erin Cathleen Rutherford

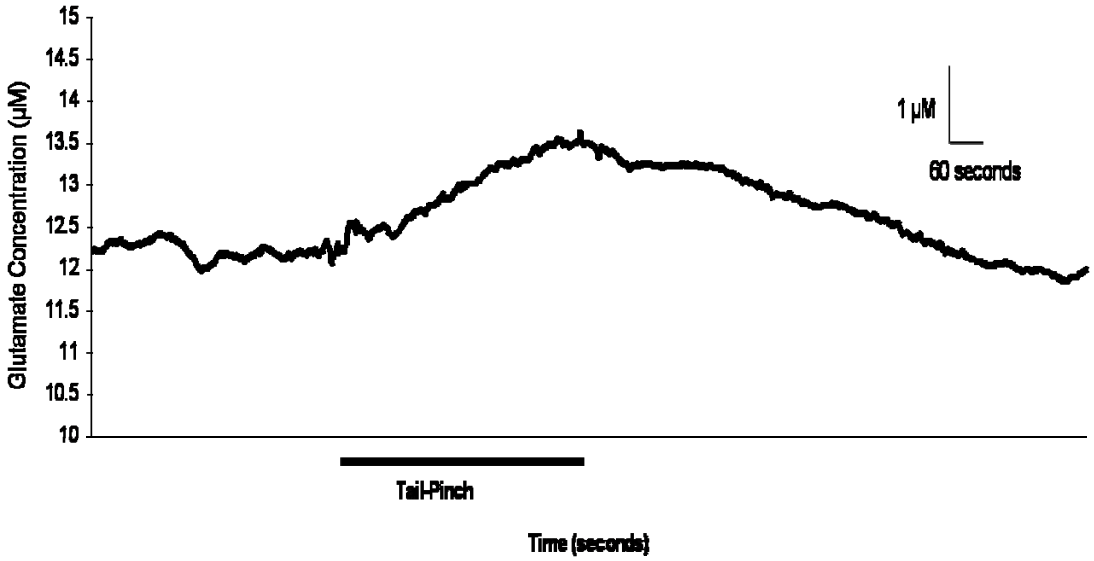

Figure 6.1: Representative Tracing of a Five Minute Tail-Pinch Response in the Striatum of a Long Evans Rat
Long Evans rats implanted in the striatum underwent a five minute tail-pinch stressor. Tail-pinch is indicated by the solid black line.

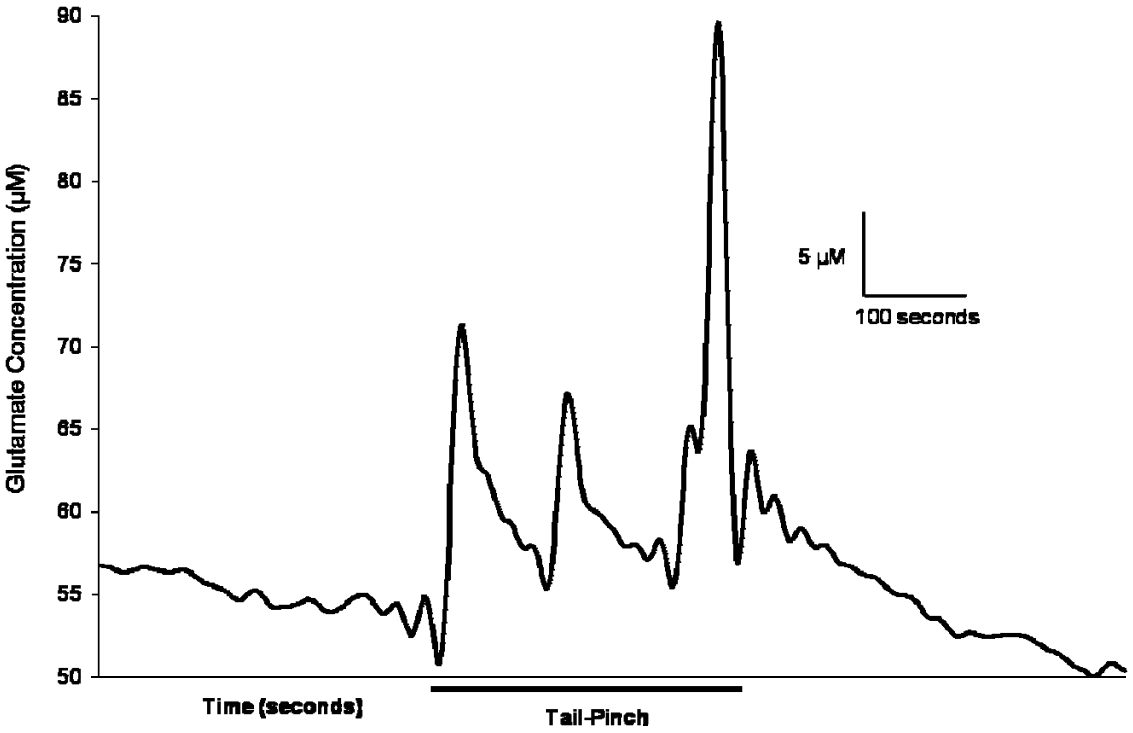

Figure 6.2: Representative Tracing of a Five Minute Tail-Pinch Response in the Prefrontal Cortex of Long Evans Rats
Long Evans rats implanted in the PFC underwent a five minute tail-pinch stressor. Tail-pinch is indicated by the solid black line.

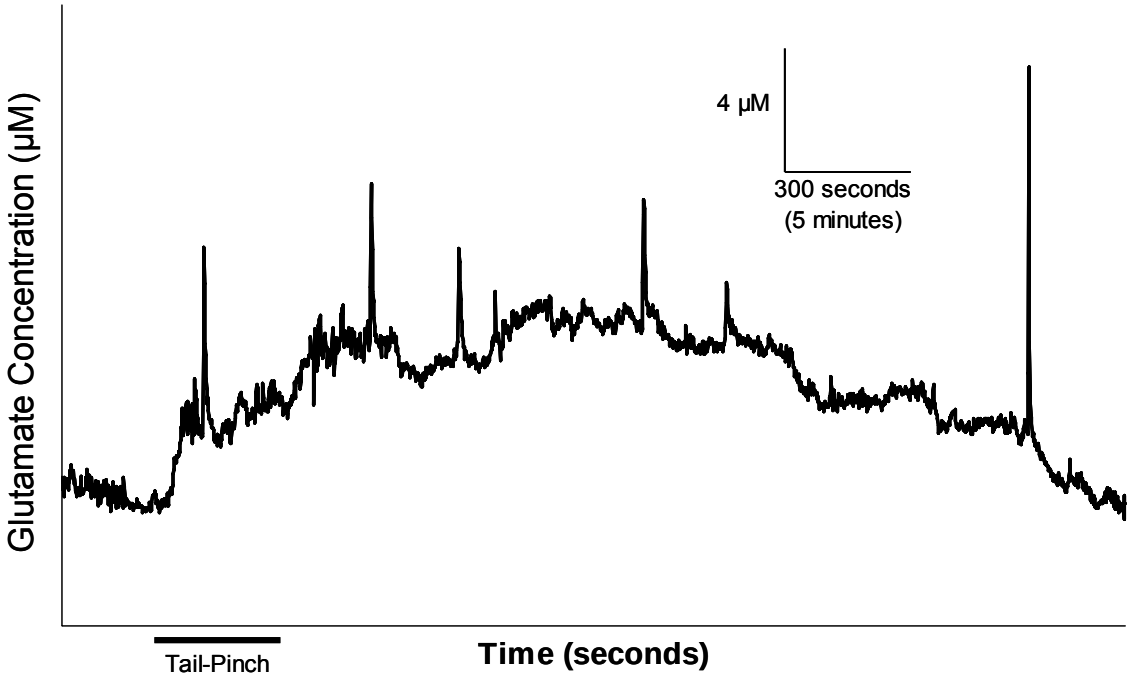

Figure 6.3: Representative Tracing of a Five Minute Tail-Pinch Response in the Striatum of Fischer 344 Rats
Fischer 344 rats implanted in the striatum underwent a five minute tail-pinch stressor. Tail-pinch is indicated by the solid black line.

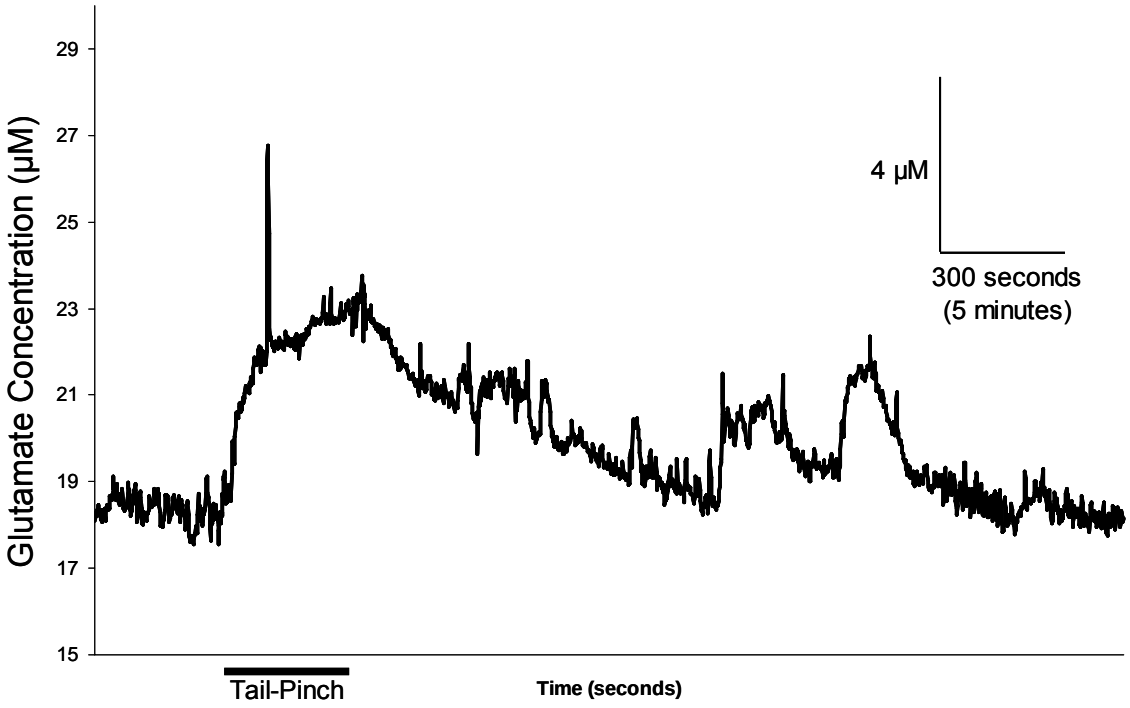

Figure 6.4: Representative Tracing of a Five Minute Tail-Pinch Response in the Prefrontal Cortex of Fischer 344 Rats
Fischer 344 rats implanted in the PFC underwent a five minute tail-pinch stressor. Tail-pinch is indicated by the solid black line.

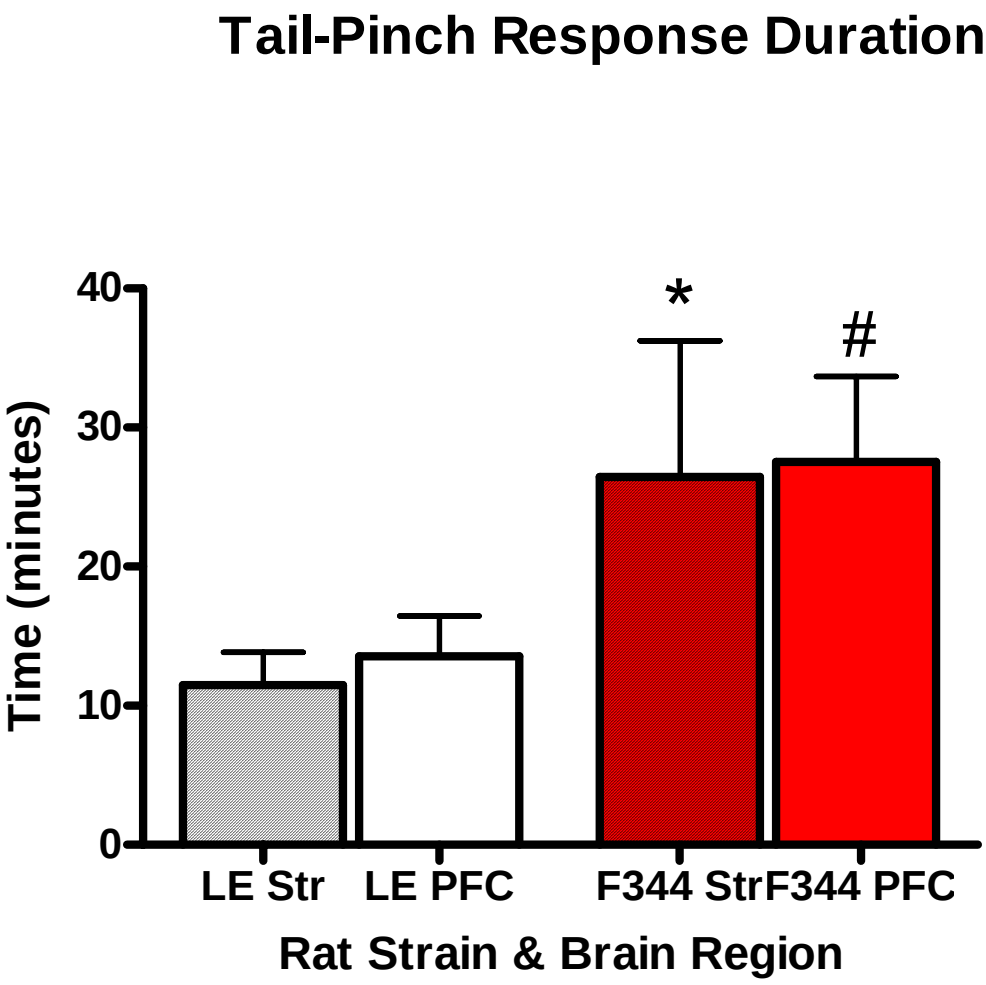

Figure 6.5: Duration of Response to a Five Minute Tail-Pinch in the Striatum and Prefrontal Cortex of Fischer 344 and Long Evans Rats
Fischer 344 (F344) and Long Evans (LE) rats were implanted in the striatum (Str) or PFC and underwent a five minute tail-pinch stressor. The duration of the Glu response to the tail-pinch was examined. Fischer 344 striatal responses were significantly increased compared to the striatum of Long Evans rats (*$p<0.05$). Fischer 344 PFC responses were significantly increased compared to the striatum of Long Evans rats ($^{\#}p<0.05$) (n=7, except Str F344 n=4).

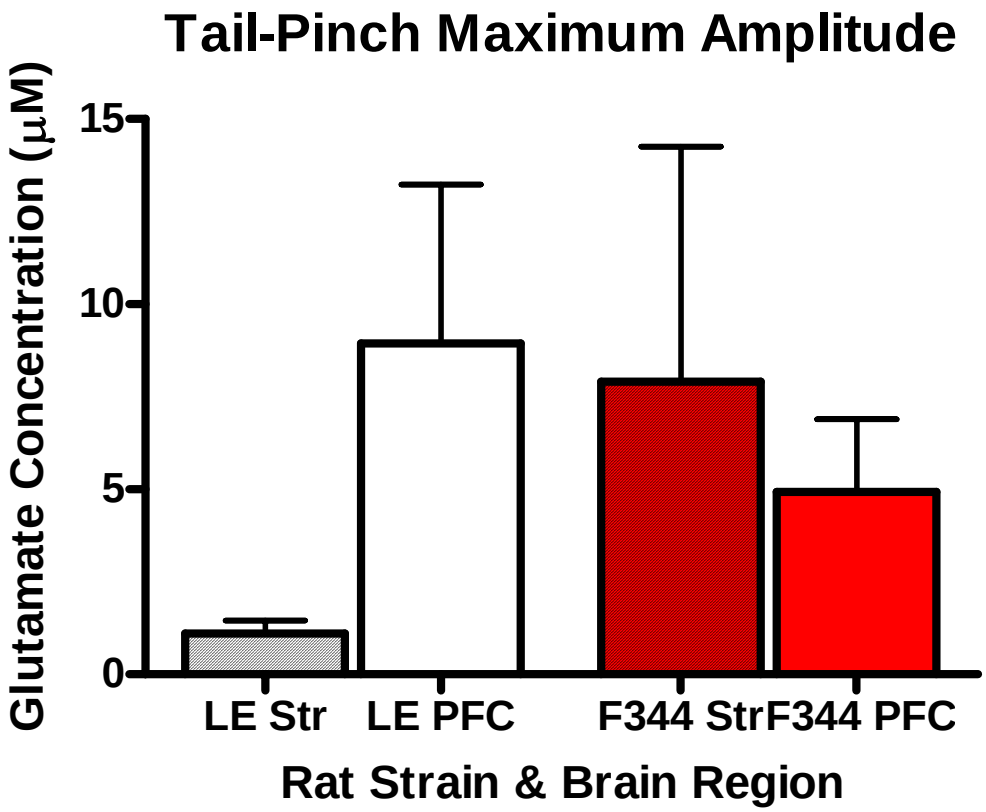

Figure 6.6: Maximum Amplitude during Tail-Pinch Response in the Striatum and Prefrontal Cortex of Fischer 344 and Long Evans Rats
Fischer 344 (F344) and Long Evans (LE) rats were implanted in the striatum (Str) or PFC and underwent a five minute tail-pinch stressor. The maximum amplitude of the Glu response to the tail-pinch was examined. No significant difference was observed (n=7, except Str F344 n=4).

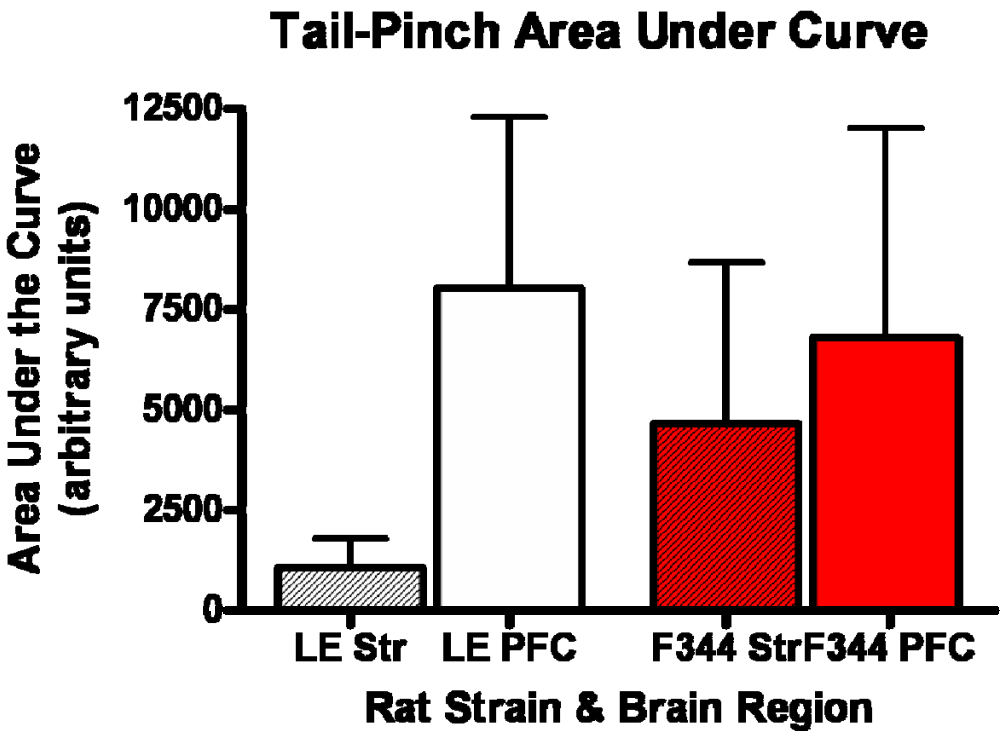

Figure 6.7: Area Under the Curve for Tail-Pinch Response in the Striatum and Prefrontal Cortex of Fischer 344 and Long Evans Rats
Fischer 344 (F344) and Long Evans (LE) rats were implanted in the striatum (Str) or PFC and underwent a five minute tail-pinch stressor. The area under the curve of the Glu response to the tail-pinch was examined. No significant difference was observed (n=7, except Str F344 n=4).

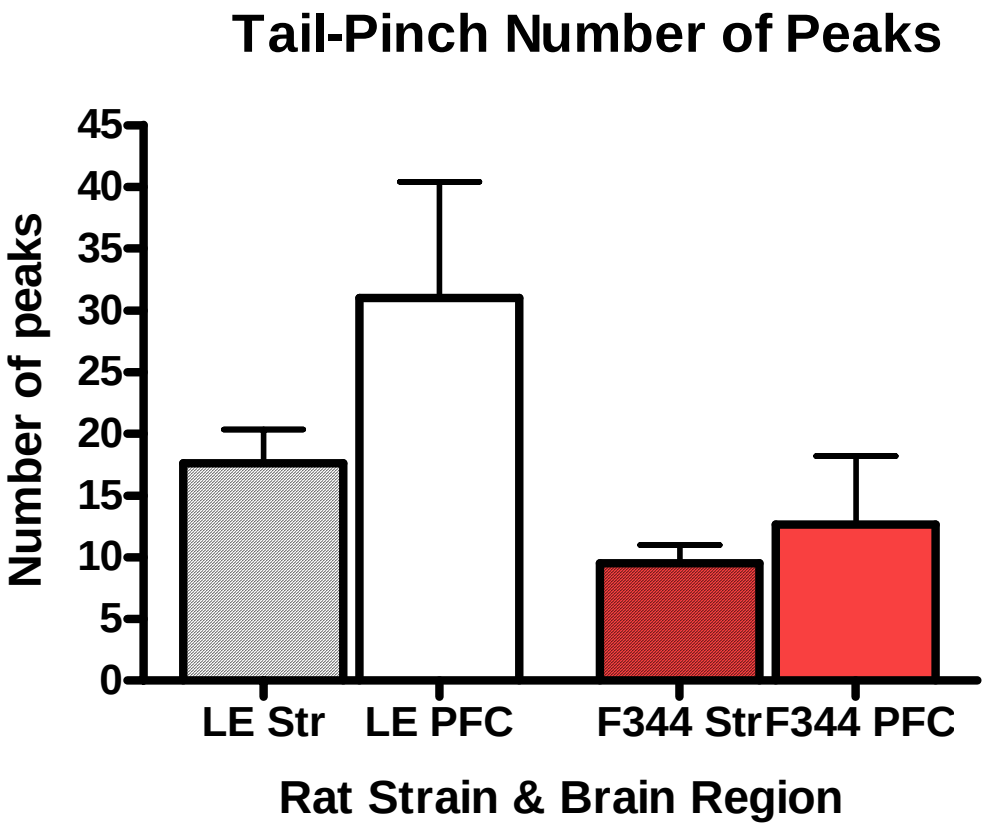

Figure 6.8: Number of Peaks during Tail-Pinch Response in the Striatum and Prefrontal Cortex of Fischer 344 and Long Evans Rats
Fischer 344 (F344) and Long Evans (LE) rats were implanted in the striatum (Str) or PFC and underwent a five minute tail-pinch stressor. The number of peaks during the Glu response to the tail-pinch was examined. No significant difference was observed (n=7, except Str F344 n=4).

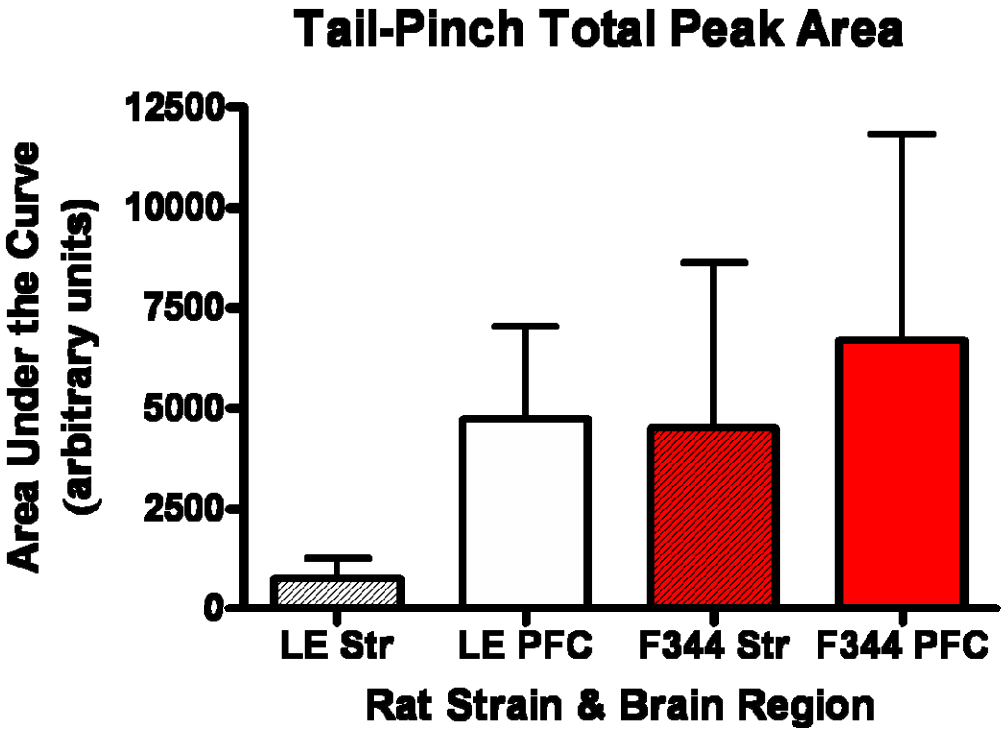

Figure 6.9: Total Peak Area for Tail-Pinch Response in the Striatum and Prefrontal Cortex of Fischer 344 and Long Evans Rats
Fischer 344 (F344) and Long Evans (LE) rats were implanted in the striatum (Str) or PFC and underwent a five minute tail-pinch stressor. The area under the curve for the peaks during the Glu response to the tail-pinch was examined. No significant difference was observed (n=7, except Str F344 n=4).

Chapter Seven: Preliminary Studies and Future Directions

Much work has been accomplished to develop and characterize the enzyme-based ceramic MEA for use in freely behaving animal recordings. Over the past several years there have been many advances in the freely moving recording system that have allowed us to optimize Glu studies in the awake rat. Our MEA design combined with our FAST-16 recording system has allowed for second-by-second measures of Glu. A new paddle design allowed for Glu recordings on four independent Pt recording sites and that number will soon increase to eight. Employing the self-referencing technique has allowed for measures of resting Glu levels and another way to verify that the analyte being measured is Glu. Our laboratory has been successful in moving freely behaving Glu recordings into a mouse model, which with the use of transgenic mouse models will give us the opportunity to greatly enhance our knowledge of how the glutamatergic system works and the possibility to study disease models more in depth (Hascup *et al*., 2006). Due to the nature of our enzyme-based MEAs, we are also capable of selectively measuring other analytes, such as dopamine and acetylcholine. This chapter is a compilation of the various trials, preliminary studies, and future directions surrounding my work in the awake, freely behaving rat.

In our initial studies (prior to the self-referencing capability) we wanted to determine if we could measure changes in Glu levels in a behaviorally relevant situation. Our laboratory was interested in stress and how it affects Glu levels in the striatum. Glu tracings of a typical tail-pinch stress in the striatum of Fischer 344 rats can be seen in Figure 7.1. The Glu response due to a 5 minute tail-pinch yielded a bimodal response. The initial phase was a rapid spike (A) lasting approximately 20 seconds. The second phase (B) of the response had a plateau appearance with a sustained increase in Glu levels compared to baseline (n=3). These fast changes in Glu levels that occurred in the freely behaving rats due to stress would not be accurately detectable using other current *in vivo* techniques, such as microdialysis, for measuring Glu. The prolonged plateau properties observed in the Glu signals due to stress is most likely the response observed in

current freely-moving microdialysis studies (Bagley and Moghaddam, 1997). Subsequent tail-pinches in the striatum of Fischer 344 rats resulted in a significantly decreased Glu response in both the spike (day 4 = 86.4 ± 7.5 μM vs. day 6 = 3.8 ± 1.9 μM) (Figure 7.2) and plateau portions (day 4 = 5.6 ± 0.1 μM vs. day 6 = 2.8 ± 0.1 μM; $p<0.001$) (Figure 7.3). These studies in the striatum of the Fischer 344 rats were performed prior to having the capability to use the self-referencing technique. Therefore, the above results reported for the Fischer 344 rat striatum tail-pinch stress data were reported as total Glu concentration and were not subtracted from sentinel sites. The oscilloscope was used in all studies and only signals matched with valid oscilloscope data were used. Taken together, these preliminary studies support that the improved temporal resolution of enzyme-based MEAs can be used for reliable second-by-second measures of Glu in the CNS of conscious freely moving rats and recordings in unanesthetized animals are necessary to accurately determine the dynamics of glutamatergic function.

We also have preliminary data in the freely moving rat that shows locally applied DA results in robust, reproducible peaks (Figure 7.4). Since DA was readily oxidized on our Pt recording surfaces, an enzyme coating was not necessary. Instead, the MEAs were coated with the exclusion layer, Nafion®, as with our Glu configured MEAs, to block interferents including DOPAC and ascorbate based on charge, but still allowed for DA to reach the recording sites. Next, two of the Pt recording sites (either 1 and 3 or 2 and 4) were electroplated with another exclusion layer, meta phenylenediamine (mPD). mPD formed a size exclusion layer that allowed molecules smaller than the matrix formed by mPD, such as H_2O_2, to pass through. However, larger molecules, such as DA, were not able to pass through the mPD layer. This coating procedure allowed oxidation of DA on the Pt recording sites that were only coated with Nafion®, but not on those coated with Nafion® and mPD. Since mPD can be selectively electropolymerized onto a Pt recording site, we can utilize side-by-side self-referencing for the DA selective MEA. We were able to record resting DA levels,

DA signals due to locally applied exogenous DA, and evoked DA release due to a physiological event, a tail-pinch stress (Figure 7.5).

The acetylcholine MEA relied on the same enzymatic principle established with the Glu configured MEA. However, the acetylcholine MEA required 2 enzymes, choline oxidase and acetylcholinesterase. Neither choline nor acetylcholine is readily oxidized at +0.7 V and therefore, they require enzymatic breakdown to H_2O_2 to be measured by our FAST-16 recording system. Acetylcholinesterase breaks down acetylcholine into acetic acid and choline. Choline is then broken down by choline oxidase into betaine and H_2O_2, which can be oxidized at +0.7 V. Again, by using the self-referencing techniques previously described for Glu selective MEAs, we were able to measure signals primarily due to acetylcholine. When the self-referencing technique is applied to acetylcholine selective MEAs, the acetylcholinesterase and choline oxidase coated sites were the analyte measuring sites and the sites coated with choline oxidase, but not acetylcholinesterase, were the self-referencing sites. Using this approach in the freely behaving rat, we were able to measure changes in acetylcholine due to tail-pinch stress (Figure 7.6).

In addition to the tail-pinch stressor, our laboratory also wanted to examine the affects of another possible stressor, such as exposure to a natural predator, the fox. To accomplish this, Glu was continuously recorded in the striatum of a Fischer 344 rat as previously described. Once baseline was established, fox urine was applied to a cotton ball and placed in the recording chamber for 50 seconds. We observed a delayed slight increase in Glu levels that immediately returned to baseline with the removal of the odor (Figure 7.7). The delay could be accounted for by the time it would take for the smell to reach all areas of the recording chamber.

We also examined another brain area, the somatosensory cortex, for Glu response to a subcutaneous injection of a NMDA receptor antagonist (MK-801) and contralateral vibrissae stimulation. There was no change in Glu levels in the somatosensory cortex associated with the injection of MK-801 (1 mg/kg). However, approximately 3.5 minutes after the MK-801 injection, the rat began to

seize (Figure 7.8). There was an increase in Glu in the somatosensory cortex that correlated in time with the seizure. When examining the affects of contralateral vibrissae stimulation on Glu in the somatosensory cortex a cotton tipped applicator was used to brush against the vibrissae for either 30 seconds or 60 seconds. Vibrissae stimulation resulted in an increase in Glu activity in the contralateral somatosensory cortex, but not an overall increase in Glu levels (Figure 7.9).

Our laboratory also wanted to study the effects of circadian rhythm on glutamatergic function on a second-by-second basis. This would give us the ability to monitor rapid changes that may occur during light and dark cycles in addition to the overall glutamatergic tone associated with these cycles. Additionally, with the capacity to measure in the awake behaving rat on a second-by-second time scale, we could couple our technology with an activity monitor to determine a direct association between activity level of the rat and changes in Glu levels. An important first step was taken to pursue this merging of technologies. We were able to continuously measure Glu in the PFC of a Long Evans rat for over 15 hours. We observed an overall increase in resting extracellular Glu levels in the PFC of a Long Evans rat that was associated with the dark cycle, the time when rats are more active (Figure 7.10).

Another area of interest is to combine the implantation of our MEAs with imaging techniques, such as magnetic resonance imaging (MRI). This capability could open the door to many research avenues. In addition to being able to determine tissue damage associated with chronic implant of our MEA, the ability to perform MRI guided implantation and recordings would allow us to strategically and accurately place the MEA in the brain area of interest and could allow us to record from small or hard to locate brain areas that would not be possible without guided placement. A specific type of MRI, functional MRI (fMRI), in conjunction with MEA recordings would allow us to correlate changes in neurotransmitter levels with functional activation of specific brain areas. We have taken a positive first step in being able to combine these two scientific methods. We have brain images from a rat that underwent chronic implantation of our MEA. The

implantation procedure followed those outlined in Chapter Two, except skull screws and guide cannula were not used since their metallic properties would interfere with the MRI scan. After one day post-implantation, the rat was anesthetized with urethane to minimize their movement in the MRI scanner and was sacrificed following imaging. Preliminary T1 MRI data showing images taken of the chronic MEA implantation clearly showed the tract from the implantation (Figure 7.11). Additionally, the MRI scan revealed that there is little to no edema associated with chronic implantation of our MEA. This supports our histopathological data of the chronic MEA implantations (see Chapter Five) which showed that our implantation materials and methods resulted in very little damage to the surrounding brain tissue as measured by GFAP (an astrocytic marker) and Iba1 (a microglial marker) that extended only approximately 50 – 100 μm into the tissue immediately surrounding the implantation site.

Many of these preliminary trials and studies have laid the groundwork for future experiments. We have been able to verify that by using our chronically implanted enzyme-based MEAs we are able to independently measure multiple analytes with our self-referencing technique. However, an important advantage of microdialysis is the ability to measure multiple analytes simultaneously. Our laboratory is in the process of developing MEAs with up to 36 recording sites. The additional recording sites will allow for multiple analytes to be measured using the self-referencing technique on a single MEA in a given brain area. These advances bring the promise of studies to evaluate neurotransmitter interactions in response to behavioral and chemical stimuli, such as the dopamine-Glu interactions that may exist in several brain areas, including the PFC and striatum.

Copyright © Erin Cathleen Rutherford

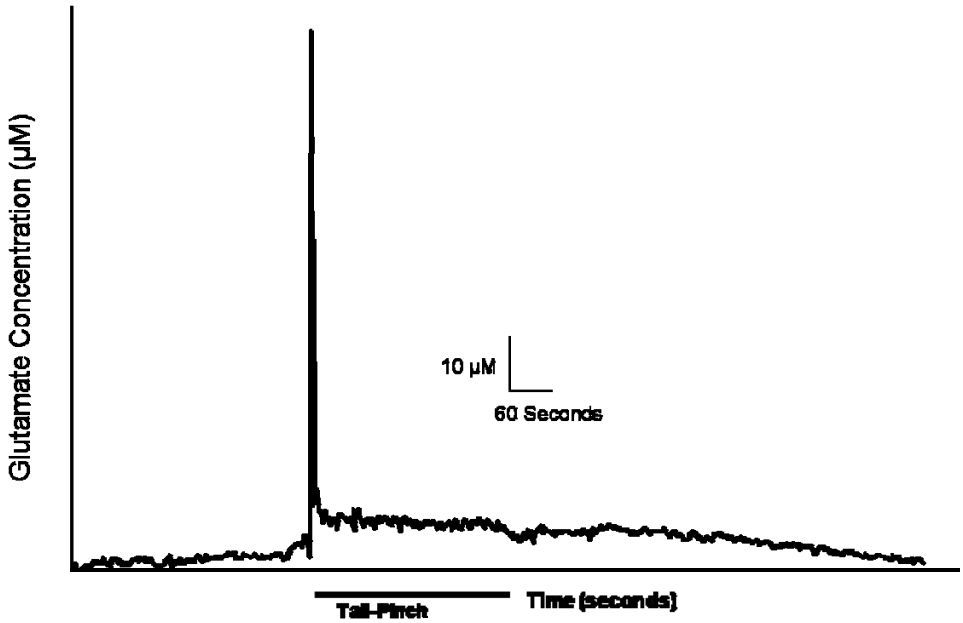

Figure 7.1: Tail-Pinch Response in the Fischer 344 Rat Striatum
Representative trace from the striatum of a Fischer 344 rats of a Glu response to a five minute tail-pinch. The response was bi-phasic with an initial rapid spike in Glu followed by prolonged plateau-like Glu levels. The duration of the tail-pinch is indicated by the solid black line.

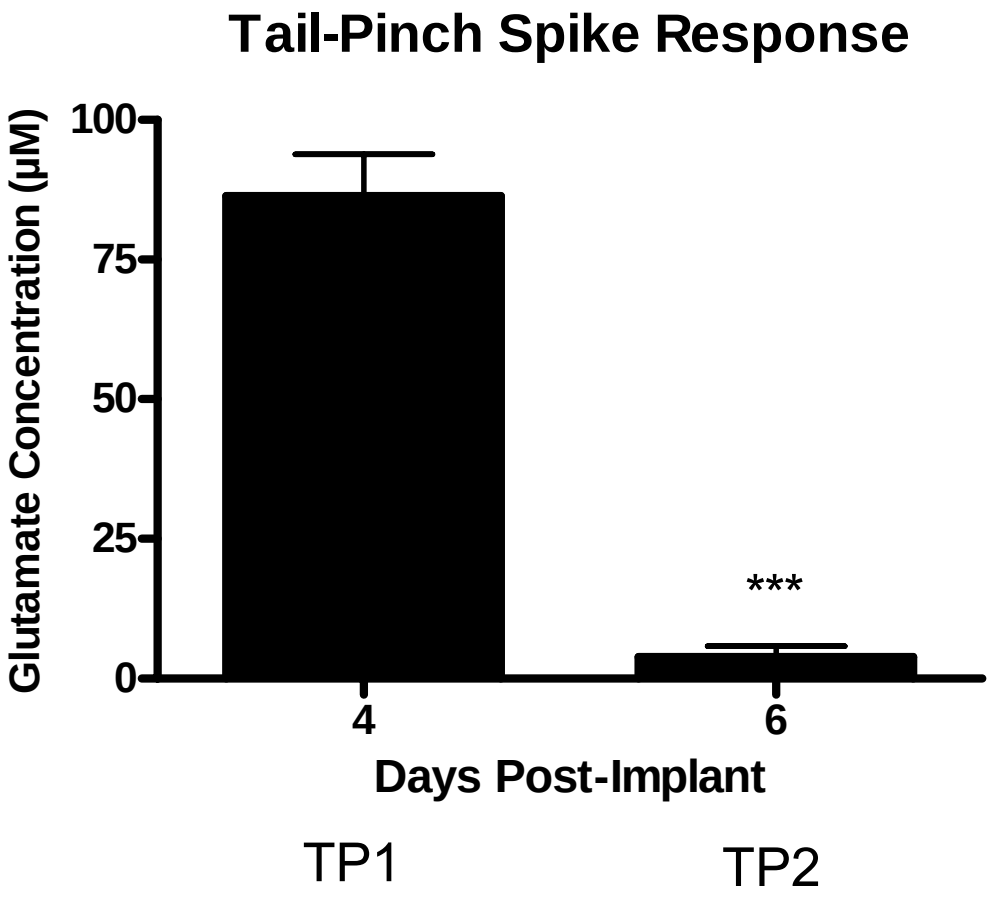

Figure 7.2: Fischer 344 Tail-Pinch Striatal Spike Response
Pedestal MEAs were implanted in the striatum of Fischer 344 rats. Rats underwent a five minute tail-pinch stressor. The maximum amplitude of the Glu response during the initial spike phase to the tail-pinch was examined. The maximum amplitude of the spike response was significantly decrease during the second tail-pinch (TP2), which occurred on day 6 post-implantation, as compared to the first tail-pinch (TP1), which occurred on day 4 post-implantation (***$p<0.001$).

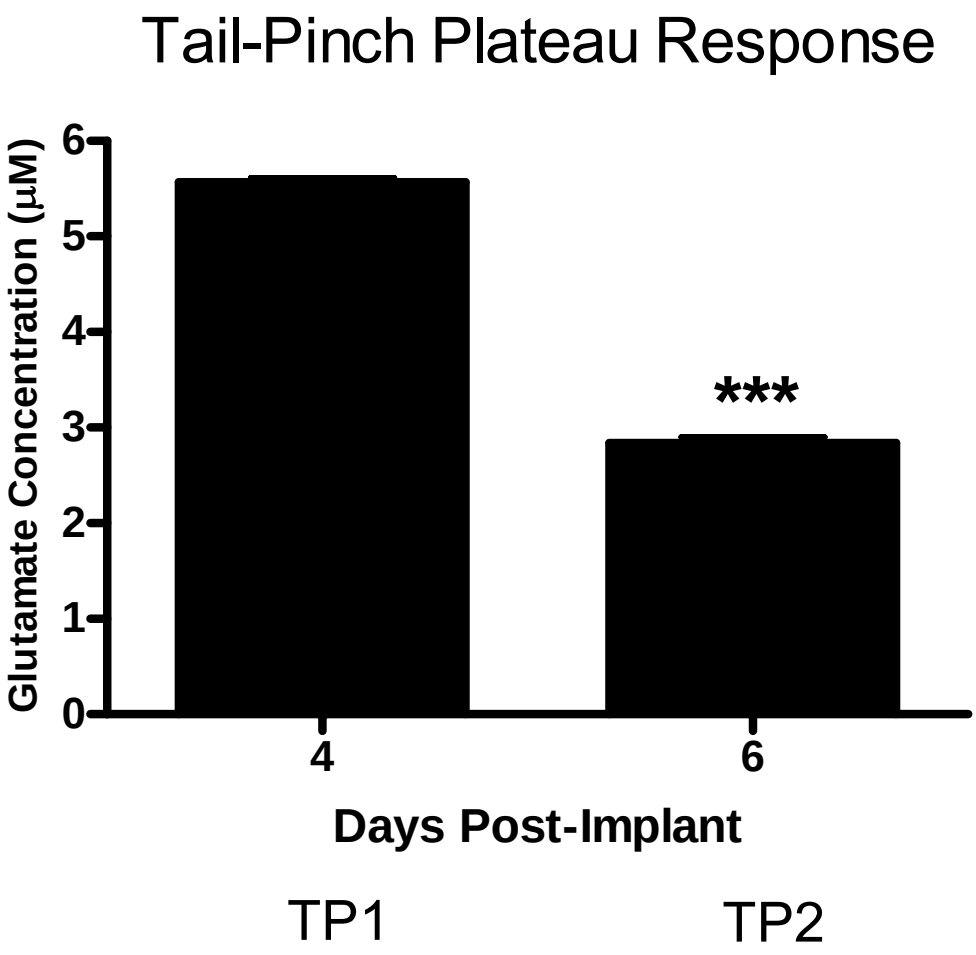

Figure 7.3: Fischer 344 Tail-Pinch Striatal Plateau Response
Pedestal MEAs were implanted in the striatum of Fischer 344 rats. Rats underwent a five minute tail-pinch stressor. The maximum amplitude of the Glu response during the plateau phase to the tail-pinch was examined. The maximum amplitude of the plateau response was significantly decrease during the second tail-pinch (TP2), which occurred on day 6 post-implantation, as compared to the first tail-pinch (TP1), which occurred on day 4 post-implantation (***$p<0.001$).

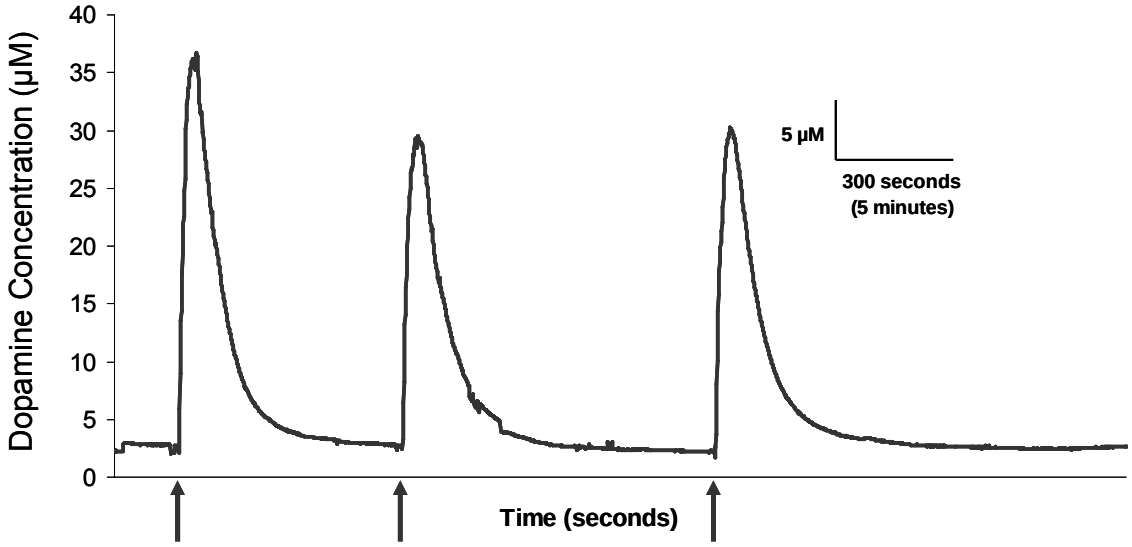

Figure 7.4: Local Application of Dopamine (200 µM, 1 µL) in the Striatum of a Long Evans Rat

Single recording of locally applied DA (200 µM, 1 µL) in the striatum of Long Evans rats. DA was locally applied (indicated by arrows) and detected using a self-referencing MEA. Tracing shown is the result of subtracting the self-referencing site (Nafion® and mPD) from the Nafion® coated site. DA peaks were robust and reproducible.

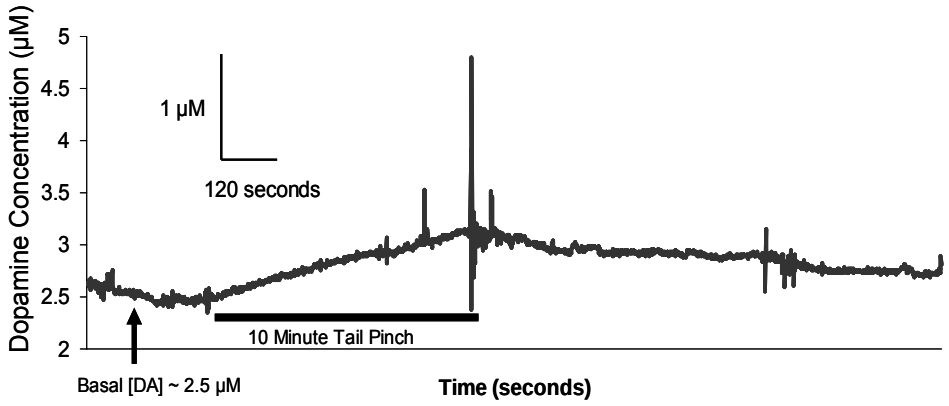

Figure 7.5: Dopamine Tail-Pinch Response in the Striatum of a Long Evans Rat
Single DA recording of a five minute tail-pinch response from the striatum of a Long Evans rat. The duration of the tail-pinch is indicated by the solid black line.

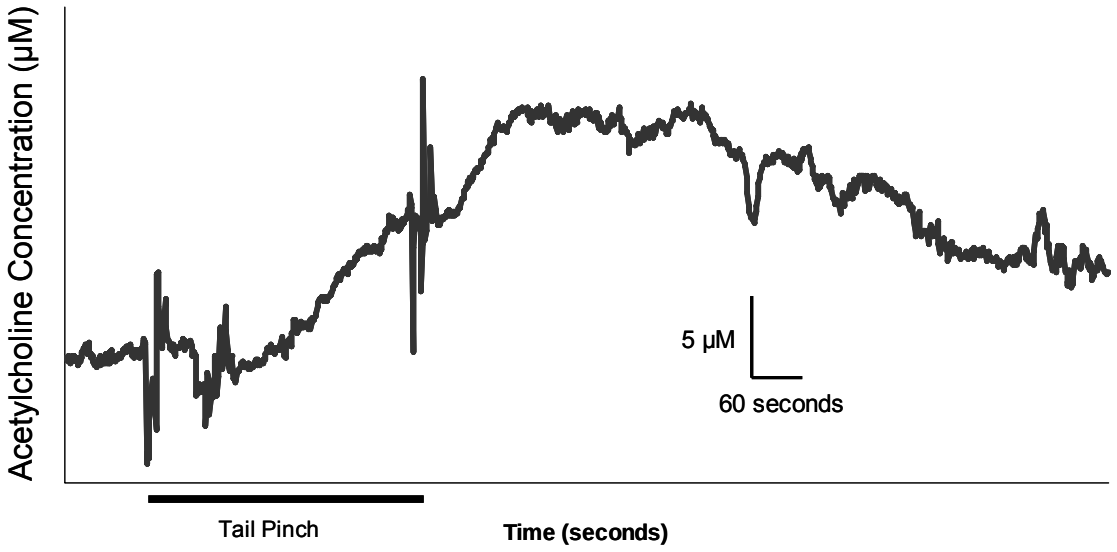

Figure 7.6: Achetylcholine Tail-Pinch Response in the Prefrontal Cortex of a Long Evans Rat
Single acetylcholine recording of a five minute tail-pinch response from the PFC of a Long Evans rat. The duration of the tail-pinch is indicated by the solid black line.

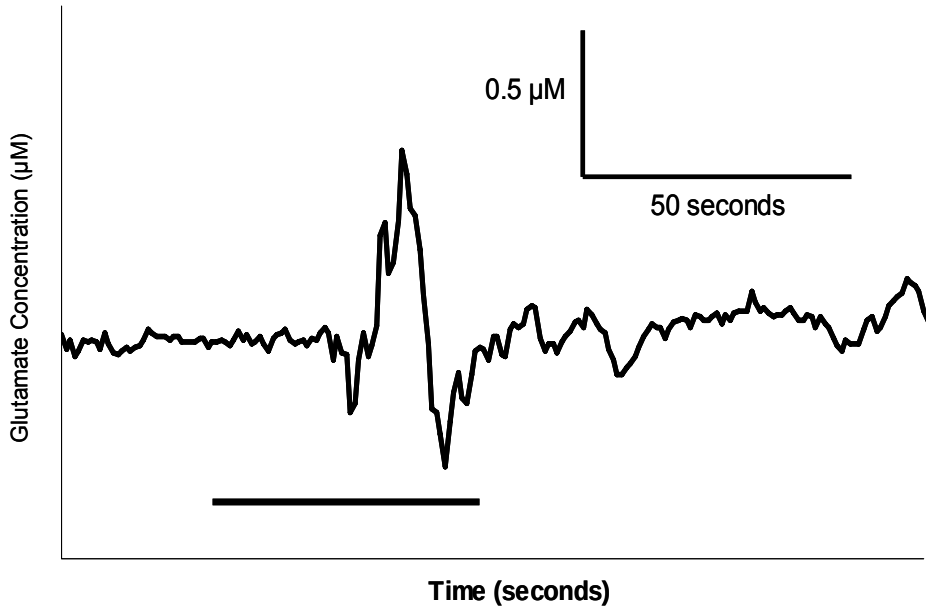

Figure 7.7: Glutamatergic Response to Fox Urine Exposure in the Striatum of a Fischer 344 Rat
Single glutamatergic recording of a response to fox urine odor in the striatum of a Fischer 344 rat. The duration of the fox urine exposure is indicated by the solid black line.

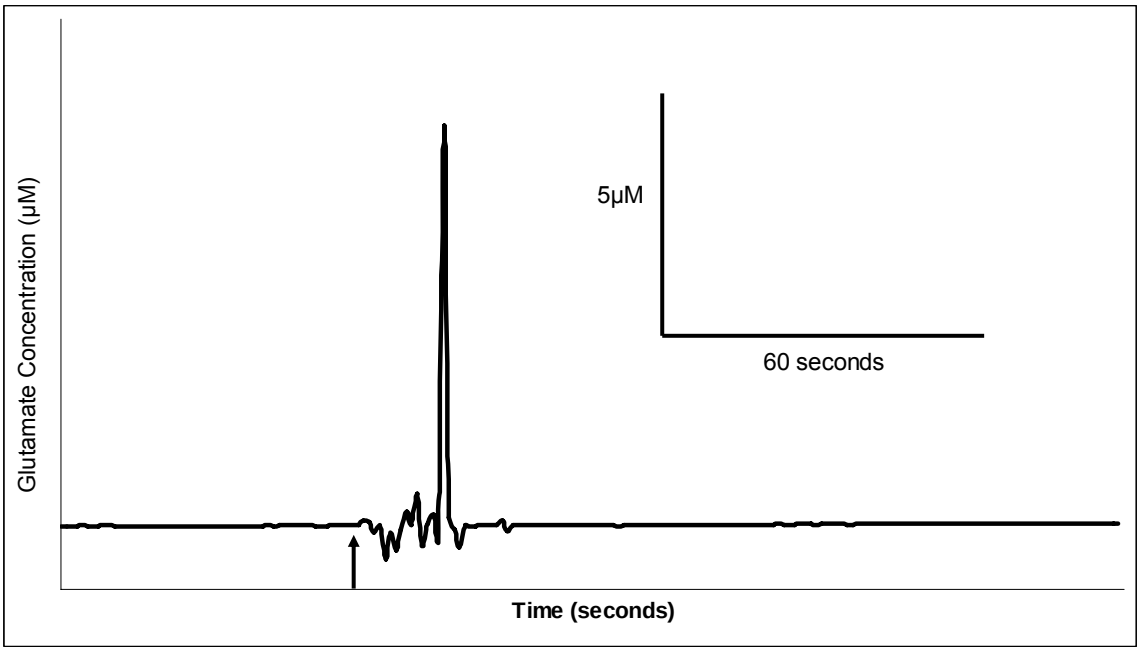

Figure 7.8: Glutamatergic Response to a NMDA Receptor Antagonist (MK-801) in the Somatosensory Cortex of a Long Evans Rat
Single glutamatergic recording of a response to a subcutaneous injection of MK-801 (1 mg/kg) in the somatosensory cortex of a Long Evans rat. Arrow indicates induction of a seizure approximately 3.5 minutes following injection.

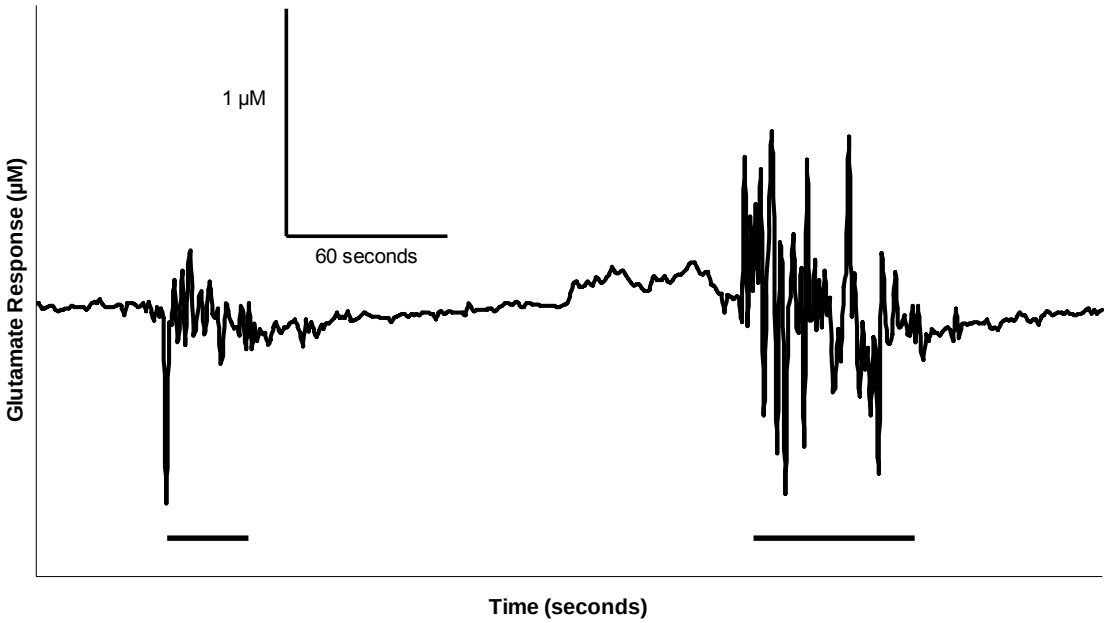

Figure 7.9: Glutamatergic Response to Contralateral Vibrissae Stimulation in the Somatosensory Cortex of a Long Evans Rat
Single glutamatergic recording of a 30 second (left) and 60 second (right) contralateral vibrissae stimulation response from the somatosensory cortex of a Long Evans rat. The duration of the vibrissae stimulation is indicated by the solid black line.

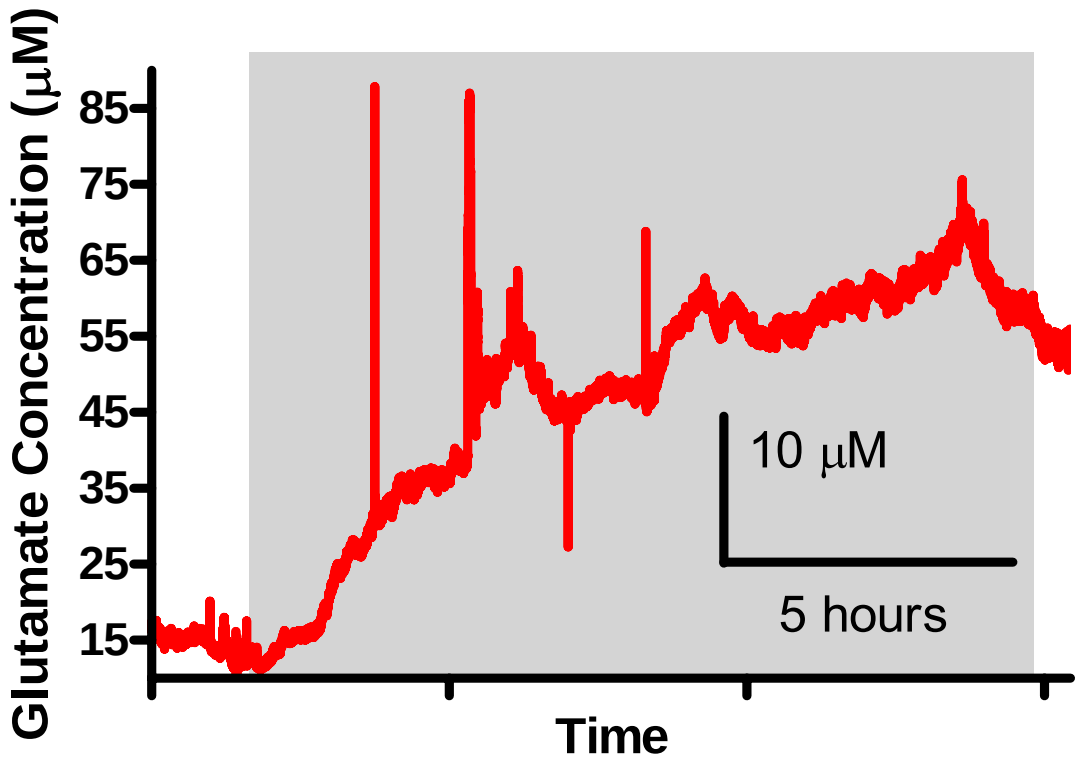

Figure 7.10: Continuous Second-By-Second Recording of L-Glutamate over Light and Dark Cycles
Single continuous recording of resting Glu levels in the PFC of a Long Evans rat encompassing the light (non-shaded region) and dark cycle (shaded region). Glu levels were elevated during the dark cycle as compared to the light cycle.

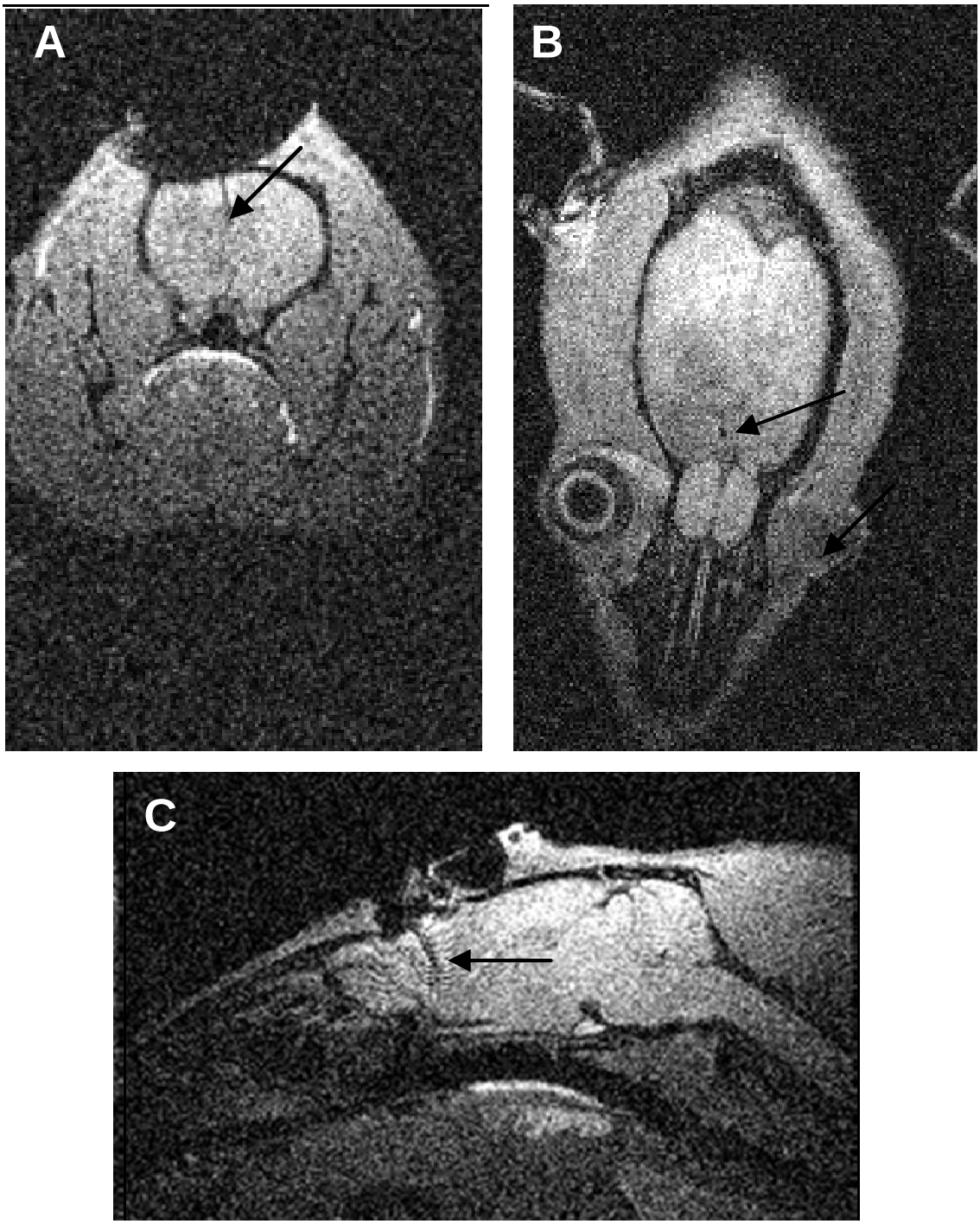

Figure 7.11: T1 MRI of an Implanted MEA in the Prefrontal Cortex of a Long Evans Rat
A) Coronal view of a T1 MRI of a MEA implanted in the right PFC of a Long Evans rat. B) Horizontal view of a T1 MRI of a MEA implanted in the right PFC of a Long Evans rat. C) Sagital view of a T1 MRI of a MEA implanted in the right PFC of a Long Evans rat. Arrows indicate MEA implant site.

References

Albrecht D, Davidowa H (1989) Action of Urethane on dorsal lateral geniculate neurons. Brain Res. Bull. 22, 923-927.

Alexander GE, DeLong, MR, and Strick PL (1986) Parallel organization of functionally segregated circuits linking basal ganglia and cortex. Ann. Review of Neurosci. 9, 357-381.

Aultman JM, Moghaddam B (2001) Distinct contributions of glutamate and dopamine receptors to temporal aspects of rodent working memory using a clinically relevant task. Psychopharmacologia. 153, 353-364.

Bagley J, Moghaddam B (1997) Temporal dynamics of glutamate efflux in the prefrontal cortex and in the hippocampus following repeated stress: Effects of pretreatment with saline or diazepam. Neuroscience. 77, 65-73.

Baker DA, Xi ZX, Shen H, Swanson CJ, Kalivas PW (2002) The orgin and neuronal function of *in vivo* nonsynaptic glutamate. J. Neurosci. 22(20), 9134-9141.

Belay A, Collins A, Ruzgas T, Kissinger PT, Gorton L, Csöregi E (1998) Redox hydrogel based bienzyme electrode for L-glutamate monitoring. J. Pharmaceutical & Biomedical Analysis 19(1-2), 93-105.

Bindman LJ, Meyer T, Prince CA (1988) Comparison of the electrical properties of neocortical neurons in slices in vitro and in the anaesthetized rat. Exp. Brain Res. 69, 489-496.

Bland ST, Gonzales RA, Schallert T (1999) Movement-related glutamate levels in rat hippocampus, striatum, and sensorimotor cortex. Neurosci. Letters. 277, 119-122.

Boatell ML, Bendahan G, Mahy N (1995) Time-related cortical amino acid changes after basal forebrain lesion: a microdialysis study. J. Neurochem. 64, 285.

Borland LM, Guoyue S, Hua Y, Michael AC (2005) Voltammetric study of extracellular dopamine near microdialysis probes acutely implanted in the striatum of anesthetized rat. J. Neurosci. Methods. 146, 149-158.

Burmeister JJ, Moxon K, Gerhardt GA (2000) Ceramic-based multisite microelectrodes for electrochemical recordings. Anal.Chem. 72, 187-192.

Burmeister JJ and Gerhardt GA (2001) Self-referencing ceramic-based multisite microelectrodes for the detection and elimination of interferences from the measurement of L-glutamate and other analytes. Anal.Chem. 73, 1037-1042.

Burmeister JJ, Pomerleau F, Palmer M, Day BK, Huettl P, Gerhardt GA (2002) Improved ceramic-based multisite microelectrode for rapid measurements of L-glutamate in the CNS. J. Neurosci. Methods. 119, 163-171.

Campagna JA, Miller KW, Phil D, Forman SA (2003) Mechanism of actions of inhaled anesthetics. N Engl J Med. 348, 2110-24.

Carlsson M, Carlsson A (1990) Interaction between glutamatergic and monoaminergic systems within the basal ganglia – implications for schizophrenia and Parkinson's disease. Trends Neurosci. 13, 272-276.

Castaneda TR, de Prado BM, Prieto D, and Mora F (2004) Circadian rhythms of dopamine, glutamate and GABA in the striatum and nucleus accumbens of the awake rat: modulation by light. J. Pineal Res. 36, 177-85.

Cellar NA, Burns ST, Meiners JC, Chen H, Kennedy RT (2005) Microfluidic chip for low-flow push-pull perfusion sampling in vivo with on-line analysis of amino acids. Anal Chem. 77(21), 7067-73.

Clapp-Lilly KL, Roberts RC, Duffy LK, Irons KP, Hu Y, Drew KL (1999) An ultrastructural analysis of tissue surrounding a microdialysis probe. J. Neurosci. Methods. 90, 129-142.

Clements JD (1996) Transmitter timecourse in the synaptic cleft: its role in central synaptic function. Trends Neurosci. 19, 163-171.

Danbolt NC (2001) Glutamate uptake. Prog. Neurobiol. 65, 1-105.

Day BK, Pomerleau F, Burmeister JJ, Huettl PF, Gerhardt GA (2006) Microelectrode array studies of basal and potassium-evoked release of L-glutamate in the anesthetized rat brain. J. Neurochem. 96(6), 1626-1635.

Del Arco A, Castaneda TR, Mora F (1998) Amphetamine releases GABA in striatum of the freely moving rat: involvement of calcium and high affinity transporter mechanisms. Nueropharmacology 37, 199-205.

Del Arco A, González-Mora JL, Armas VR, Mora F (1999) Amphetamine increases extracellular concentrations of glutamate in striatum of the awake rat: involvement of high affinity transporter mechanisms. Neuropharmacology 38, 943-954.

Delatour B, Grisquet-Verrier P (1996) Prelimbic cortex specific lesions dirupt delayed-variable response tasks in the rat. Behav. Neurosci. 110, 1282-1298.

Deptula D, Singh R, Pomara N (1993) Aging, emotional stress, and memory. Am. J. Psychiatry 150, 429-434.

Di Cara B, Dusticier N, Forni C, Lievens JC, Daszuta A (2001) Serotonin depletion produces long lasting increase in striatal glutamatergic transmission. J. Neurochem. 78, 240.

Doherty MD, Gratton A (1996) Medial prefrontal cortical D_1 receptor modulation of the meso-accumbens dopamine response to stress: an electrochemical study in freely-behaving rats. Brain Res. 715, 86-97.

Doherty MD, Gratton A (1997) NMDA receptors in nucleus accumbens modulate stress-induced dopamine release in nucleus accumbens and ventral tegmental area. Synapse. 26, 225-234.

Dyer RS, Rigdon GC (1987) Urethane affects the rat visual system at subanesthetic doses. Physiol. Behav. 41, 327-330.

Fillenz M (1995) Physiological release of excitatory amino acids. Behavioral Brain Research. 71, 51-67.

Fitzpatrick JS, Akopian G, Walsh JP (2001) Short-term plasticity at inhibitory synapses in rat striatum and its effects on striatal output. J Neurophysiol. 85, 2088-2099.

Floresco SB, Seamans JK, Phillips AG (1996) Differential effects of lidocaine infusions into the ventral CA1/subiculum or the nucleus accumbens on the acquisition and retention of spatial information. Behav. Brain Res. 81, 163-172.

Fornieles F, Peinado JM, Mora F (1986) Endogenous levels of amino acid neurotransmitters in different regions of frontal and temporal cortex of the rat during the normal process of aging. Neurosci. Lett. Suppl. 26, 150.

Gerhardt GA, Oke AF, Nagy G, Moghaddam B, Adams RN (1984) Nafion-coated electrodes with high selectivity for CNS electrochemistry. Brain Res. 290, 390-395.

Gerhardt GA, Ksir C, Pivik C, Dickinson SD, Sabeti J, and Zahniser NR (1999) Methodology for coupling local application of dopamine and other chemicals with

rapid in vivo electrochemical recordings in freely-moving rats. J. Neurosci Meth. 87, 67-76.

Gilad GM, Gilad VH, Wyatt RJ, Tizabi Y (1990) Region-selective stress-induced increase of glutamate uptake and release in rat forebrain. Brain Research. 525, 335-338.

Girman SV, Suave Y, Lund RD (1999) Receptive field properties of single neurons in rat primary visual cortex. J. Neurophysiol. 82, 301-311.

Glass JD, Hauser UE, Blank JL, Selim M, and Rea MA (1993) Differential timing of amino acid and 5-HIAA rhythms in suprachiasmatic hypothalamus. Am. J. Physiol. 265, R504-11.

Grace AA (1991) Phasic versus tonic dopamine release and the modulation of dopamine system responsivity: a hypothesis for the etiology of schizophrenia. Neuroscience 41, 1-24.

Granon S, Poucet B (1995) Medial prefrontal lesions in the rat and spatial navigation: Evidence for impaired learning. Behav. Neurosci. 109, 474-484.

Greenamyre JT (1993) Glutamate – dopamine interactions in the basal ganglia: relationship to Parkinson's disease. J. Neural Transm. 91, 255-269.

Greengard P (2001) The neurobiology of slow synaptic transmission. Science 294-1024-1030.

Hascup KN, Rutherford EC, Quintero JE, Day BK, Nickell JR, Pomerleau F, Huettl P, Burmeister JJ, Gerhardt GA (2006) Second-by-Second Measures of L-Glutamate and Other Neurotransmitters Using Enzyme-Based Microelectrode Arrays. Chapter 19 of Electrochemical Methods for Neuroscience.

Honma S, Katsuno Y, Shinohara K, Abe H, Honma K (1996) Circadian rhythm and response to light of extracellular glutamate and aspartate in rat suprachiasmatic nucleus. Am. J. Physiol. 271, R579-85.

Hostenpillar G, Wolf ME (2002) Extracellular glutamate levels in prefrontal cortex during the expression of associative responses to cocaine related stimuli. Neuropharm. 43, 1218-1229.

Hurley KM, Herbert H, Moga MM, Saper CB (1991) Efferent projections of the infralimbic cortex of the rat. J. Comp. Neurol. 308, 249-76.

Imai Y, Ibata I, Ito D, Ohsawa K, Kohsaka S (1996) A novel gene iba1 in the major histocompatibility complex class III region encoding an EH hand protein expressed in a monocytic lineage. Biochem Biophys. Res. Comm. 224, 855-862.

Ingram DK (1985) Analysis of age-related impairments in learning and memory in rodent models. Ann. N.Y. Acad. Sci. 444, 312-331.

Ito D, Imai Y, Ohsawa K, Makajima K, Fukuuchi Y, Kohsaka S (1998) Microglia-specific localization of a novel calcium binding protein, Iba1. Mol. Brain Res. 57, 1-9.

Jedema HP, Moghaddam, B (1994) Glutamatergic control of dopamine release during stress in the rat prefrontal cortex. J. Neurochem. 63, 785-788.

Kennedy RT, Watson CJ, Haskins WE, Powell DH, Strecker RE (2002) In vivo neurochemical monitoring by microdialysis and capillary separations. Current Opinion in Chem. Biol. 6, 659-665.

Kalivas PW, McFarland K (2003) Brain circuitry and the reinstatement of cocaine-seeking behavior. Psychopharm. 168, 44-56.

Kalivas PW (2004) Glutamate systems in cocaine addiction. Curr. Opin. Pharm. 4, 23-29.

Kesner RP, Hunt ME, Williams JM, Long JM (1996) Prefrontal cortex and working memory for spatial response, spatial location and visual object information in the rat. Cereb. Cortex. 6, 311-318.

Krnjevic K (1986) Amino acid transmitters: 30 year's progress in research. "Fast and Slow Signaling in the Nervous System" (Iversen, LL and Goodman E, Eds.), pp .3-15. Oxford University Press, Oxford.

Kullmann DM, Asztely F (1998) Extrasynaptic glutamate spillover in the hippocampus: evidence and implications. Trends Neurosci. 21, 8-14.

Laurenzi MA, Arcuri C, Rossi R, Marconi P, Bocchini V (2002) Effects of microenvironment on morphology and function of the microglial cell line BV-2. Neurochem. Res. 26 (11), 1209-1216.

Liachenko S, Tang P, Somogyi GT, Xu Y (1998) Comparison of anaesthetic and non-anaesthetic effects on depolarization-evoked glutamate and GABA release from mouse cerebrocortical slices. Brit. J. of Pharm. 123, 1274.

Liachenko S, Tang P, Somogyi GT, Xu Y (1999) concentration-dependent isoflurane effects on depolarization-evoked glutamate and GABA outflows from mouse brain slices. Brit. J. of Pharm. 127, 131.

McFarland K, Davidge SB, Lapish CC, Kalivas PW (2004) Limbic and motor circuitry underlying footshock-induced reinstatement of cocaine-seeking behavior. J. Neurosci. 24, 1551-1560.

Melendez RI, Vuthiganon J, Kalivas PW (2005) Regulation of extracellular glutamate in the prefrontal cortex: focus on the cystine glutamate exchanger and

group I metabotropic glutamate receptors. J. Pharm. and Experimental Therapeutics 314(1), 139-147.

Michaelis EK (1997) Molecular biology of glutamate receptors in the central nervous system and their role in excitotoxicity, oxidative stress, and aging. Prog. Neurobiol. 54, 369-415.

Moghaddam B (1993) Stress preferentially increases extraneuronal levels of excitatory amino acids in the prefrontal cortex: comparison to hippocampus and basal ganglia. J. Neurochem. 60, 1650-1657.

Moghaddam B (2002) Stress Activation of Glutamate Meurotransmission in the Prefrontal Cortex: Implications for Dopamine-Associated Psychiatric Disorders. Society of Biological Psychiatry. 51:775-787.

Mufson EJ, Stein DG (1980) Behavioral and morphological aspect of aging: an analysis of rat frontal cortex. In: Stein DG (Ed.), The Psychobiology of Aging: Problems and Perspectives. Elsevier, New York, 99-125.

Murray AM, Waddington JL (1991) Age-related changes in the regulation of behavior by D1:D2 dopamine receptor interactions. Neurobiol. Aging 12, 431-435.

Nickell J, Pomerleau F, Allen J, Gerhardt GA (2005) Age-related changes in the dynamics of potassium-evoked L-glutamate release in the striatum of Fischer 344 rats. J.Neural Transm. 112, 87-96.

Oldenziel WH, Dijkstra G, Cremers TIFH, Westerink B.H.C. (2006a) In vivo monitoring of extracellular glutamate in the brain with a microsensor. Brain Research 1118, 34-42.

Oldenziel WH, Dijkstra G, Cremers TIFH, Westerink B.H.C. (2006b) Evaluation of hydrogel-coated glutamate microsensors. Anal. Chem. 78, 3366-3378.

Paxinos G, Watson C (2005) The rat brain: in stereotaxic coordinates, 5th addition. ElsevierAcademic Press: Massachusetts.

Pomerleau F, Day BK, Huettl P, Burmeister JJ, Gerhardt GA (2003) Real time in vivo measures of L-glutamate in the rat central nervous system using ceramic-based multisite microelectrode arrays. Ann.N.Y.Acad.Sci. 1003, 454-457.

Ranft A, Kurz J, Deuringer M, Haseneder R, Dodt H, Zieglgänsberger W, Kochs E, Eder M, Hapfelmeier G (2004) Isoflurane modulates gluamatergic and GABAergic neurotransmission in the amygdala. E. J. of Neurosci. 20, 1276-1280.

Rocha L, Briones M, Ackermann RF, Anton B, Maidment NT, Evans CJ, Engel J Jr. (1996) Pentylenetetrazol-induced kindling: early involvement of excitatory and inhibitory systems. Epilepsy Research 26, 105-113.

Rutherford EC, Pomerleau F, Huettl P, Strömberg I, and GA Gerhardt (2007) Chronic second-by-second measures of L-glutamate in the CNS of freely moving rats. (in press - *Journal of Neurochemistry*).

Sabeti J, Adams CE, Burmeister J, Gerhardt GA, Zahniser NR (2002) Kinetic analysis of striatal clearance of exogenous dopamine recorded by chronoamperometry in freely-moving rats. J. Neurosci. Meth. 121, 41-52.

Sabeti J, Gerhardt GA, Zahniser NR (2003) Chloral hydrate and ethanol, but not urethane, alter the clearance of exogenous dopamine recorded my chronoamperometry in striatum of unrestrained rats. Neurosci. Letters 343 (1), 9-12.

Sceniak MP, MacIver MB (2006) Cellular actions of urethane on rat visual cortical neurons in vitro. J. Neurophysiol. 95, 3865-3874.

Schoepp DD (2001) Unveiling the functions of presynaptic metabotropic glutamate receptors in the central nervous system. J. Pharm and Exp. Therapeutics. 299(1), 12-20.

Seamans J, Floresco, Phillips A (1995) Functional differences between the prelimbic and anterior cingulated regions of the rat prefrontal cortex. Behav. Neurosci. 109, 1063-1073.

Segovia G, Del Arco A, Prieto L, Mora F (2001) Glutamate-glutamine cycle and aging in striatum of the awake rat: effects of a glutamate transporter blocker. Neurochemical Research 26(1), 37-41.

Segovia G, Porras A, Del Arco A, Mora F (2001b) Glutamatergic neurotransmission in aging: a critical perspective. Mechanisms of Ageing and Development. 122 (1): 1-29.

Shou M, Smith AD, Shackman JG, Peris J, Kennedy RT (2004) In vivo monitoring of amino acids by microdialysis sampling with on-line derivatization by naphthalene-2,3-dicarboxyaldehyde and rapid micellar electrokinetic capillary chromatography. J. Neurosci. Methods 138, 189-197.

Stevenson CW, Gratton A (2003) Basolateral amygdala modulation of the nucleus accumbens dopamine response to stress: role of the medial prefrontal cortex. Euro. J. Neurosci. 17, 1287-1295.

Stevenson CW, Sullivan RM, Gratton A (2003) Effects of basolateral amygdala dopamine depletion on the nucleus accumbens and medial prefrontal cortical dopamine responses to stress. Neuroscience. 116, 285-293.

Stevenson CW, Gratton A (2004) Basolateral amygdala dopamine receptor antagonism modulates initial reactivity to but not habituation of the acoustic startle response. Behav. Brain Res. 153, 383-387.

Takahata R, Moghaddam B (1998) Glutamatergic regulation of basal and stimulus-activated dopamine release in the prefrontal cortex. J. Neurochem. 71: 1443-1449.

Timmerman W, Westerink BHC (1997) Brain microdialysis of GABA and glutamate: What does it signify? Synapse 27, 242-261.

Tucci S, Rada P, Sepulveda MJ, Hernandez L (1997) Glutamate measured by 6-s resolution brain microdialysis: capillary electrophoretic and laser-induced fluorescence detection application. J. Chromatography 694, 343-349.

Valdes TI, Moussy F (2000) In vitro and in vivo degradation of glucose oxidase enzyme used for implantable glucose biosensor. Diabetes Technology and Therapuetics 2 (3), 367-376.

Waagepetersen HS, Sonnewald U, Larsson OM, Schousboe A (2000) A possible role of Alanine for ammonia transfer between astrocytes and glutamatergic neurons. J. Neurochem. 75, 471-479.

Watkins JC (1986) Twenty-five years of excitatory amino acid research: The end of the beginning? "Excitatory Amino Acids" (Roberts, PJ, Storm-Mathisen, J, and Bradford, J, Eds), pp 1-39. Macmillan, London.

Wisniewski N, Reichert M (2000) Methods for reducing biosensor membrane biofouling. Colloids and Surfaces 18, 197-219.

VITA

Name: Erin Cathleen Rutherford

Date of Birth: 10/17/1978

Birthplace: Cincinnati, Ohio

Education

2001	B.S. Biochemistry with Honors, Hobart and William Smith Colleges, Geneva, New York 14456
1996	High School Diploma, Cincinnati Country Day School Cincinnati, Ohio 45243

Professional Experience

2002-2007	Doctoral candidate, University of Kentucky, Department of Anatomy and Neurobiology, Greg Gerhardt, Ph.D., Supervisor
2003-2007	Undergraduate/Graduate Student Mentor, University of Kentucky, Department of Anatomy and Neurobiology, Greg Gerhardt, Ph.D., Supervisor
2006	FAST-16 Installation and Training, Karolinska Institute, Department of Pharmacology, Stockholm, Sweden

2004, 2005, 2006	Center for Sensor Technology Training Course, University of Kentucky, Greg Gerhardt, Ph.D., Supervisor
2004	Teaching assistant, University of Kentucky, Department of Anatomy and Neurobiology, Pam Stein, Supervisor
2002	Student researcher, University of Kentucky, Department of Anatomy and Neurobiology, Paul Glaser, Ph.D., Supervisor
2002	Student researcher, University of Kentucky, Department of Biochemistry, Rebecca Dutch, Ph.D., Supervisor
2001-2002	Research assistant, Los Alamos National Laboratory, Bioscience Division, Theresa Ruscetti, Ph.D., Supervisor
2000-2001	Student researcher, Hobart and William Smith Colleges, Department of Biochemistry, Paul Pyenta, Ph.D., Supervisor
1999-2000	Student researcher, Hobart and William Smith Colleges, Department of Biochemistry, Joel Kerlan, Ph.D., Supervisor

Scholastic and Professional Honors

2007	Invited Speaker 12th Institute of Biological Engineering Meeting St. Louis, Missouri Czarena Crofcheck, Ph.D., Chairman
2007	Graduate Student Outstanding Poster Award Bluegrass Chapter, Society for Neuroscience University of Kentucky Michael Bardo, Ph.D., Chairman
2004-2006	National Institute for Drug Abuse Fellowship University of Kentucky Lou Hersh, Ph.D., Chairman
2006	Graduate Student Outstanding Poster Award Monitoring Molecules in Neuroscience – 11th International Congress on *In Vivo* Methods Sardinia, Italy Gaetano Di Chiara, Ph.D., Chairman
2006	Graduate Student Outstanding Poster Award Bluegrass Chapter, Society for Neuroscience University of Kentucky Joe Springer, Ph.D., Chairman
2005	Graduate Student Outstanding Poster Award Bluegrass Chapter, Society for Neuroscience University of Kentucky Greg Gerhardt, Ph.D., Chairman

2001	Honors for Outstanding Original Undergraduate Research Department of Biochemistry Hobart and William Smith Colleges Paul Pyenta, Ph.D., Chairman
1997-2001	Hobart and William Smith Colleges Tuition Scholarship

Publications

Manuscripts:

Rutherford EC, Pomerleau F, GA Gerhardt (2007) Real time effects of stress on L-glutamate in the prefrontal cortex and striatum of freely moving rats. (manuscript in preparation).

Rutherford EC, Pomerleau F, Huettl P, Strömberg I, GA Gerhardt (2006) Chronic second-by-second measures of L-glutamate in the CNS of freely moving rats. In press- *Journal of Neurochemistry*.

Currier Thomas C, Kruzich PJ, Joyce BM, Gash CR, Suchland KL, Rutherford EC, Surgener SP, Grandy DK, Gerhardt GA, Glaser PEA (2006) Dopamine D4 Receptor Knockout Mice Exhibit Behavioral and Neurochemical Changes Consistent with Decreased Dopamine Release (in press *Journal of Neuroscience Methods*).

Rutherford E, Max T, Nickololoff JA, Ruscetti T (2007) Strict Regulation of Homologous Recombination in Ribosomal DNA is Largely Sir2p Independent (submitted to *Molecular and Cellular Biology*).

Rutherford E, Pyenta PS (2001) Investigation of the Relative Distance Between Antigen Combining Sites of IgE. Honors Thesis, Hobart and William Smith Colleges.

Book Chapters

M.L. Stephens, D.D. Spencer, I. Cavus, M.C. Hsiao, D. Song, S.H. Courellis, S.A. Deadwyler, R.E. Hampson, D. Putz, J.E. Quintero, M.K. Bensalem-Owen, K.N. Hascup, E.C. Rutherford, B.K. Day, J.R. Nickell, F. Pomerleau, P. Huettl, J.J. Burmeister, P.M. Talauliker, V.Z. Marmarelis, J.J. Granacki, T. Berger, G.A. Gerhardt. (in press, 2007) Microelectrode-Based Eplilepsy Therapy: A Hybrid Neural Prothesis Incorporating Seizure Prediction and Intervention with Biomimetic Maintenance of Normal Hippocampal Function. Computational Neuroscience in Epilepsy.

Hascup KN, Rutherford EC, Quintero JE, Day BK, Nickell JR, Pomerleau F, Huettl P, Burmeister JJ, Gerhardt GA (2006) Second-by-Second Measures of L-Glutamate and Other Neurotransmitters Using Enzyme-Based Microelectrode Arrays. Chapter 19 of Electrochemical Methods for Neuroscience.

Abstracts

Rutherford EC, Pomerleau F, Huettl P, Strömberg I, Johnson KW, Gerhardt GA. Second-by-Second Enzyme-Based Amperometric Recordings of L-Glutamate in Awake Rats. 12th Institute of Biological Engineering Meeting. St. Louis, Missouri March, 2007.

K.N. Hascup, E.C. Rutherford, F. Pomerleau, P. Huettl, G.A. Gerhardt. Second-by-Second Measures of L-glutamate Resting Levels Using Enzyme-Based Microelectrode Arrays in the CNS of Conscious Freely Moving Mice. 12th Institute of Biological Engineering Meeting. St. Louis, Missouri March, 2007.

G. A. Gerhardt, E. Rutherford, K. Hascup, J.E. Quintero, P. Talauliker, T. Currier Thomas, M. L. Stephens, J. Fuqua, T. Coates, J. J. Burmeister, F. Pomerleau, P. Huettl . Second-by-Second Measurements of L -Glutamate and Other Neurochemicals in the CNS of Animal Models and Humans. 12th Institute of Biological Engineering Meeting. St. Louis, Missouri March, 2007.

P.M. Talauliker, F. Pomerleau, E. Rutherford, P. Huettl, J.T. Hastings, G.A. Gerhardt**.** Evaluation of Ceramic-based Microelectrode Arrays for In Vivo Recordings. 12th Institute of Biological Engineering Meeting. St. Louis, Missouri March, 2007.

P. Huettl, G. E. Quintero, E.C. Rutherford, F. Pomerleau, K.W. Johnson, D.D. Schoepp and G.A. Gerhardt. Pharmacological Studies of $mGlu_{2/3}$ Drugs on Glutamate Release Utilizing Ceramic-Based Microelectrode Arrays. 40th Winter Conference on Brain Research. Snowmass, Colorado January 2007.

Rutherford EC, Pomerleau F, Huettl P, Strömberg I, Johnson KW, Gerhardt GA. Second-by-Second Enzyme-Based Microelectrode Recordings of Basal L-Glutamate in the Prefrontal Cortex of Awake Rats. Monitoring Molecules in Neuroscience: 11th International Conference on *In Vivo* Methods. Villasimius-Cagliari, Italy May, 2006.

Hascup KN, Rutherford EC, Pomerleau F, Huettl P, Gerhardt GA. Second-By-Second Measures of L-Glutamate Using Enzyme-Based Microelectrodes in the CNS of Conscious, Freely Moving Mice. Monitoring Molecules in Neuroscience: 11th International Conference on *In Vivo* Methods. Villasimius-Cagliari, Italy May, 2006.

Gerhardt GA, Pomerleau F, Huettl P, Nickell J, Rutherford E, Hascup K, Quintero JE, Day BK, Currier Thomas T, Stephens ML, Burmeister JJ. Ceramic Enzyme-Based Microelectrode Arrays for Second-by-Second Measurements of L-Glutamate and Other Neurochemicals in CNS. Monitoring Molecules in Neuroscience: 11th International Conference on *In Vivo* Methods. Villasimius-Cagliari, Italy May, 2006.

Talauliker PM, Rutherford EC, Pomerleau F, Huettl P, Stephens ML, Hastings JT, Gerhardt GA. Multisite Microelectrode Array Studies of L-Glutamate Dynamics in the Rodent Hippocampus. Monitoring Molecules in Neuroscience: 11th International Conference on *In Vivo* Methods. Villasimius-Cagliari, Italy May, 2006.

Rutherford E, Pomerleau FP, Gerhardt GA. Second-by-Second Recordings of Stress Induced L-Glutamate Release in the Striatum and Prefrontal Cortex of Unanesthetized Rats: Strain Differences. Society for Neuroscience Meeting. Washington D.C. November, 2005.

Pomerleau FP, Rutherford E, Huettl P, Hampson RE, Deadwyler SE, Strömberg I, Gerhardt GA. Histopathology Studies of Long-Term Implantation of Ceramic-Based Microelectrodes in the rat Prefrontal Cortex. Society for Neuroscience Meeting. Washington D.C. November, 2005.

Hascup KN, Rutherford EC, Pomerleau FP, Gerhardt GA. Real time (second-by-second) *in vivo* measures of L-glutamate in the CNS of conscious, freely moving mice. Society for Neuroscience Meeting. Washington D.C. November, 2005.

Talauliker PM, Rutherford E, Pomerleau F, Huettl P, Hastings JT, Gerhardt GA. Surface analysis of chronically implanted ceramic based microelectrode arrays using scanning electron microscopy. Society for Neuroscience Meeting. Washington D.C. November 2005.

Allen J, Rutherford E, Burmeister JJ, Huettl PF, Pomerleau FP, Gerhardt GA. Basal glutamate measures using m-phenylenediamine coated vs. Nafion® coated ceramic microelectrode arrays. Society for Neuroscience Meeting. Washington D.C. November, 2005.

Rutherford E, Pomerleau FP, Strömberg I, Johnson KW, Gerhardt GA. Second-by-second recordings of L-glutamate due to stress in the striatum and prefrontal cortex of unanesthetized rats. 5th International mGluR Meeting. Taoramina-Sicily, Italy September, 2005.

Pomerleau FP, Rutherford E, Gerhardt GA. Improvements in real time (second-by-second) in vivo measures of L-glutamate in the striatum of conscious, freely moving rats: Effects of stress. Society for Neuroscience Meeting. San Diego, CA. October 2004.

Rutherford E, Gash CR, Joyce BM, Surgener S, Currier TD, Grandy D, Gerhardt GA, Glaser PEA. Dopamine Neuron Dynamics are Altered in the Nucleus Accumbens of Mice Lacking the D4 Dopamine Receptor. Society for Neuroscience Meeting. New Orleans, LA. November 2003.

Pomerleau FP, Rutherford EC, Gerhardt GA. Real Time (second-by-second) *in vivo* Measures of L-Glutamate in the CNS of Conscious, Freely Moving Rats Using Multisite Microelectrode Arrays. Society for Neuroscience Meeting. New Orleans, LA. November 2003.

Martin JC, Parsons J, Rutherford E, Ruscetti T, Ambrose WP. Development of an Imaging Flow Cytometer. International Society for Analytical Cytology (ISAC) Conference. San Diego, CA. May 2002.

Rutherford E, Max T, Nickoloff JA, Ruscetti T. Strict Regulation of Ribosomal DNA Homologous Recombination. Radiation Research Society Meeting. Reno, NV. April, 2002.

Rutherford E, Ruscetti T. Aging Process Linked to Homologous Recombination in Specific DNA Sequence. Symposium 2001—Championing Scientific Careers. Santa Fe, NM. August 2001.

Signed: Erin Cathleen Rutherford